EVALUATION OF A CELL MIGRATION- AND AUTOPHAGY-RELATED KINASE AS A NOVEL DRUG TARGET IN PEDIATRIC GLIOMA

by

GAMZE DEVECİ

A Dissertation Submitted to the
Graduate School of Health Sciences
in Partial Fulfillment of the Requirements for
the Degree of

Master of Science

in

Cellular and Molecular Medicine

August, 2023

MSc Thesis Title

Koç University

Graduate School of Health Sciences

This is to certify that I have examined this copy of a master's thesis by

Gamze DEVECİ

and have found that it is complete and satisfactory in all respects,
and that any and all revisions required by the final
examining committee have been made.

Committee Members:

Prof. Dr. Devrim Gözüaçık (Advisor)

Prof. Dr. Tuğba Bağcı Önder

Assoc. Prof. Dr. N. C. Tolga Emre

Assoc. Prof. Dr. Elif Damla Arısan

Prof. Dr. Mehmet Fatih Erbey

Date: 08.08.2023

I dedicate this thesis to the founder of the Republic of Turkey, Mustafa Kemal ATATÜRK, and Turkish science.

ABSTRACT

Evaluation of a Cell Migration- and Autophagy-Related Kinase as a Novel Drug Target in Pediatric Glioma

Gamze Deveci

Master of Science in Cellular and Molecular Medicine

August 8, 2023

Pediatric gliomas are aggressive brain tumors that pose serious difficulties in terms of prognosis and treatment options. The purpose of this thesis is to assess a novel therapeutic target for pediatric glioma, a cell migration- and autophagy-related kinase. This kinase was discovered as a prospective therapeutic target by a thorough study of proteomic datasets due to its altered expression and interaction with important pathways involved in cell migration and autophagy in glioblastoma.

This thesis examines the functional importance and expression of the discovered kinase in pediatric glioma cell lines and patient tumour samples. We observed that migration and drug resistance of pediatric glioma cells are more sensitive to changes in autophagic flux. Also, its expression and localization in patient samples is evaluated using quantitative PCR, Western blotting, and immunohistochemistry. To determine the influence of targeting this kinase on glioma cell migration and autophagy, functional tests such as cell migration assays, autophagy flux analysis, and cell viability assays were carried out.

The findings from this study could aid in facilitating the improvement of pediatric glioma-targeted treatments. Understanding the functions of this kinase protein will help researchers develop novel pharmaceutical candidates that selectively limit the growth of gliomas while minimizing side effects. The interaction between the interested kinase protein and one of the main autophagy proteins, ATG5, was displayed. The changes in the autophagic degradation with wild-type, kinase overexpressing and CRISPR-Cas9 mediated knockout cell lines were revealed. Moreover, cellular migration was significantly influenced upon depletion of the protein. Besides, drug resistance against

various commonly used chemotherapeutic agents was not changed with gene deletion and kinase inhibition. To summarize, this research on the interested kinase protein as a druggable target may pave the door for individualized treatment plans that develop the prognosis and quality of life for children with gliomas.

Key Words: Pediatric glioblastoma, cellular migration, serine-threonine kinase, focal adhesion, cytoskeleton

ÖZETÇE

Hücre Göçü ve Otofaji ile İlişkili Bir Kinazın Pediatrik Glioma'da Yeni Bir İlaç Hedefi Olarak Değerlendirilmesi

Gamze Deveci

Hücresel ve Moleküler Tıp, Yüksek Lisans

8 Ağustos, 2023

Pediatrik gliomalar, prognoz ve tedavi seçenekleri açısından ciddi zorluklar oluşturan agresif beyin tümörleridir. Bu tez, hücre göçü ve otofajiyle ilişkili bir kinaz olan pediatrik glioma için yeni bir terapötik hedefi değerlendirmeyi amaçlamaktadır. Bu kinaz, değiştirilmiş ekspresyonu ve glioblastomada hücre göçü ve otofajide yer alan temel yollarla etkileşimi nedeniyle proteomik veri kümelerinin kapsamlı bir çalışmasıyla ileriye dönük bir terapötik hedef olarak keşfedildi.

Bu tez, pediatrik glioma hücre dizilerinde ve hasta tümör örneklerinde keşfedilen kinazın fonksiyonel önemini ve ekspresyonunu incelemektedir. Pediatrik glioma hücrelerinin göçü ve ilaç direncinin, otofajik akıştaki değişikliklere karşı daha duyarlı olduğunu gözlemledik. Ayrıca kantitatif PCR, Western blotlama ve immünohistokimya, hasta örneklerinde ekspresyonunu ve lokalizasyonunu değerlendirdi. Bu kinazın glioma hücre göçü ve otofaji üzerindeki etkisini belirlemek için hücre göçü analizleri, otofaji akı analizi ve hücre canlılığı analizleri gibi çeşitli fonksiyonel testler yapıldı.

Bu çalışmadan elde edilen bulgular pediatrik glioma hedefli tedavilerin iyileştirilmesini kolaylaştırmaya yardımcı olabilir. Bu kinaz proteininin işlevlerini anlamak, araştırmacıların, yan etkileri en aza indirirken gliomaların büyümesini seçici olarak sınırlayan yeni farmasötik adaylar geliştirmelerine yardımcı olacaktır. İlgili kinaz proteini ile ana otofaji proteinlerinden biri olan ATG5 arasındaki etkileşim gösterildi. Vahşi tip, aşırı kinaz ekspresyonu ve CRISPR-Cas9 aracılı nakavt hücre çizgileri ile otofajik bozulmadaki değişiklikler ortaya çıktı. Üstelik hücresel göç, proteinin tükenmesinden önemli ölçüde etkilenmiştir. Ayrıca gen delesyonu ve kinaz inhibisyonu,

yaygın olarak kullanılan çeşitli kemoterapötik ajanlara karşı ilaç direncini değiştirmedi. Özetlemek gerekirse, ilaç verilebilir bir hedef olarak kinaz proteini üzerine yapılan bu araştırma, gliomlu çocukların prognozunu ve yaşam kalitesini geliştiren bireyselleştirilmiş tedavi planlarının kapısını açabilir.

Anahtar Kelimeler: Pediyatrik glioblastoma, serin-threonine kinazlar, hücre göçü, fokal adezyon, hücre içi iskeleti.

ACKNOWLEDGEMENTS

I would like to express my deepest gratitude to all those who have contributed to completing my master's degree in Cellular and Molecular Medicine.

First and foremost, I am immensely grateful to my supervisor, Prof. Dr Devrim Gözüaçık, for their guidance, expertise, and unwavering support throughout this journey. Their invaluable insights, encouragement, and patience have been instrumental in shaping my research and academic growth.

I am indebted to all G Lab members for their camaraderie, intellectual discussions, and shared experiences. Their collaboration and support have enriched my learning and made this academic endeavor even more rewarding.

I am grateful to my family for their unwavering love, encouragement, and belief in my abilities. Their constant support and understanding have been a source of motivation and strength throughout this academic pursuit. I would like to thank Samet Ertürk endlessly for always believing in me, encouraging me during rough periods, and being the most magnificent partner along this journey.

Lastly, I would like to acknowledge the KUTTAM and TÜBİTAK that have financially and technically supported my research. Their investment in scientific exploration has made this study possible.

In conclusion, this master's degree would not have been possible without the collective efforts and support of all those mentioned above. I am truly fortunate to have had the opportunity to study in such a research group and to have been surrounded by such remarkable individuals.

TABLE OF CONTENTS

LIST OF TABLES

LIST OF FIGURES

ABBREVIATIONS

GBM	Glioblastoma
pHGG	Pediatric high-grade glioma
CNS	Central Nervous System
WHO	World Health Organization
IDH	Isocitrate dehydrogenase
EGFR	Epithelial growth factor receptor2
CDKN2A	Cyclin-dependent kinase inhibitor 2A
pHGG	Pediatric high-grade glioma
PDGFR	Platelet-derived growth factor receptor
ECM	Extracellular matrix
MMP	Matrix metalloproteinase
TNF	Tumor necrosis factor
TGF-ß	Transforming growth factor beta
EGF	Epithelial growth factor
ERM	Ezrin/Radixin/Moesin
FA	Focal adhesion
EMT	Epithelial mesenchymal transition
mTORC	Mammalian target of rapamycine complex
DIPG	Diffuse intrinsic pontine glioma
LOK	Lymphocyte-oriented kinase
SLK	Ste20-like kinase
FAK	Focal adhesion kinase
MAPK	Mitogen-activated protein kinase

Chapter 1:
INTRODUCTION

1.1 PEDIATRIC HIGH-GRADE GLIOMA

Glioblastoma is an aggressive and incurable type of brain cancer that accounts for over half of all diagnosed cases. It is characterized by rapid tumor growth, invasion into surrounding brain tissue, and resistance to conventional therapies. The prognosis for glioblastoma patients is poor, with a median survival rate of only 15 months, highlighting the urgent need for further research and innovation in the field (Hanif et al., 2017). The classification system for gliomas is based on the level of malignancy determined by histopathological criteria, with grades I to IV. Grade I gliomas are characterized by low proliferative potency and can be treated with surgical operation. In contrast, grades II to IV gliomas are thoroughly invasive and malignant. Glioblastoma multiforme, designated Grade IV by WHO, is the most invasive, aggressive, and undifferentiated type of tumor (Louis et al., 2007). Pediatric glioblastoma is a rare but aggressive type of brain cancer that primarily affects children and adolescents. Epidemiological studies have shown that pediatric glioblastoma accounts for a small proportion of all pediatric brain tumors, with an incidence rate ranging from 5 to 20% of all brain malignancies in children. The age of onset varies, with the peak incidence observed between the ages of 3 and 7 years. Boys are slightly more affected by the disease compared to girls (Fangusaro, 2009). Although GBM is the most prevalent lethal brain tumor in adults, it accounts for maximum 15% of primary central nervous system tumors (CNS) in pediatric patients. As we can see in Figure 1.1, pediatric high-grade glioma has the lowest overall survival ratio compared to other types of pediatric brain tumors (Petralia et al., 2020). Classification of WHO was based on cellular origin of tumor types until 2016. Following the explorations of different molecular and genetic features between pediatric and adult glioblastoma thanks to advancements in genetic studies, pediatric brain tumors were discriminated from adult brain tumors. Glioblastomas have also been divided into different categories based on their IDH immunoreactivity. Glioblastomas can presently be classified as IDH-mutant, IDH-wild type, or IDH-NOS (Hoshide & Jandial, 2016).

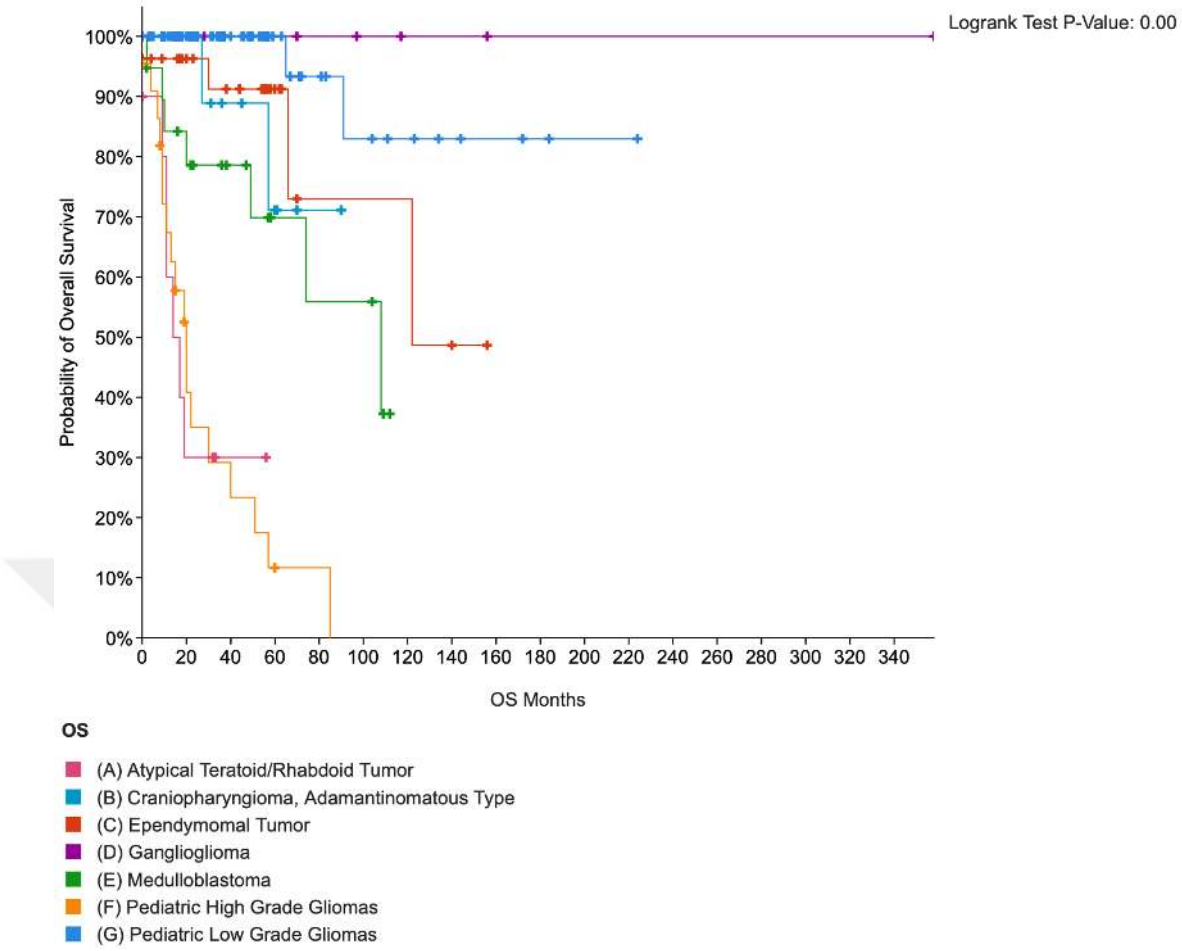

Figure 1.1 Overall survival rate of pediatric brain cancer cases. Data was obtained from cBioportal website by analyzing 218 tumors across 7 histological types of childhood brain cancer (Petralia et al., 2020).

1.1.1 Molecular Biology of Pediatric High-Grade Glioma

Glioblastoma is a highly aggressive type of brain cancer that arises from glial cells in the central nervous system. It is characterized by its rapid growth and invasive nature. Molecularly, glioblastoma has several distinguishing characteristics including genetic alterations, chromosomal abnormalities, tumor suppressor gene inactivation, increased angiogenesis, and tumor heterogeneity.

Numerous genetic mutations, including those in important genes like TP53, PTEN, and EGFR, are associated with glioblastoma. These modifications frequently interfere with biological processes such cell cycle regulation, apoptosis, and signal transmission, which results in unchecked cell proliferation and survival (Diaz & Baker, 2014).

Chromosome instability and intricate chromosomal rearrangements are frequently seen in glioblastoma cells. Specific chromosome regions are frequently amplified or deleted, which might have an impact on gene expression and function (Rickert et al. 2001).

Some of tumor suppressor genes, such as CDKN2A, RB1, and NF1, are frequently inactivated in glioblastoma in addition to the TP53 and PTEN. These genes' capacity to control DNA repair and cell cycle advancement is eliminated when they stop working. (Rizzo et al., 2015).

Glioblastomas are highly vascularized tumors. They induce angiogenesis, the formation of new blood vessels, by secreting various pro-angiogenic factors such as VEGF (vascular endothelial growth factor). The presence of abundant blood vessels supports the rapid growth and survival of glioblastoma cells (Ahir et al., 2020).

Inter- and intra-patient glioblastoma demonstrates high intratumoral heterogeneity. This heterogeneity develops because of genetic, epigenetic, and microenvironmental effects, giving rise to variations in the tumor's molecular profiles, cellular characteristics, and therapeutic responses (Friedmann-Morvinski, 2014). Understanding these molecular characteristics is essential for developing targeted therapies and personalized treatment approaches for glioblastoma.

Pediatric high-grade gliomas are a highly aggressive and malignant brain tumor that occurs in children. It is characterized by uncontrolled proliferation of glial cells, particularly astrocytes, in the brain (Faury et al., 2007). Several molecular alterations have been identified in pediatric high-grade glioma, which contribute to its development and progression. These alterations include:

- TP53 Mutation: TP53 is one of the well-known tumor suppressor gene having important role in cell-cycle control. In pHGG, the tumor suppressor gene TP53 frequently develops mutations. Due to TP53 mutations, the tumor suppressor function is lost, allowing for unbounded cell proliferation and survival (Pollack et al., 2002).
- PTEN Mutation: Various cellular actions such as proliferation and migration are under control of phosphatidylinositol-4,5,-biphosphate, PI3K, pathway. PI3K was

phosphorylated and formed phosphatidylinositol-3.4.5-triphosphate (PIP3) upon activation by several growth factors such EGFR and PDGFR. PIP3 formation leads to recruitment of AKT protein and phosphorylation at Thr308 and Ser473 residues. Downstream of Akt is initiated upon its activation and inhibits apoptosis (Hemmings & Restuccia, 2012). PI3K/Akt pathway is inhibited by the PTEN tumor suppressor gene encoding a phosphatase protein product. Phosphatase exhibits its action by dephosphorylating PIP3. A mutation of the PTEN tumor suppressor gene causes the Akt to be stacked in active form and programmed cell death are impaired in tumor cells (Chen et al., 2018). Up-to date studies represented the increased Akt activation in malignant pediatric glioma and associated the weak survival rate with RAS/Akt pathway (Pollack et al., 2010).

- PDGFRA Amplification: Platelet-derived growth factor is mainly responsible for angiogenesis, motility of nervous system cells, neuronal differentiation, and proliferation regulation (Lokker et al., 2002). Pediatric high-grade glioma commonly exhibits amplification of the platelet-derived growth factor receptor alpha (PDGFRA) gene. A receptor tyrosine kinase called PDGFRA encourages tumor growth and cell division. (Paugh et al., 2013)
- EGFR Overexpression: Overexpression of the epidermal growth factor receptor (EGFR) is found in a subset of adult glioblastomas. EGFR activation leads to the activation of downstream signaling pathways that promote cell proliferation and survival (J. Li et al., n.d.). However, amplification of EGFR in pHGG is rare than adult counterparts (Bredel et al., 1999).
- IDH Mutation: Isocitrate dehydrogenase (IDH) mutations, commonly found in adult glioblastoma, are rare in pediatric cases. IDH mutations lead to the accumulation of an oncometabolite called 2-hydroxyglutarate, which alters cellular metabolism and promotes tumorigenesis (Korshunov et al., 2017).
- H3F3A Mutation: A specific mutation in the H3F3A gene encoding histone protein H3.3, known as K27M, is frequently found in pHGG. This mutation disrupts normal epigenetic regulation, leading to altered gene expression and tumorigenesis (Schwartzentruber et al., 2012).

It is essential to comprehend the molecular biology of pediatric high-grade glioma in order to create tailored treatment plans and targeted medicines for these young patients.

Researchers hope to enhance treatment outcomes and lower the overall morbidity and death linked to this terrible disease by focusing on specific genetic abnormalities.

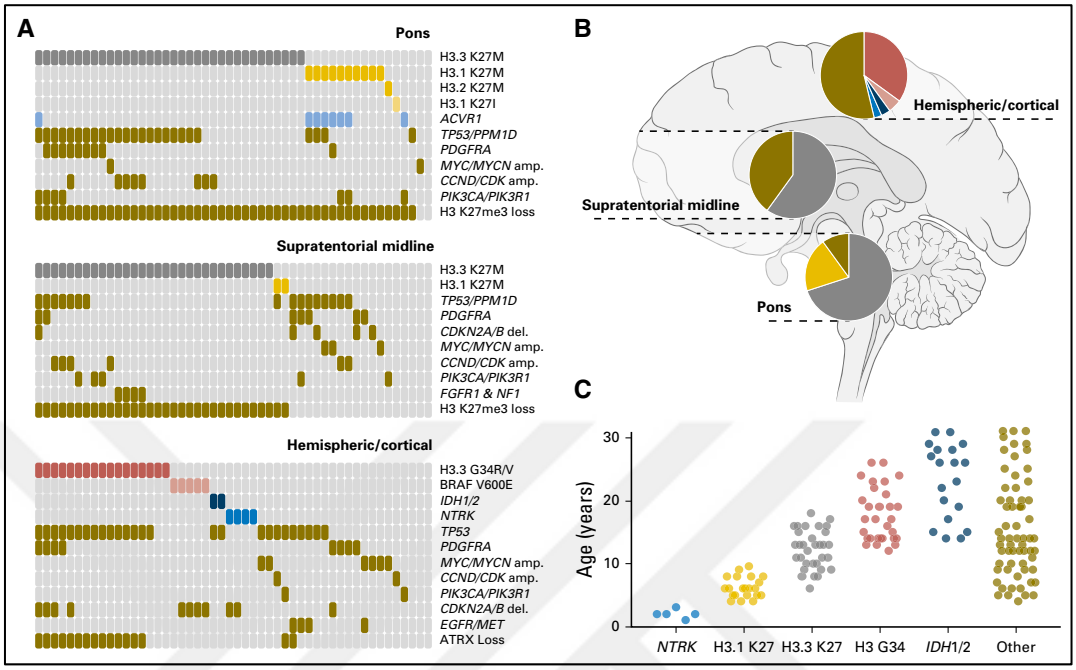

Figure 1.2 Clinical characteristics and molecular variance in groups of pediatric high-grade gliomas. (A) Common mutations in pediatric high-grade gliomas according to brain settlement is schematically depicted. (B) Frequency of prevalent molecular variances in pediatric high-grade glioma is depicted in pie chart by colors matching to A. (C) distribution of molecular variances according to ages in young adults and children (Sturm et al., 2017). License number: 5618701266400

1.1.2 Current Treatments for Pediatric High-Grade Glioma

Glioblastomas in children have unique characteristics, making their treatment challenging. Over the years, various treatment approaches have been developed to tackle this complex disease. The primary treatment for pHGG involves a combination of surgery, radiation therapy, and chemotherapy. However, the optimal treatment strategy depends on various factors such as the size, location, and genetic characteristics of the tumor, as well as the age and overall health of the child (Wyss et al., 2022).

Surgery plays a pivotal part within the administration of pediatric high-grade glioma. Neurosurgeons endeavor to evacuate as much of the tumor as conceivable without

causing harm to basic brain structures. Total resection of the tumor is by and large troublesome due to its obtrusive nature, which regularly leads to tumor repeat. All things considered; surgery upgrades the adequacy of consequent medications by decreasing the tumor burden (Broniscer, 2006)

The treatment for pediatric high-grade glioma must also include chemotherapy. Physicians enforce chemotherapic drugs in oral or intravenous routes to target the primary cancer cells and tumor cells dispersed from the prior tumor site. It is possible to utilize several chemotherapy regimens, which frequently include medications such as temozolomide, vincristine, and carboplatin. These drugs may be administered in cycles to give the child's body a chance to recuperate in between doses (Wolff et al., 2010). It was shown that concomitant therapy with temozolomide could improve the two-year survival rate compared to treatment with only radiotherapy (Stupp et al., n.d.)

Pediatric high-grade has been the subject of contemporary research into precision medicine methods. To pinpoint specific biomarkers that may inform treatment choices, analysis of the tumor's genetic features is being used more frequently. Then, targeted therapies can be applied to obstruct molecules or signaling pathways connected to the development of tumors. Some tyrosine kinase receptors are currently used as anticancer drugs in treating pHGG (MacDonald et al., 2011). For example, erlotinib, an EGFR inhibitor, is using with radiotherapy in newly diagnosed and relapsed pHGGs Yet, recommended drug doses are higher in pediatric patients than adults, and intratumoral bleeding is a severe side effect in children (Geoerger et al., 2011). Moreover, imatinib, a PDGFR inhibitor, was recruited in the Phase II clinical trial, but there was no clinically significant activity in relapsed gliomas (Raymond et al., 2008).

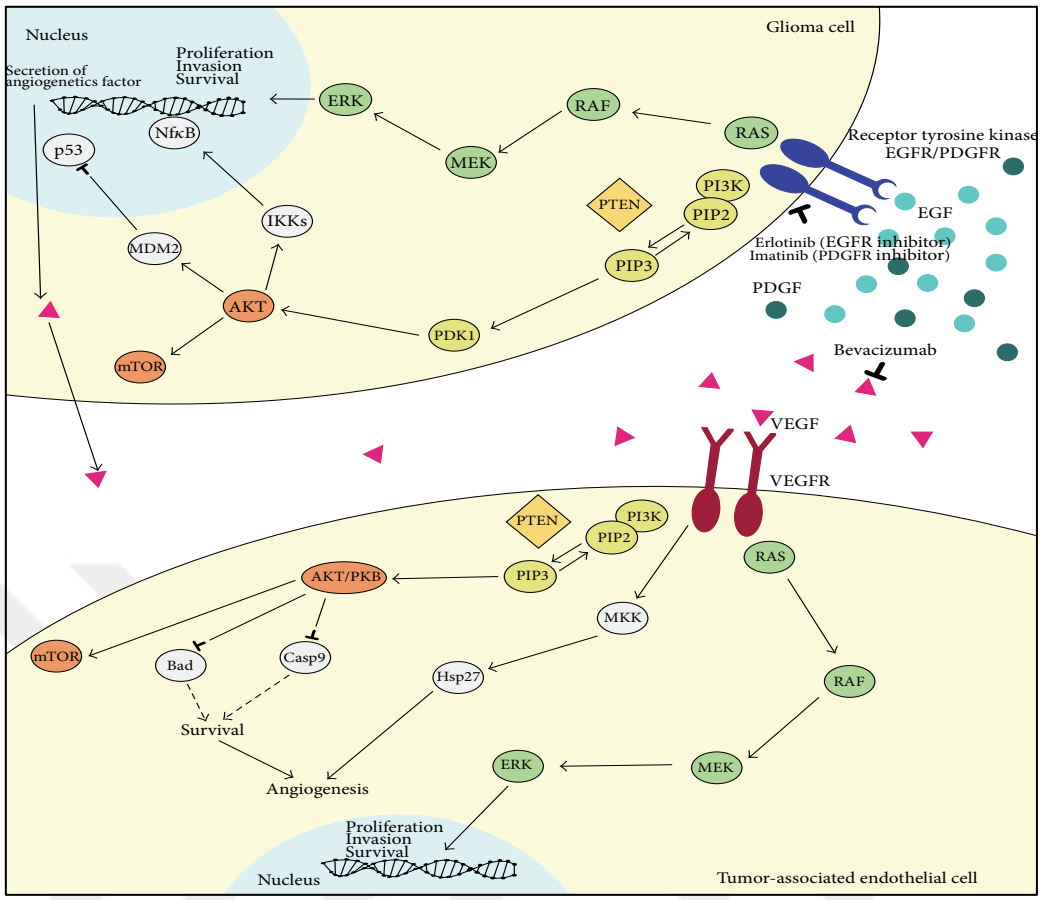

Figure 1.3 Molecularly targeted therapy for pHGG (Rizzo et al., 2015). (Copyright © 2015 Daniela Rizzo et al. This is an open access article distributed under the Creative Commons Attribution License, which permits unrestricted use, distribution, and reproduction in any medium, provided the original work is properly cited.)

Despite improvements in available therapies, pediatric high-grade glioma is still difficult to treat. The disease's aggressiveness frequently causes tumor recurrence, necessitating additional treatments. In order to improve the quality of life for affected children and their families, numerous active research projects concentrate on developing novel targeted medicines, optimizing existing treatment regimens, and enhancing supporting care (Vanan & Eisenstat, 2014).

As a conclusion, surgery, radiation therapy, and chemotherapy are all used in the current management of pHGG. In order to improve results, precision medicine strategies and immunotherapy are also being investigated. Even while there is still much work to be done, current research holds out a lot of hope for improving the prognosis and broadening the range of available treatments for kids with this life-threatening condition.

1.1.3 Invasion and Infiltration in Glioblastoma

Glioblastoma is known as the most aggressive brain tumor due to its highly complicated biochemistry and undiscovered properties. Even though the maximum tumor resection is performed with chemotherapy and radiotherapy as a primary treatment method, the extreme migration/invasion capability of GBM cells causes tumor recurrence (Ramirez et al., 2013). The uncertain boundary between the tumor and normal brain tissue is another challenge of surgical resection. This challenge also increases the risk of causing damage to central nervous system (Sales et al., 2022). Recurrence of the GBM is represented with the MRI image in Figure 1.4.

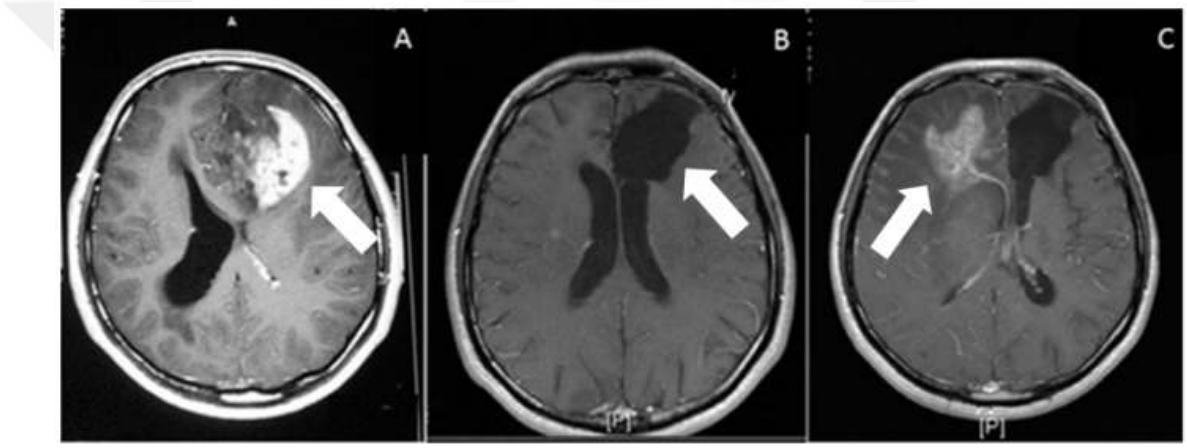

Figure 1.4 Radiology image of GBM. (A) Tumor before surgery in left frontal lobe of the brain. (B) No residual tumor after tumor resection. (C) Relapsed tumor in contralateral hemisphere of the brain after 18 months (Seker-Polat et al., 2022).

The primary route of the glioblastoma cells is the perivascular area to supply the requirements for nutrients and oxygen. Besides, glioblastoma cells can prefer to invade the brain parenchyma and white-matter tracts (Cuddapah et al., 2014). Brain parenchyma includes various cell types, such as neurons, astrocytes, microglia, and progenitor cells release molecules that can induce the proliferation and motility of the tumor cells. The dynamics of the microenvironment and tumor-stroma connections can affect the behavior

of glioblastoma cells. On the other hand, white-matter tract is a known route for diffuse pediatric high-grade glioma cells (de Gooijer et al., 2018).

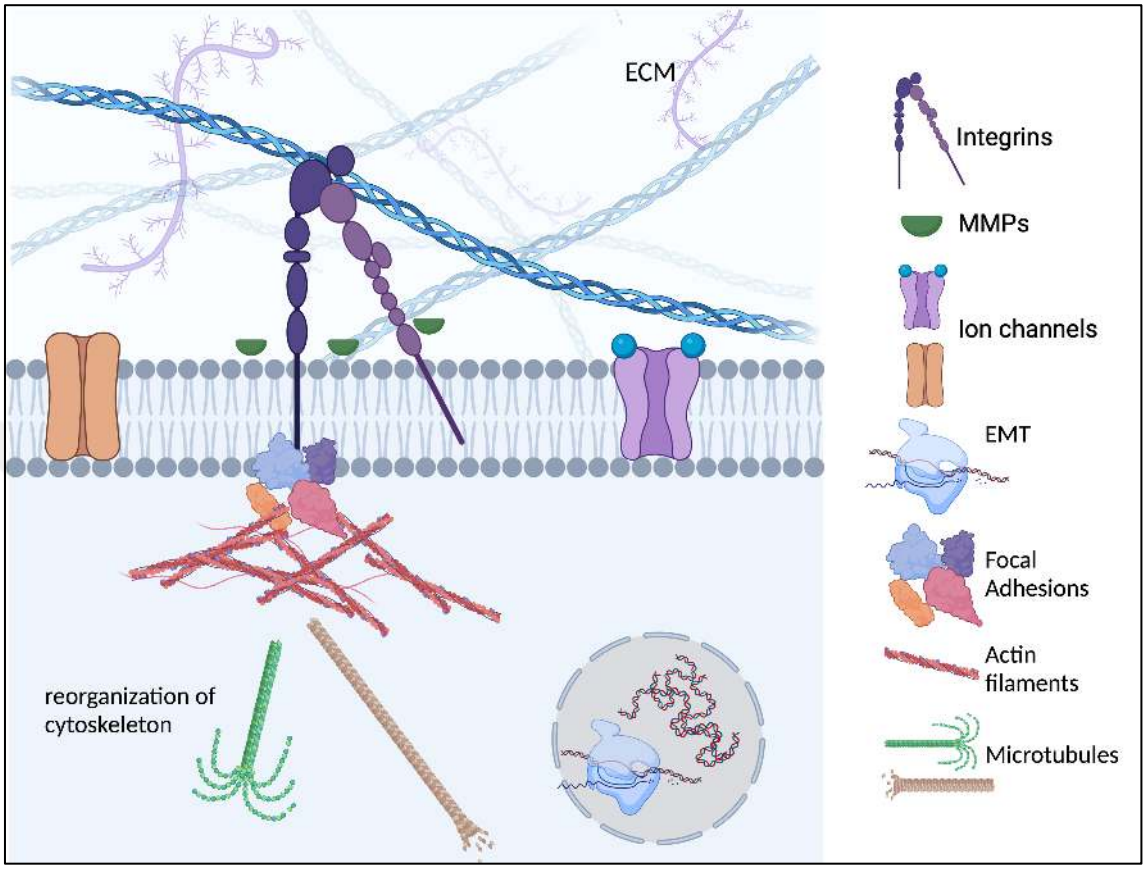

Figure 1.5 Cell invasion related factors is GBM. Created in Biorender.

- **Extracellular Matrix (ECM)**

The extracellular matrix (ECM) is formed by surrounding cells and accounts for a major amount of the brain volume. It is important not just for structural reasons, but also for migration, brain development, differentiation, cell survival, maturation, and tissue homeostasis. Proteoglycans, hyaluronan, link-proteins like TN-C, and other proteins are important components of brain ECM. ECM dynamics become dysregulated in the context of cancer, notably glioblastoma (Mahesparan et al., 2003). Glioma ECM differs from that of a healthy brain, with fibrous proteins and laminin upregulated in high-grade glioma. Glioma cell invasion into healthy brain tissue is dependent on the interaction of the ECM molecule hyaluronan and its receptor CD44, both of which are overexpressed in glioma cells. This invasion entails the breakdown and modification of the intact ECM, which is aided by a variety of ECM-degrading and remodeling enzymes that are controlled at several levels (Goldbrunner et al., 1999).

- **Adhesion molecules**

Regulation of extracellular matrix (ECM) interactions is required for cell mobility and invasion. To enable directed migration, tumor cells detach from the ECM and subsequently reconnect. Adhesion qualities are important in determining tumor cell invasive capacity, and several adhesion-associated proteins have been proposed as potential targets to prevent invasion (Friedl & Alexander, 2011). Specific cell adhesion molecules, such as CD44, neural cell adhesion molecule (NCAM), and cadherins, are involved in glioblastoma invasion. CD44 interacts with hyaluronic acid in the brain ECM and is linked to the grade of glioma (Ranuncolo et al., 2002). NCAM functions as a paracrine inhibitor, reducing glioma cell motility (Prag et al., 2002).

Cadherins, namely the alteration from E-cadherin to N-cadherin, are connected to cell mobility and a shift to a more invasive phenotype in glioblastoma. Cadherin-mediated junction instability and disorder contribute to enhanced invasion in glioblastoma cells. Overall, these adhesion-related proteins are important in regulating glioblastoma invasion and may be therapeutic targets (Cavallaro & Christofori, 2004).

Tenascin-C and Integrins are critical proteins in the reattachment of infiltrating cells to the ECM. Integrins, the most common type of adhesion molecule, are essential for interacting with ECM proteins and other cell surface attachment molecules. They serve as links between extracellular contacts and the intracellular cytoskeleton, allowing cells to move by creating and dissolving Integrin-mediated ECM connections (Horwitz, 1997). Integrin family members are overexpressed in glioma cells. Integrins, in addition to inducing cell adhesion and migration, contribute in intracellular signaling, transducing extracellular signals, and orchestrating cytoskeleton reorganization via Focal adhesion kinase (FAK). FAK binds cytoskeletal proteins and triggers Rho GTPases to enhance cell migration when activated by Integrin-mediated ECM adhesion and growth stimuli. FAK overexpression is linked to glioma invasiveness and recurrence, especially near the invasive margins of glioblastoma cells (Cary, 1999; Cox & Huttenlocher, 1998).

- **Matrix metalloproteinases (MMPs)**

Matrix metalloproteinases (MMPs) are endoproteinases that degrade and alter the extracellular matrix (ECM). MMP expression is modest in the normal brain, but it is overexpressed or activated in glioma. MMP-2 and MMP-9 are particularly important in

glioma invasion, and their levels correlate with tumor grade and development (Yu & Stamenkovic, 2000). MMP-2 and MMP-9 participate in a feedback loop with transforming growth factor (TGF)-, which promotes cell motility. MMP-9 expression or activity is regulated by a number of factors, including STAT3, EGF, FN, VN, IL-1, TNF-, and TGF-. Glioma cells use MMP-14 from nearby microglia cells to activate MMP-2. MMP-3, -7, -12, -13, -16, -19, and -26 are also strongly expressed and linked to enhanced glioma invasion (M. Wang et al., 2003).

- **Ion Channels**

Tumor invasion requires alterations in the extracellular matrix and cytoskeleton, as well as ion channel modulation. Ion channels are essential in cancer cells for cell homeostasis, membrane potential, cell volume, and gene expression. To protrude and traverse through limited spaces, glioma cells change their ionic equilibrium and volume (Litan & Langhans, 2015). Diverse ion channels, including KCa1.1, NKCC1, KCa3.1, and CLC3, play a role in glioma migration of cells by controlling ion flux on both the leading and trailing edges (Catacuzzeno & Franciolini, 2018). Downstream pathways of signaling activated by ion channels include NF-KB, Ca2+-dependent routes, and STAT3 and Notch signaling (M. Liu et al., 2014). In glioma cells, acid-sensing ion channels are overexpressed, causing acidosis as the cells migrate (Shah et al., 2021). Inhibiting certain ion channels has showed promise in reducing glioma cell invasion. Ion channels play a diverse role in glioblastoma invasion beyond volumetric regulation, altering signaling pathways and contributing to glioma cell invasion (Caramia et al., 2019).

- **Cytoskeleton Rearrangement**

Cell mobility is dependent on cytoskeleton reorganization. Tumor cells become polarized, with leading and trailing edges, and protrude to allow movement. Microtubules and intermediate filaments maintain cell structure and organelle placement, whereas actin polymerization and depolymerization reorganize the cytoskeleton for cell mobility (Bølge Tysnes & Mahesparan, 2001). Protrusion development and actin polymerization are aided by the Arp2/3 complex, nucleation-promoting factors, capping proteins, cofilin, and profilin (Nicholson-Dykstra et al., 2005). Rac1 and Cdc42 regulate lamellipodia and filopodia, which are actin membrane protrusions that cause cell movement (Whale, 2011). Podosomes and invadopodia are essential protrusions in glioblastoma invasion that

release matrix-degrading enzymes and act as leading structures for invasion. Cortactin, an actin-binding protein generated by WASP/N-WASP activity, is involved in the development of invadopodia and podosomes (Yamaguchi & Oikawa, 2010). RhoA and Rac are key molecules in glioma cells that regulate cytoskeletal rearrangements that allow for cell migration and invasion (H. Wang et al., 2014).

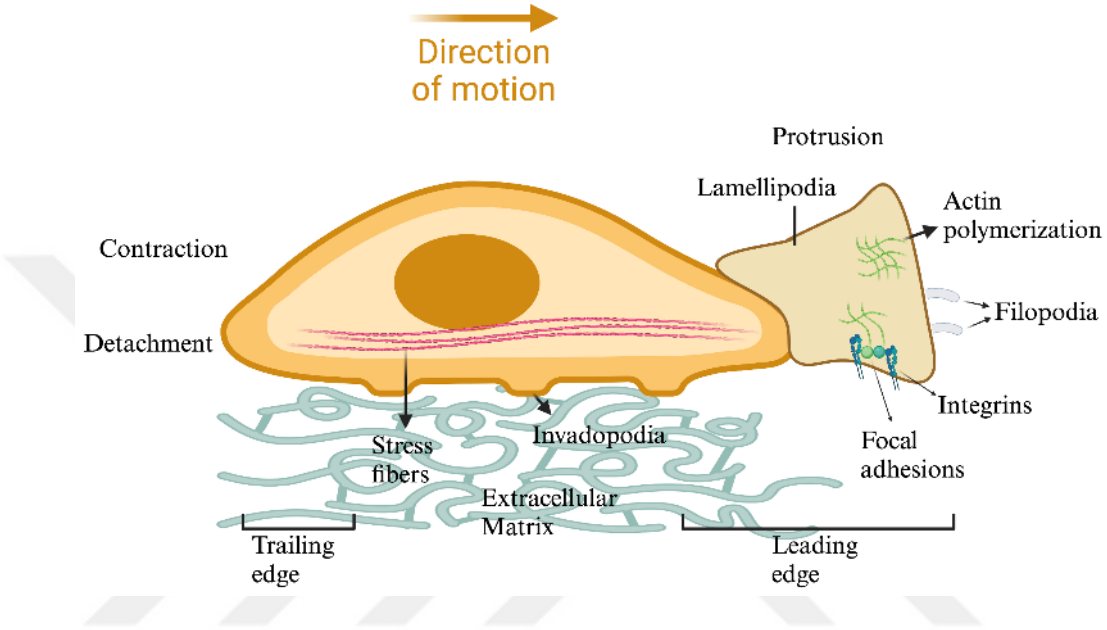

Figure 1.6 Cytoskeleton Arrangement during Cellular Movement (Boyle & Kopecki, 2020)

- **Epithelial-to-Mesenchymal Transition (EMT)**

The epithelial-to-mesenchymal transition (EMT) is a process in which epithelial cells undergo modifications to become mesenchymal cells. This change results in enhanced cell motility, apoptosis resistance, and the generation of pro-invasive proteins, all of which contribute to cancer growth and dissemination (Kalluri & Weinberg, 2009). Gene expression and cellular behavior change during EMT, influencing cell motility and interactions with the extracellular matrix (ECM). In cancer cells, EMT is related with increased chemoresistance, invasiveness, and stem cell-like features. EMT-like processes also contribute to invasion and metastasis in gliomas, a kind of brain tumor. ZEB1, Decorin, Twist, Snail, Slug, and P4HA2 are key EMT regulators that regulate glioma invasion (Iser et al., 2017).

1.2 AUTOPHAGY

Autophagy is a highly conserved degradation mechanism that engulfs targets in double-membrane autophagosomes (autophagic vesicles) and degrades the cargo in autolysosomes that result from autophagosome-lysosome fusion. Autophagy regulates the half-life of long-lived proteins and organelles, as well as the elimination of protein aggregates and the destruction of intracellular invaders. Furthermore, as a major stress response, autophagy permits cells to survive under adverse situations such as food and growth factor deficiency, oxidative stress, and drug and toxin exposure. Autolysosomal breakdown of cargoes into their fundamental components provides building blocks for cellular processes, allowing macromolecule synthesis and energy production under stress situations (Mizushima, 2007).

The mammalian target of rapamycin (mTOR) is a serine/threonine kinase that participates in mTORC1 and mTORC2. mTORC1 is required for autophagy regulation and is controlled by food availability, growth factors, and stress signals (Bar-Peled & Sabatini, 2014). The tuberous sclerosis protein (TSC)1/2 complex regulates mTORC1 by directly regulating the activator RHEB. mTORC1 suppresses autophagy by phosphorylating ULK1 and ATG13, rendering them inactive in nutrient-rich circumstances (González & Hall, 2017). Starvation or a drop in energy levels inhibits mTORC1, allowing ULK1 and ATG13 to activate autophagy. The ULK1 complex phosphorylates the components of the class III PI3K complex I (VPS34 complex), increasing the synthesis of phosphatidylinositol 3-phosphate (PI3P) at the omegasome, which are ER membrane fragments (Hosokawa et al., 2009; Karanasios et al., 2013). This pathway promotes the recruitment of PI3P-interacting proteins for phagophore growth, such as DFCP1 and WIPI proteins. Two ubiquitylation-like systems are involved in phagophore expansion: ATG12-ATG5-ATG16L1 and ATG8/LC3 family proteins, which include GABARAP and LC3. Lipidated ATG8/LC3 proteins are autophagy indicators that signal the number of autophagosomes (Slobodkin & Elazar, 2013).

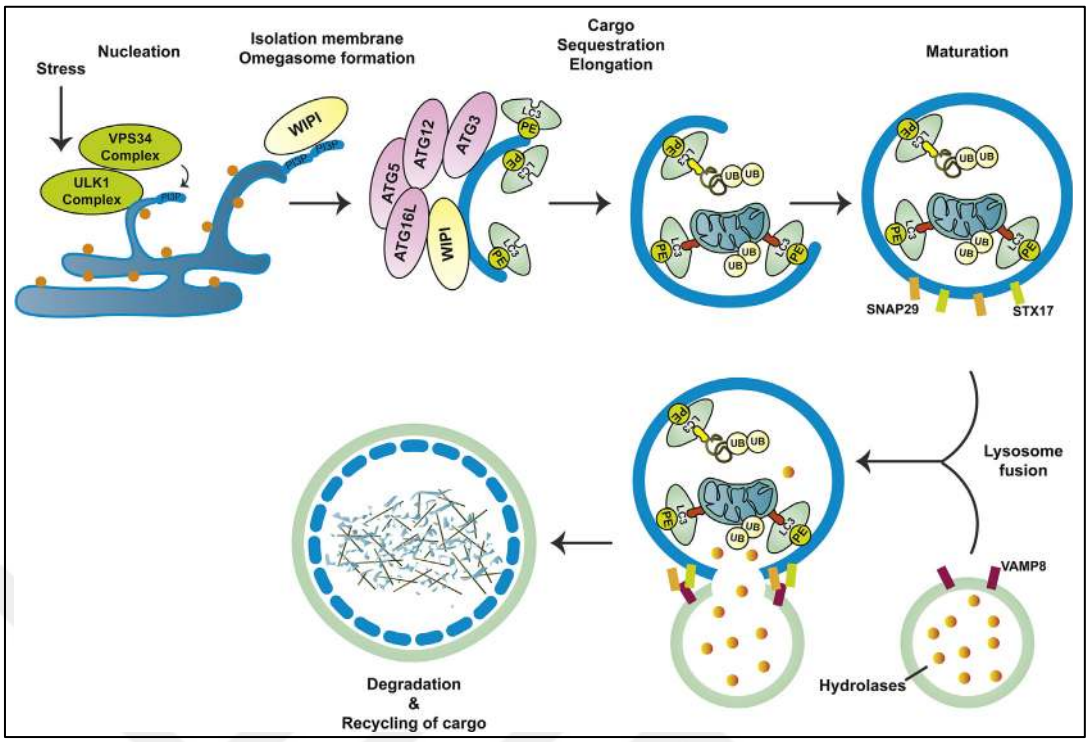

Figure 1.7 Representative progress of autophagic degradation.(Peker & Gozuacik, 2020)

Autophagy can be selective or nonselective, and various autophagy receptors have been identified for their function in selective autophagy, including NBR1, SQSTM1/P62, NDP52, and optineurin (OPTN) (Johansen & Lamark, 2020). Autophagosomes fuse with lysosomes via SNARE proteins, resulting in cargo destruction by lysosomal acidic hydrolases (R. Liu et al., 2015). Aside from its protein-level function, mTORC1 works for also transcriptional regulation of autophagy by detecting the level of amino acid and inactivating transcription factors involved in autophagy amplification and lysosomal formation (Sardiello et al., 2009).

Furthermore, autophagy is regulated by small noncoding RNAs (snRNAs) and microRNAs (miRNAs), which control important autophagy proteins at various phases of the autophagy process, from vesicle nucleation to lysosome fusion (Gozuacik et al., 2017).

1.2.1 Autophagy in Cancer

It has been understood that autophagy has functions related to cancer formation, development, spread, and drug resistance. While autophagy plays a suppressive role during the cancerization of normal cells, it contributes to the survival of tumor cells that

overgrow and are exposed to metabolic stress after cancer formation (Karakaş & Gözüaçik, 2014). Autophagy exerts an anti-cancerous effect by controlling ROS accumulation in the early stages of cancer, preventing DNA damage, and regulating the removal of damaged organelles and misfolded proteins (Mathew et al., 2009). Autophagy has been shown to have a tumor-promoting role in established and actively growing tumors (e.g., tumors with K-RAS activation). Autophagy is known to compensate for the metabolic demands of cancer cells resulting from nutrient and energy deficiencies, hypoxia, and acidosis (Levine, 2007). It is also involved in a variety of tumor growth and metastasis-related processes, including autophagy, cell cycle regulation, stem cell behavior, extracellular matrix interactions, epithelial-mesenchymal transition (EMT), anoikis, tumor cell-stroma interactions, angiogenesis, immune responses, and treatment resistance (Akkoc et al., 2023; Gerada & Ryan, 2020; Z. Li & Zhang, 2017). In line with these observations, a number of autophagy genes and proteins are known to exhibit tumor-suppressive or oncogenic activity.

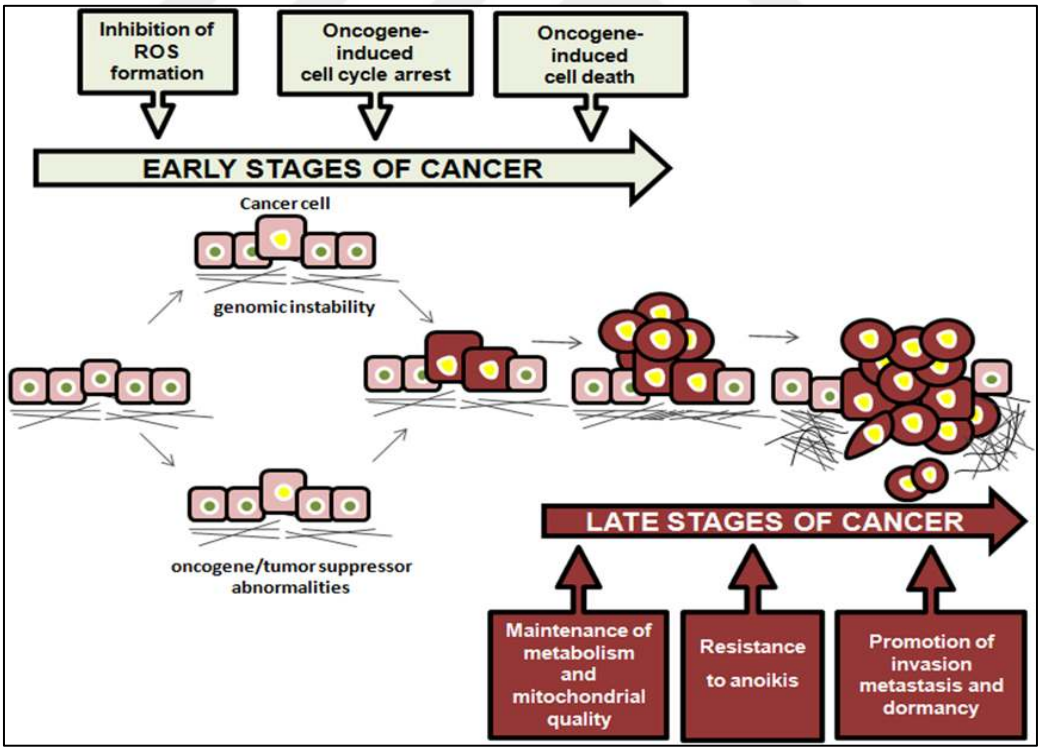

Figure 1.8 Binary roles of autophagy in various stage of cancer (Karakaş & Gözüaçik, 2014).

1.2.2 Impact of Autophagy in Metastasis of Tumor Cells

Cancer metastasis, or the spread of tumor cells to other regions of the body, is a major problem in cancer treatment. When cancer cells spread, they develop the ability to live and travel in a detached state. Clinical investigations have indicated increased synthesis of autophagic proteins in human metastatic lesions, suggesting that autophagy plays a role in cancer metastasis (Weiss et al., 2022). Sharifi et al. discovered that suppressing autophagy reduced tumor invasion in 4T1 breast cancer and decreased lung metastasis in a mouse mammary tumor model. This was accomplished by degrading paxillin, a focal adhesion (FA)-associated adaptor protein, via LC3-dependent processes, resulting in the breakdown of FA complexes (Sharifi et al., 2016). Autophagosomes were discovered to disrupt these complexes by weakening cell-matrix connections and enhancing cell motility (Kenific et al., 2016).

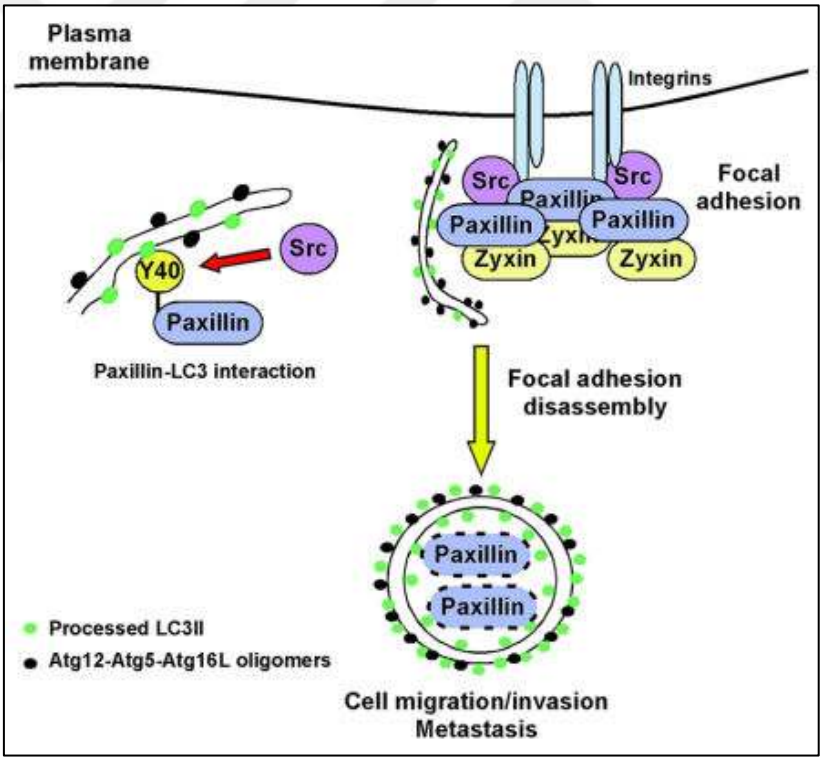

Figure 1.9 Effect of autophagy in FA dissambly by direct interaction of paxillin and LC3 in metastatic cells (Sharifi et al., 2016). (Permission is presented in Appendix G.)

Autophagy, a kind of cellular self-degradation, is important in regulating metastatic cancer pathways. Because it prevents the degradation of the pro-metastatic transcription factor Twist1, the autophagy adaptor p62 has been identified as a critical link between

autophagy and cancer (Qiang et al., 2014). Autophagy inhibition causes p62 accumulation, which stabilizes Twist1 and promotes tumor development and metastasis. Twist1 then suppresses autophagy via PI3K/Akt/mTOR signaling, resulting in a positive feedback loop (W. Xu et al., 2015). Furthermore, in malignant melanoma, p62 is expected to preserve the expression of pro-metastatic proteins by increasing their mRNA half-life. Also, it has been shown that inhibition of mTORC enhanced EMT in lung cancer and hepatocellular carcinoma cells, which points out improved metastatic ability (Kim et al., 2016).

Autophagy has an impact on metastasis in the secondary location as well. Tumor cells can lie dormant for a long time before reactivating and replicating at the metastatic location, contributing to tumor recurrence after treatment (Pranzini et al., 2022). Autophagy is important in the acquisition and maintenance of the latent phenotype and has the potential to turn dormant cells into malignant ones by maintaining energy balance during metabolic stress and managing ROS generation. Autophagy suppression can cause mitochondrial malfunction, ROS generation, and apoptotic cell death in quiescent tumor cells in some situations (Vera-Ramirez et al., 2018). However, there are contradicting results, and further research is needed to determine the real regulatory functions and targets of autophagy in dormant cancer cells.

The significance of autophagy in cancer is still being debated, with some studies suggesting that it promotes tumor growth while others suggest that it suppresses it. Understanding the mechanisms that enhance autophagic cell death while limiting its cytoprotective function is critical for creating effective autophagy-targeted cancer treatments.

1.2.3 Autophagy in Pediatric High-Grade Glioma

In recent years, it has been obvious that HGGs and DIPGs in children differ from HGGs in adults on a molecular level. Many of the molecularly targeted methods that have been adopted based on adult glioblastoma research have minimal application in the pediatric environment (Knizhnik et al., 2013). The main focus of autophagy research has been its role in causing chemoresistance. Studies have shown that the alkylating drug temozolomide (TMZ), commonly used as a first-line treatment for gliomas, induces an autophagic response in adult glioblastoma, which leads to apoptosis and senescence,

ultimately affecting its cytotoxic impact. The effect of TMZ was inhibited by the action of O6-methylguanine-DNA methyltransferase (MGMT) in adults and children. Therefore, methylation of MGMT promoter might be an epigenetic defense mechanism for tumor cells by modulating autophagy indirectly (Donson et al., 2007; Mazurek et al., 2020). Multiple miRNAs have been discovered as epigenetically regulating autophagy in both adult and pediatric high-grade gliomas (pHGGs).

In particular, the downregulation of ATG7 via miR-17 hindered autophagy in adult glioblastoma cells (Miele et al., 2014). When compared to adult cells, the combination of euphol, a tetracyclic triterpene alcohol, and TMZ (Temozolomide) displayed the highest cytotoxic effect in the context of pHGG. By promoting autophagic cell death, this combination limits migration and cell growth. Moreover, when euphol is combined with the autophagy inhibitor Bafilomycin A1, its cytotoxicity is increased. However, the underlying mechanism is still unknown (Howarth et al., 2019)

A study was carried out to examine the levels of autophagy-related proteins in glioma patients before and after particular pharmacological therapies. Interestingly, they discovered that after delivering a rigorous chemotherapy regimen containing many medicines, the levels of Beclin 1 and LC3 A/B proteins considerably raised. This finding suggests that autophagy is a critical chemoresistance mechanism in pediatric high-grade gliomas (pHGG), making it a possible target for overcoming drug resistance and improving tumor cell death, particularly in relapsed illnesses (Tsoli et al., 2018). The authors believe that targeting autophagy might take advantage of the entire pHGG cohort, regardless of subgroup, because autophagy is a common route in all pHGG subgroups. Autophagy-inhibiting methods with subgroup-specific therapy could be a potential technique for dealing with medication resistance in pHGG. The precise involvement of autophagy in pHGG is still being disputed (Gatto et al., 2021).

1.2.4 Autophagy and Cytoskeleton

Autophagosomes, double-membrane autophagic vesicles, are originated on omegasomes which are on ER-membrane. Expansion of autophagosomes is accompanied with several membrane sources such as plasma membrane, endosomes, ER, and Golgi aparatus (Hamasaki et al., 2013). At the end, biogenesis of autophagosomes is completed with the closure step following the lipidation of LC3 and insertion on the membrane of

autophagosomes (Fujita et al., 2008). Fusion of autophagic vesicles with lysosomes into the cytoplasm is occurred by the transportation of autophagosomes on actin and microtubule network (Aplin et al., 1992).

Actin is a globular, multifunctional protein found in eukaryotic cells that is essential for many cellular activities. It is an important component of the cytoskeleton, which is a dynamic network of filamentous proteins that offers structural support, sustains cell shape, and allows for intracellular transport. Actin is classified into two types: monomeric (G-actin) and filamentous (F-actin). Polymerization of G-actin molecules results in the formation of long, helical F-actin filaments (Mondal et al., 2021).

Firstly, it was shown that the process of initial steps in the formation of autophagosomes involves actin and RhoA activity, which are essential molecules for the cytoskeleton network (Aguilera et al., 2012). Also, in autophagosome maturation, myosinVI, actin-based protein, have an important function for selective autophagy. The binding of myosinVI to some aytophagy receptor proteins such as NDP52, TAX1BP, and OPTN(Reggiori et al., 2005; Tumbarello et al., 2012). On the other hand, it was demonstrated that autophagosome formation was interrupted in ATG7-deleted mouse epithelial cells, and the expression of proteins related to regulation of the actin dynamic was diminished. The dramatic change in cytoskeleton of MEF cells is displayed by phalloidin staining (Zhuo et al., 2013).

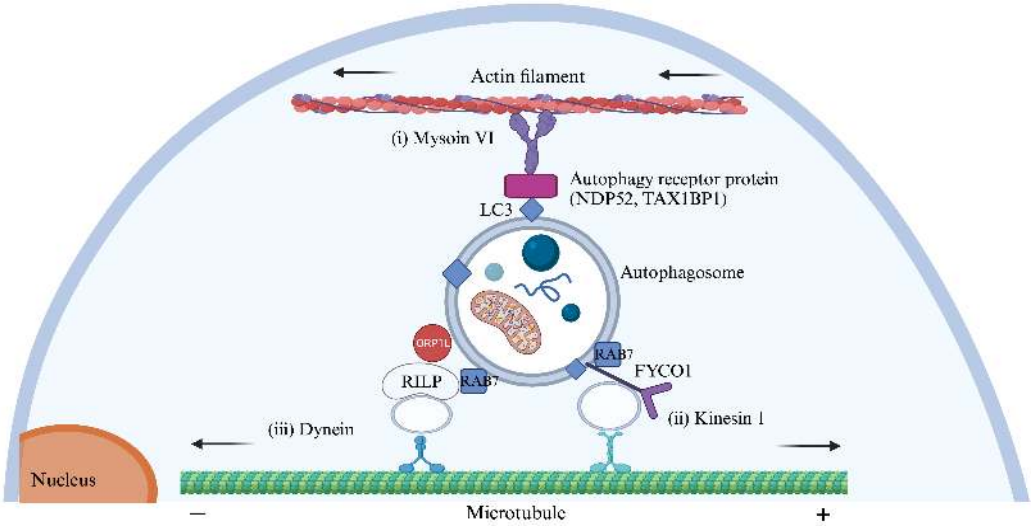

Figure 1.10 Autophagosome transportation via cytoskeleton components. (i) Interaction of myosinVI with autophagosome via autophagy receptor (NDP52, OPTN, TAX1BP1). (ii) Autophagosome trafficking is also performed by motor proteins (Kinesin) on+ end of microtubule. FYCO1 is a RAB7-effector protein intervening the

binding of kinesin and autophagosomes. (iii) Dynein, another motor protein, facilitate transportation of autophagosomes along microtubules toward the – end of the cell (cell's center) (Søreng et al., 2018)

Microtubules are also another component of cytoskeleton. They have various role in vesicle transportation, chromosome segregation and nucleus localization. Microtubules have a highly dynamic and polar structure. α-tubulin unit is extended to the inner side of the cell facing the nucleus (- end), whereas ß-tubulins are toward to cellular membrane, forming the + end of the cell. The action of kinesin and dynein proteins facilitates the transportation of the organelles and the cargo (Desai & Mitchison, 1997; Hunt & Stephens, 2011). Autophagosomes formed somewhere in the cytoplasm must be transported to the area close to lysosomes for fusion. Dependency on dynein protein for transportation of autophagosome to proximity to lysosomes and autophagic degradation of the protein aggregates were observed in a study (Kimura et al., 2008; Ravikumar et al., 2005). Moreover, nocodazole treatments, a chemical leading to microtubule depolymerization, causes retardation of autophagosome-lysosome fusion and decreases LC3-lysosome colocalization (Jahreiss et al., 2008; Köchl et al., 2006).

The RAB7 effector protein RILP is essential for autophagosome transport within cells by attaching dynein-dynactin motor complexes to RAB7-containing late endosomes, causing them to migrate toward the cell's perinuclear region along microtubules(Jordens et al., 2001). The recruitment of RILP to RAB7-positive autophagic vesicles during autophagy induction indicates its role in autophagy. Overexpression of RILP causes an accumulation of autophagosomes towards the nucleus, whereas a mutant RILP that is unable to recruit dynein inhibits minus-end directed autophagosome trafficking (Wijdeven et al., 2016). On the other hand, the kinesin family of motor proteins, which is responsible for plus-end directed microtubule transport, regulates autophagosome trafficking and lysosome placement during autophagy (Korolchuk et al., 2011).

We detected an important interaction of ATG5 protein with Ste20-like kinase in starvation condition. This examination is presented in section 3.1. When we make further investigations about the protein, we realized that it has essential functions in neurodevelopment. Also, the expression of the kinase protein is observed brain tissues and adult and pediatric glioblastoma. Therefore, we planned various experiments to investigate the functions of this serine/threonine kinase.

1.3 STE20-LIKE KINASE

Ste20-like kinase (SLK) protein is an important member of the serine/threonine protein kinase family. It is essential for several biological activities, including cell division, proliferation, apoptosis, and differentiation. By transferring phosphate groups to target proteins and regulating their activity, the SLK protein functions as a signaling molecule. The SLK protein has been linked to several human diseases, including cancer, neurological diseases, and cardiovascular ailments. Its activity is strictly regulated to ensure optimal cellular function. Uncovering the Ste20-like kinase protein's therapeutic potential and creating targeted therapies for different pathological disorders depend on an understanding of the molecular workings and functional activities of the protein (Garland et al., 2021).

1.3.1 Structure and Regulation of SLK

SLK expression was determined and studied in many species, including pigs, trematodes, mice, and humans (Hipfner & Cohen, 2003) (Itoh et al., 1997) (Ellinger-Ziegelbauer et al., 2000). It is well investigated in yeasts as a mating response upstream regulator of the mitogen-activated protein kinase (MAPK) cascade. Several families of mammalian Ste20-like kinases were discovered after the first yeast investigations. According to the domains and primary sequence, they have separated into the p21-activated kinase (PAKs) and germinal center kinase (GCKs) families. In the PAK family, the kinase domain of the protein is in the C terminus, while in the GCK family N terminus of the protein covers the kinase domain. Lymphocyte-oriented kinase (LOK) is the closest relative of SLK and classified into subgroup V of the GCK family (Dan et al., 2001). In the Figure 1.4, a tree diagram showing subgroups of Ste20 protein kinase family.

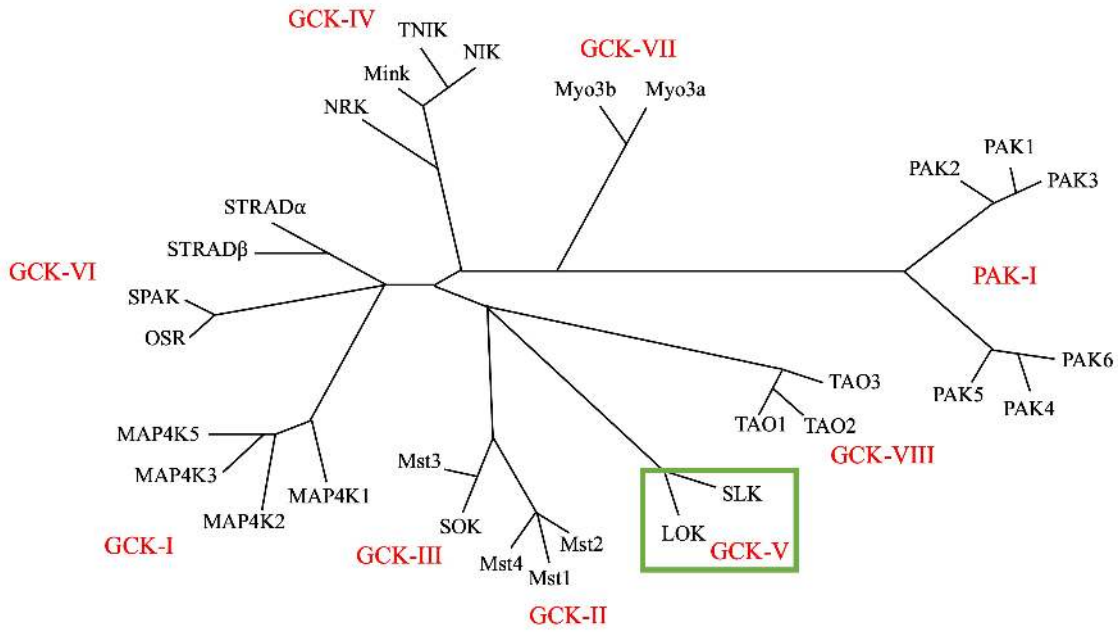

Figure 1.11 Taxonomic relationship of SLK (Gagnon & Delpire, 2012)

SLK protein has three domains: the kinase domain, an unstructured coiled-coil region, and the AT1-46/LOK homology (ATH) domain. The kinase domain is presented between amino acids 1-338 in the N-term, the region between amino acids 339-788 confines the coiled-coil part, and in the C-term of protein, the ATH domain consists of amino acids 789-1202 (Sabourin et al., 2000). In the kinase region, the protein exhibits 74% similarity with LOK and a signature sequence for Ste20 kinase, TPYWMAPE, located at position amino acid 193.

Likely many other kinase proteins, SLK is known to undergo autophosphorylation at residues T183 and S189 (Pike et al., 2008a). To enable substrate binding, autophosphorylation causes a conformational shift in the activation region. Important post-translational changes for SLK activation include these phosphorylation processes (Cybulsky et al., 2007). The amount of SLK kinase activity is considerably reduced by mutations at these phosphorylation sites (Luhovy et al., 2012a). Since both residues are not fully phosphorylated at the same time in SLK crystals, autophosphorylation happens in a primary and secondary manner successively. T183 is highly conserved across species and members of the same family, highlighting its significance in activating SLK. SLK activation, also known as activation segment exchange, involves dimer formation and trans-autophosphorylation (Pike et al., 2008a). The C-terminal coiled-coil region promotes dimerization, which enables the catalytic core of SLK to approach the activation

section on the other molecule for phosphorylation (Delarosa et al., 2011). Like other GCK-related kinases, deletion of the C-terminal region of SLK dramatically increases its kinase activity (Sabourin et al., 2000). Current research aims to clarify the precise mechanism of SLK activation. In addition, 56% similarity is observed between C terminus of SLK and ATH domain of LOK protein (Sabourin & Rudnicki, 1999)

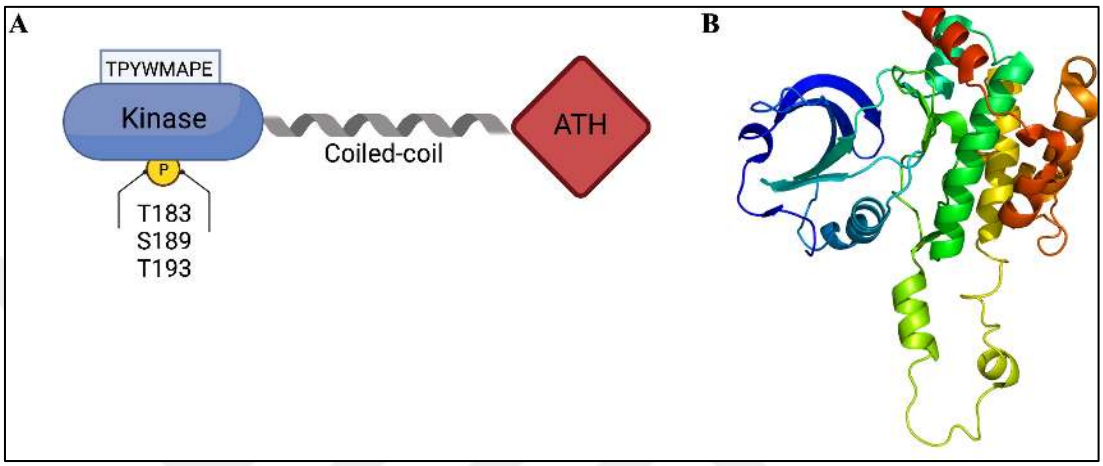

Figure 1.12 Structure of SLK protein. (A) Schematic representation of SLK domains. Kinase domain is located at the N terminus and ATH domain presents at the C terminus. T183, S189, and T193 residues are autophosphorylation sites. 'TPYWMAPE' is recognition site of Ste20 kinase protein family. Figure was constructed with BioRender online tool. (B) 3D structure of SLK protein. Figure was obtained from Uniprot database (*Https://Www.Uniprot.Org/Uniprotkb/Q9H2G2/Entry#structure*, n.d.).

1.3.2 SLK Interacting Proteins

STE20-like kinases interact with a wide range of proteins, creating complexes and controlling several cellular processes. According to STRING protein interaction network, interacting proteins with SLK is shown in Figure 1.6. Among these proteins ezrin, radixin and moesin proteins (ERM) is showed the highest 5 strong interaction which are key regulators of the actin cytoskeleton and cell membrane interactions (STRING Interaction Network, n.d.). Cellular functions like cell adhesion, migration, and cytoskeletal structure are modulated by the interaction between SLK and ERM proteins. It has been demonstrated that SLK phosphorylates ERM proteins, mainly moesin, which activates them and subsequently controls the dynamics of the actin cytoskeleton (Hipfner et al., 2004). The control of cell shape, membrane protrusions, and cellular responses to external

signals are all facilitated by this phosphorylation-dependent interaction between the proteins SLK and ERM (Machicoane, de Frutos, Fink, Rocancourt, Lombardi, Gare, et al., 2014). The precise molecular processes and functional effects of the protein interaction between SLK and ERM in various cellular situations still need to be clarified through additional research.

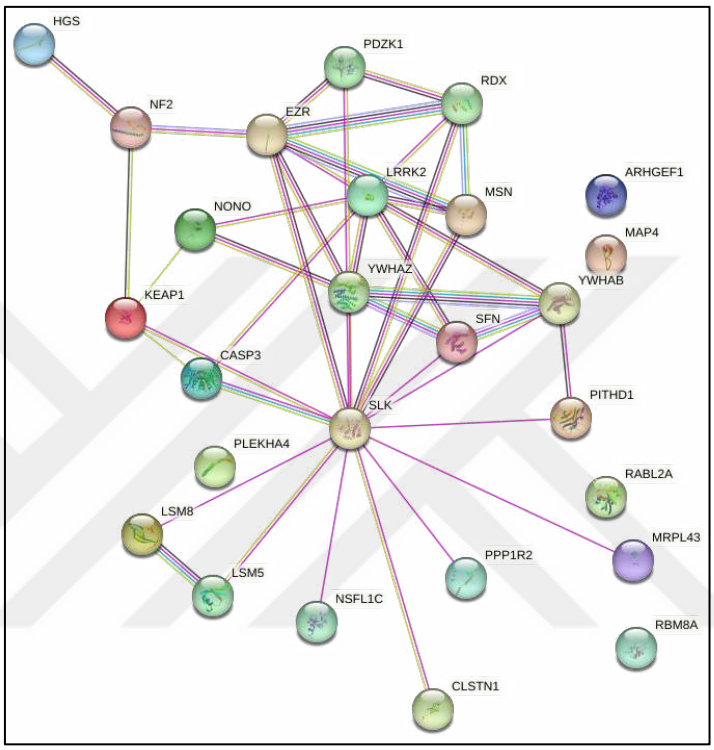

Figure 1.13 Interacting Proteins for SLK gene (STRING Interaction Network, n.d.).

It has been demonstrated that SLK (STE20-like kinase) phosphorylates various proteins, playing a role in the control of numerous physiological processes. Table 1.1 represents a few examples of proteins that SLK has reportedly been shown to phosphorylate.

Table 1-1 Interactors of SLK. This table only shows the experimentally proved interactions.

SLK-Interacting Protein	Cell Line	Stimulus	Reference
Trp	COS1 C2C12	No stimulus	(Jaberi et al., 2015)
α-actinin-4	COS1 C2C12	No stimulus	(Jaberi et al., 2015)
LDB1/2	MEF	No stimulus	(Storbeck, Wagner, O'Reilly, et al., 2009)
LMO4	MEF3T3	Scratch wounding	(Baron et al., 2015a)

Table 1-2 Phosphorylated protein by SLK based on literature review.

Target	Cell line	Stimulus	Reference
Polo-like kinase1 (Plk1) (Thr210)	HASM (Human airway smooth muscle)	Knockdown of SLK + Acetylcholin treatment	(J. Li et al., 2016)
Paxillin (Ser250)	MEF3T3, HEK293T	SLK overexpression and K63R mutant SLK expression	(Quizi et al., 2013a)
ASK1 (n.d.)	COS Monkey kidney fibroblast-like cell	Overexpression of SLK and ASK1	(Hao et al., 2006)
RhoA (Ser188)	Rat aortic smooth muscle cells	Angiotensin II	(Guilluy et al., 2008)
ERM prot (Ezrin at T567, Radixin at T564, Moesin at T558)	HeLa	Knockdown of SLK	(Machicoane, de Frutos, Fink, Rocancourt, Lombardi, Gare, et al., 2014)
P38	GEC	Overexpression of SLK	(Luhovy et al., 2012b)
JNK	GEC	Overexpression of SLK	(Luhovy et al., 2012b)
Dynactin (P150)	Green monkey kidney Vero epithelia-like cells	Centrosomal localization	(Zhapparova et al., 2013a)

1.3.3 Functional Roles of SLK Protein in Various Cellular Processes

SLK is a serine/threonine protein kinase that participates in signaling pathways that regulate cell motility, cytoskeleton organization, cell adhesion, and cell survival. Understanding SLK's various roles offers great potential for deciphering the intricacies of cellular activities and their implications in health and disease.

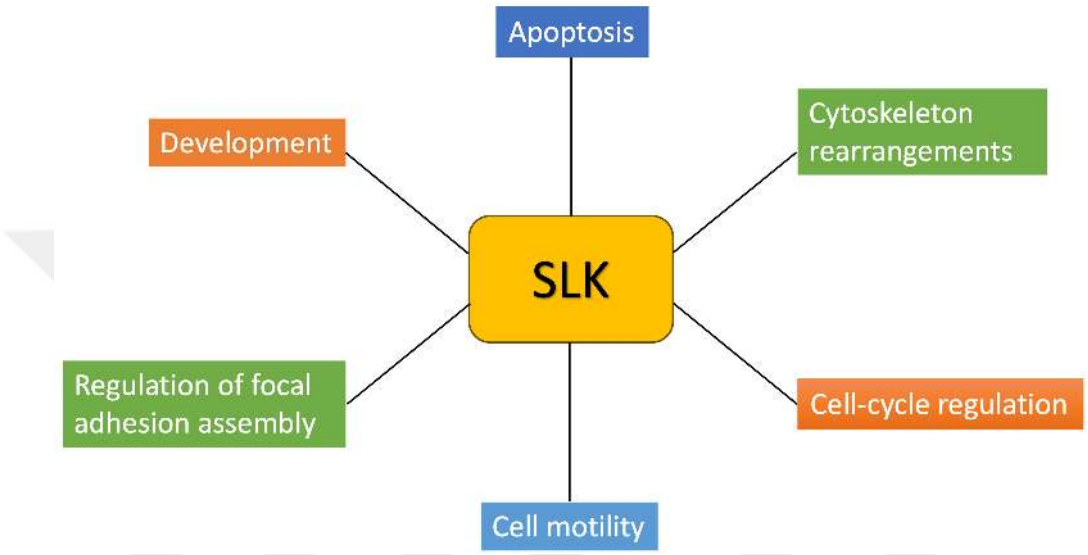

Figure 1.14 SLK have various functions in many cellular processes.

1.3.3.1 Apoptosis

The SLK protein has become a vital component of the complex apoptosis machinery, acting as a regulatory control over essential signaling pathways and cellular functions that result in programmed cell death. Firstly, it is shown that SLK overexpression in C2C12 (myoblast) and Swiss 3T3 (mouse embryo fibroblast) induces apoptosis with JNK activation. Moreover, the requirement of the kinase activity of SLK was indicated by using kinase-dead mutant (K63R) of SLK protein. Cells transfected with K63R mutant SLK were negative for apoptotic markers (Sabourin & Rudnicki, 1999). Also, in another study, it was shown that smSLK, SLK homolog in *Schistosoma mansoni*, could also activate JNK1, suggesting that it may help control the activation of the MAPK cascade during host-parasite interactions (Yan et al., 2007). By transfecting cells with SLK1-373, it was demonstrated that unregulated kinase activity of SLK strongly induces apoptosis. Presence of kinase regulating ATH domain causes late apoptosis and leads to actin

disorganization. In addition, treatment of cells with apoptotic inducers results in cleavage of SLK after apoptotic induction (Sabourin et al., 2000).

In models of renal damage, the function of SLK (STE20-like kinase) in apoptosis has been studied. This research found that renal damage and acute renal failure resulted in increased SLK expression and activity (Cybulsky et al., 2004). Tubular epithelial cells were the main site of SLK overexpression. Under anoxic conditions, SLK overexpression enhanced cell death by promoting apoptosis in renal epithelial cells . It was discovered that stress-activated kinases ASK1 and p38, as well as the tumor suppressor protein p53, were implicated in SLK-mediated cell death(Hao et al., 2006 . SLK activation caused apoptotic reactions like the release of cytochrome c and the activation of caspases while impairing the endoplasmic reticulum stress response (Hao et al., 2006). Additionally, in glomerular epithelial cells, SLK overexpression induced JNK1-dependent death (Cybulsky et al., 2009). An elevation in heat-shock factor 1 (HSF1) transcriptional activity mediated by Plk was observed upon cell death induced by SLK (Cybulsky et al., 2016). These findings imply that SLK is involved in the dysregulation of mitotic elements, such as ERM proteins and PLK1, and stress responses that result in cell death, as well as their role in triggering apoptosis in response to renal damage (Garland et al., 2021).

Apoptosis-dependent physiological processes, such as those that occur during development and following damage, may be significantly influenced by SLK, and therapeutic targeting of SLK may be advantageous for some renal and muscle diseases. For instance, SLK upregulation was monitored in mouse models possessing muscular dystrophy. Leukocyte infiltration was decreased while myogenin and utrophin expression, both indicators of muscle differentiation, were elevated in mdx mice with muscle-specific deletion of SLK (Pryce et al., 2017). In newly produced myofibers of dystrophic muscles, SLK is markedly elevated. Furthermore, myogenin (MyoG) expression and the percentage of embryonic myosin heavy chain (MHC) positive myofibers increased, and p38 MAPK is activated in mdx animals with deleted SLK gene in a skeletal muscle-specific manner (Pryce et al., 2021).

1.3.3.2 Cell-Cycle

The SLK (STE20-like kinase) protein is a significant player in the complex control of the cell cycle, orchestrating essential signaling pathways and activities required for

healthy cell division. The function of SLK in cellular proliferation was first shown in the regulation of Plk1 protein during mitotic cycle (Ellinger-Ziegelbauer et al., n.d.). Research in Drosophila showed that SLK overexpression promotes proliferation and apoptosis. Excessive tissue growth was observed upon inhibition of apoptosis, suggesting that SLK-induced proliferation can be compensated by programmed cell death (Hipfner & Cohen, 2003). Inhibiting cell proliferation through the expression of kinase-inactive mutants or SLK small interfering RNAs led to an accumulation of dormant cells that were prompted to resume the cell cycle again in the G2 phase. This study also shows the regulatory role of SLK by pointing out its colocalization with alpha tubulin molecules on mitotic spindles during mitotic stage (O'Reilly et al., 2005).

Furthermore, it has been discovered that a lack of SLK results in disordered microtubules which leads to aberrant centrosome anchoring, scattered spindles, and defective microtubule organization (Burakov et al., 2008, Carreno et al., 2008). p150 subunit of dynactin protein is phosphorylated by SLK and facilitated for targeting centrosome (Zhapparova et al., 2013b). Recently, it was discovered that in Drosophila S2 cells, a gradual enrichment of SLK was seen near the cell cortex as cells got closer to the start of metaphase. According to one theory, this cortical link is crucial for the activation of ERM proteins, the cytoskeletal dynamics (paxillin phosphorylation), and the FA breakdown required for cell shape changes and cytokinesis and mitosis (De Jamblinne et al., 2020).

1.3.3.3 Development

SLK preferentially expresses in neural and muscular lineages during embryonic development despite being widely expressed in adult tissues of mice and the large number of cell lines (Sabourin & Rudnicki, 1999, Y.-H. Zhang et al., 2002). Through various findings, has shown that SLK protein is involved in how muscles work. When muscle regenerates in vivo, it turns into active form during myoblast development and is turned on in active satellite cells (Storbeck et al., 2004). It is interesting to note that transgenic mice that express a kinase-inactive form of SLK exhibit poor muscle growth, small litter numbers, and exhaustion. Despite the reduced kinase activity in the muscles of these transgenic animals, muscle regeneration is improved in vivo, demonstrating that SLK plays different roles in developing myoblasts and mature muscles (Storbeck et al., 2013). In one of the studies, the modification was performed on exon 10 of the SLK gene that,

diminishes the SLK activity. Embryos that are homozygous for the altered gene could not survive and displayed various anomalies in the developmental stage and blood vessel formation (Al-Zahrani et al., 2013). The deletion of SLK from the Myf5 gene in mice originally produced muscles that appeared to be normal. However, mature mice displayed a gradual myopathy with centrally established nuclei in myofibers, decreased force production, and elevated p38 MAPK activation. SLK appears to play a crucial role in preserving muscle integrity, as evidenced by the fact that muscle specific SLK deletion resulted in delayed muscle regeneration and decreased myofiber stability and function (Pryce et al., 2017). Recent research has shown that targeted deletion of SLK in mouse podocytes causes albuminuria and cellular structural alterations that point to compromised kidney function. This deletion also caused podocyte loss and decreased podocyte marker expression, highlighting the critical function of SLK in preserving podocyte integrity (Cybulsky et al., 2018).

1.3.3.4 Cancer

The activity of SLK was pointed out in the invasion of NMuMG cells (epithelial cells from mouse mammary glands as a novel mediator of cell migration downstream of Neu. Neu stimulates MEK-, PI3K-, and PLCg-dependent SLK activation through two of its autophosphorylation sites, which is necessary to disrupt focal adhesions (FA) during Neu-mediated cell motility (Roovers et al., 2009). Recently, it has been shown that as the cancer level increases, the protein expression level is also elevated in breast cancer cells. In contrast to in vitro cell culture model, deletion of SLK in mammary gland cause higher tumor formation and a reduction in overall survival. Expectedly, upregulation of Sox10, a triple-negative breast cancer marker, was detected in SLK-depleted tumors. Furthermore, activated proteins from Akt family and phosphoinositide-dependent kinase-1 (PDK1) were shown in this study (Al-Zahrani et al., 2020).

The function of SLK was also shown in epithelial-mesenchymal transition (EMT) process. Repression in SLK expression resulted in a significant decrease in migration and invasion capability of NMuMG cells especially upon transforming growth factor beta-1 (TGFß-1). Also, EMT markers including Snai1, vimentin, and E-cadherin, were reduced upon TGFß-1 treatment in SLK depleted cell culture. Altogether the study suggests that TGFß-1 induced EMT process requires SLK protein in a kinase activity-independent manner (Conway et al., 2017). Despite the kinase activity of SLK, a disruption on

interaction with LIM-domain binding 1 (Ldb1) and with LIM-domain binding 2 (Ldb2) caused augmented migration and higher EMT in vivo and in vitro (Storbeck, Wagner, O'reilly, et al., 2009, Ahmed et al., 2018). Scientists suggest that the fluctuations between in vitro and in vivo studies are related to the dissimilarity of microenvironments.

Last and the most importantly for this study, SLK upregulation was confirmed in glioma samples compared to normal brain tissue and the expression is increasing with the higher malignancy degree of the tumor. A negative correlation with E-Cadherin was clear with enhancing malignancy. Suppression of SLK expression SLK elevated E-Cadherin level while decreased Snai1 and Vimentin expression in U87 MG glioma cell lines. When we consider that Snai1 inhibits the E-Cadherin, this result is expected. Furthermore, wound healing and transwell migration assay demonstrated the migration capability of glioma cells upon SLK repression. This study clearly suggests that SLK is involved in the development of gliomas and may represent a novel glioma prognostic marker (K. Wang et al., 2018).

1.3.3.5 Cytoskeleton Organization and Cell Motility

The association of SLK protein with cytoskeleton components and cell migration was observed in various studies. It is well known that RhoA activation facilitates the formation of focal adhesion (FA) complexes and stress fibers (Nobes & Hall, 1995). RhoA has been identified to interact with SLK, which affects the activity of RhoA in many cell types. SLK-mediated phosphorylation of RhoA in vascular smooth muscle cells prevents cell contraction during vasodilation (Guilluy et al., 2008). However, renal epithelial cells did not exhibit similar modulation, indicating tissue-specific effects. It has also been demonstrated that SLK interacts with RhoA which is active, possibly increasing its kinase activity (Bagci et al., 2020). RhoA-SLK interaction observed in overexpression models indicates the kinase activity of SLK on ERM proteins. Additionally, SLK controls Plk1, a cell cycle regulator that affects smooth muscle contraction. Also in this study, SLK is recognized as a significant upstream regulator of the smooth muscle contractile apparatus and works via Plk1 (J. Li et al., 2016). Focused adhesion kinase (FAK) is activated when fibroblast monolayers are scratched, which causes FA turnover when cells move into the wound. Activated FAK-Src complex was recruited for migration, FA turnover, and cytoskeletal remodelling following phosphorylation at tyrosine residue 397 (pY397) (Etienne-Manneville & Hall, 2001) (Mitra et al., 2005). Rapid localization of

SLK near the leading edge of migrating fibroblasts increases in its kinase activity, which is c-Src and MEK1 dependent(Wagner et al., 2008). In order to stimulate SLK's kinase activity, LMO4, a transcriptional regulator essential for embryonic development, interacts with SLK. LMO4 deletion prevents SLK activation, cell migration, and recruitment (Baron et al., 2015b). By affecting LMO4 expression, the kinases Src, Yes, and Fyn control SLK activity, while v-Src indirectly suppresses SLK activity through casein kinase II (CK2) (Chaar et al., 2006). These findings highlight the intricate regulatory mechanisms of SLK in cell migration and FA turnover during wound healing.

Nocodazole interferes with the dynamics of microtubule organization by binding to beta-tubulin and FA turnover. Changes in phosphorylated FAK level at residue Y397 and FA turnover can reverse the nocodazole affect and provide development of microtubules (Bershadsky et al., 1996). It is shown that SLK is essential for FA turnover and migration because nocodazole washout in fibroblasts expressing a kinase-dead mutant SLK or SLK-targeted siRNAs causes delayed FA turnover, larger adhesions, and elevated levels of FAK pY397 which is indication to hindered cell motility. No increase in kinase activity of SLK in FAK depleted culture may propose the FAK-dependent activation of SLK which is necessary for FA turnover with the induction of FAK-Src complex (Wagner et al., 2008).

Importantly, it was demonstrated that SLK causes the dismantlement of FA in murine fibroblast by phosphorylating the serine residue of Paxillin, an adapter for FA molecules, at position 250. Weakened cellular migration and FA turnover were observed, arising from the presence of stable FAK pY397 upon S250a mutant paxillin. Again, it can be suggested that SLK might be a component of a complex linked to microtubules that specifically targets FAs for disintegration (Quizi et al., 2013b).

Several studies conducted with Drosophila revealed a function of SLK on ERM proteins. ERM proteins are mainly responsible for binding to actin cytoskeleton to cellular membrane and they can be activated by phosphorylation of the conserved threonine residue (Tsukita et al., 1997). Phosphorylation of ERM protein directly by SLK and LOK was also displayed in human cells. Reduction in this phosphorylation upon deletion of SLK caused microvilli loss. In Drosophila, the tumor suppressor Merlin is phosphorylated by Slik, which results in its activation and localization to the apical surface, favoring cell proliferation (Hughes & Fehon, 2006a). In addition, SLK can directly activate ERM

proteins in mammalian cells, contributing to the direction of the mitotic spindle by encouraging the interaction of the essential components of cell polarization, LGN and NuMA (Machicoane, de Frutos, Fink, Rocancourt, Lombardi, Garel, et al., 2014a).

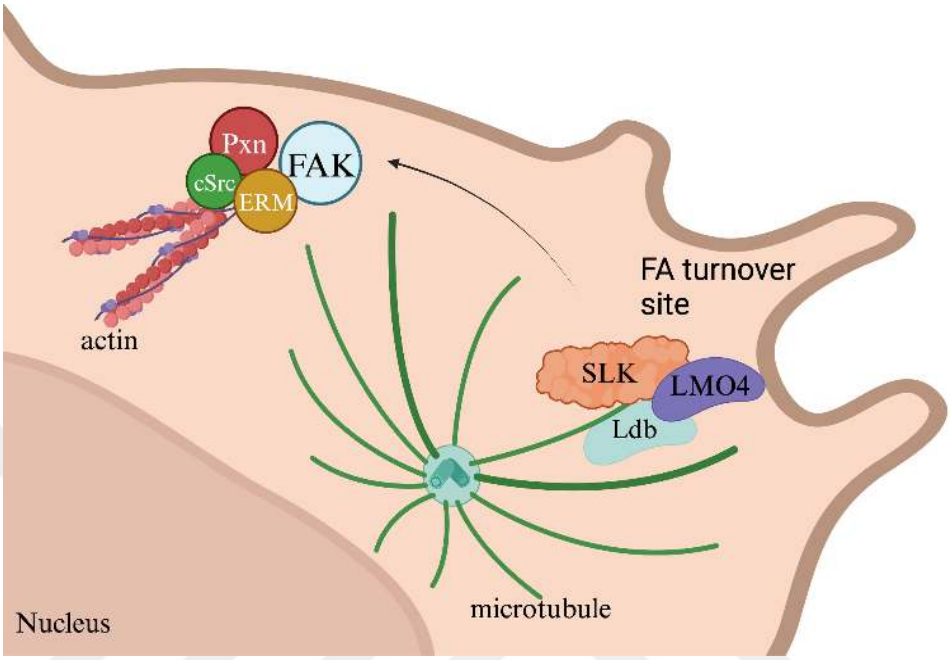

Figure 1.15 Representation of remodeling of SLK and cytoskeleton in migrating fibroblast cells. SLK is activated and driven to focal adhesions (FAs) in together with microtubules. FAK, c-Src activity, and the LMO4 adapter protein are all necessary for this. FA disintegration is triggered by direct phosphorylation of the adaptor protein paxillin (Pxn) by SLK. Once again assembled, FAs can produce the contractile forces essential for cell migration by fillipodial elongation and cytoskeletal modification. (Garland et al., 2021)

1.3.4 ERM Proteins

Ezrin, radixin, and moesin proteins together form the ERM molecules. They are among the specialized membrane domains that connect cell membrane proteins and the cytoskeleton. The expression of these molecules is based on the tissue and developmental stage in which they reside. When we look at the structure, we can see a FERM domain in the N terminus that mediate the association to membrane and in the C terminus they possess a C-terminal ERM-association domain (C-ERMAD) that binding the FERM domain to filamentous actin (F-actin). In dormant state, actin binding site was masked

through binding of FERM and C-ERMAD region of the protein. When F-actin binding region on C-ERMAD is released, the protein is turned to active state (Ivetic & Ridley, 2004).

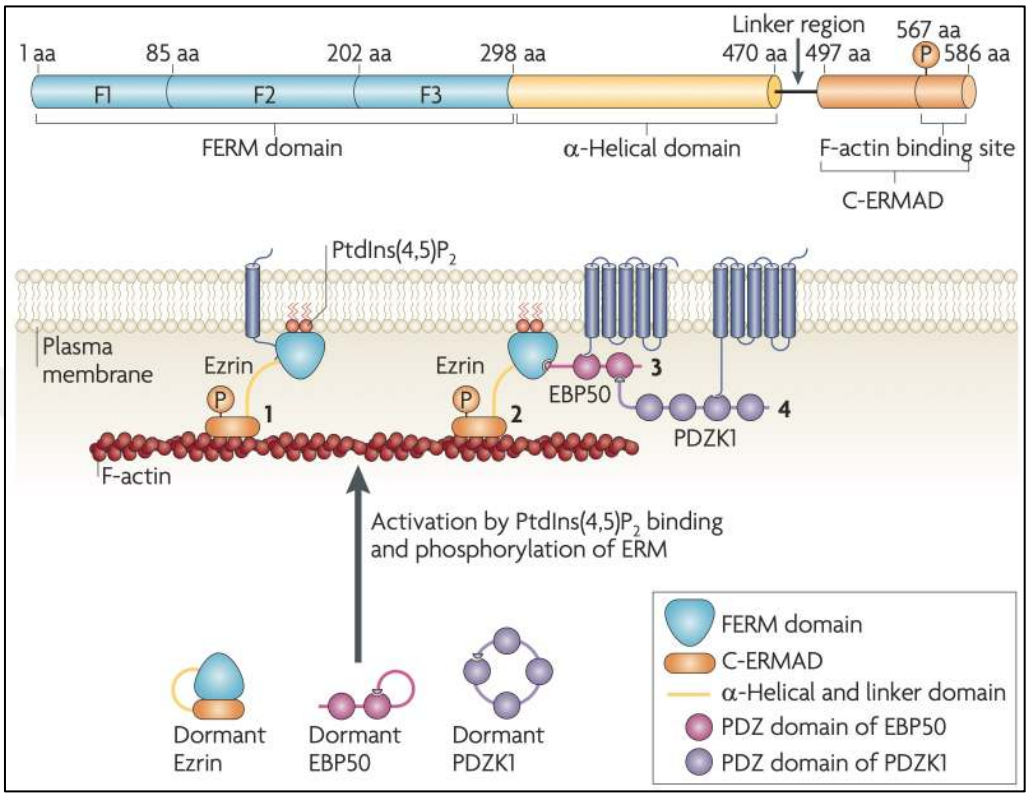

Figure 1.16 Common structure of ERM proteins on the upper part. Representation of activation model of ezrin on the lower side (Fehon et al., 2010). License number: 5618721082425

The finding that moesin is phosphorylated on Thr558 during platelet activation led to an initial understanding of how ERMs are regulated (Nakamura et al., 1995). Subsequent research revealed that the corresponding residues in ezrin (Thr576) and radixin (Thr564) also cause activation (Fievet et al., 2004). The conserved Thr residue is made more accessible for phosphorylation by several kinases, such as Rho kinase, protein kinase Cα (PKCα), NF-inducing kinase (NIF), MST4, and lymphocyte-oriented kinase (LOK), by the recruitment of ERMs to membrane regions rich in phosphatidylinositol 4,5-bisphosphate (PIP_2), according to a two-step activation model (Matsui et al., 1998). Subsequently, it was shown that SLK is also responsible for ERM phosphorylation (Hughes & Fehon, 2006b). It was also demonstrated that ezrin Thr235, which is located on the FERM-C-ERMAD interface next to Thr567, can be phosphorylated by the cyclin-

dependent kinase 5 (CDK5). There have been diverse tyrosine kinases compromising EGFR can phosphorylate ezrin on various residues (Krieg & Hunter, 1992; Yang & Hinds, 2003).

ERMs are perfectly situated to control the emergence of specialized membrane domains since they have the capacity to mediate several interactions at the cell cortex. Because they connect receptors and downstream signaling components together, such domains are crucial for signal transduction. Direct proof that RhoA and Hedgehog signaling are regulated by ERM has been presented by genetic research in the D. melanogaster species. ERMs are likely involved in other signaling pathways as well, though, given that they can interact with transmembrane receptors (Fehon et al., 2010).

- **Function of ERM proteins in metastasis**

Ezrin is thought to play a part in encouraging tumor spread, and metastatic tumors frequently exhibit elevated levels of the protein's expression and activity, particularly rhabdomyosarcomas and osteosarcomas in humans and mice (Hunter, 2004). According to recent research, ezrin is dynamically controlled at various stages of osteosarcoma metastasis (Ren et al., 2009). It is downregulated during the development and survival of metastatic nodules but elevated early during the advancement of existing metastases, indicating its involvement in tumor invasion and metastatic expansion. Additionally, ezrin interacts with a number of transmembrane proteins that have been independently linked to tumor metastasis, including CD44, podoplanin, and podocalyxin (Wicki et al., 2006). When CD44 and ezrin bind, CD44 may act as a co-receptor for certain receptor Tyrosine kinases, facilitating cell motility and tumor invasion (Bourguignon, 2008).

1.3.5 Paxillin Family Proteins

Paxillin, is one of the focal adhesion proteins binding integrin transmembrane proteins to ECM and providing signal transduction between extra and intracellular environment. Signal transduction by paxillin is related to arrangement of actin cytoskeleton and cell migration. Paxillin is present together with vinculin and interacts with the cytoskeleton (Turner, 2000). Paxillin family proteins have a structure containing helical leucine, short amphipathic, aspartate rich LD motifs at the N terminal and four different conserved LIM domains forming double-zinc-finger structure at the C terminal.

LIM-domain containing proteins have essential functions in cytoskeletal organization. N terminal is associated with multiple protein interactions while C terminal part is related to targeting of paxillin to focal adhesion molecules. Paxillin is widely expressed, but Hic-5 protein is found largely in smooth muscle tissues, including the vasculature. Leupaxin expression is primarily found in leukocytes, but it has also been found in smooth muscle tissues and several cancers (Yuminamochi et al., 2003).

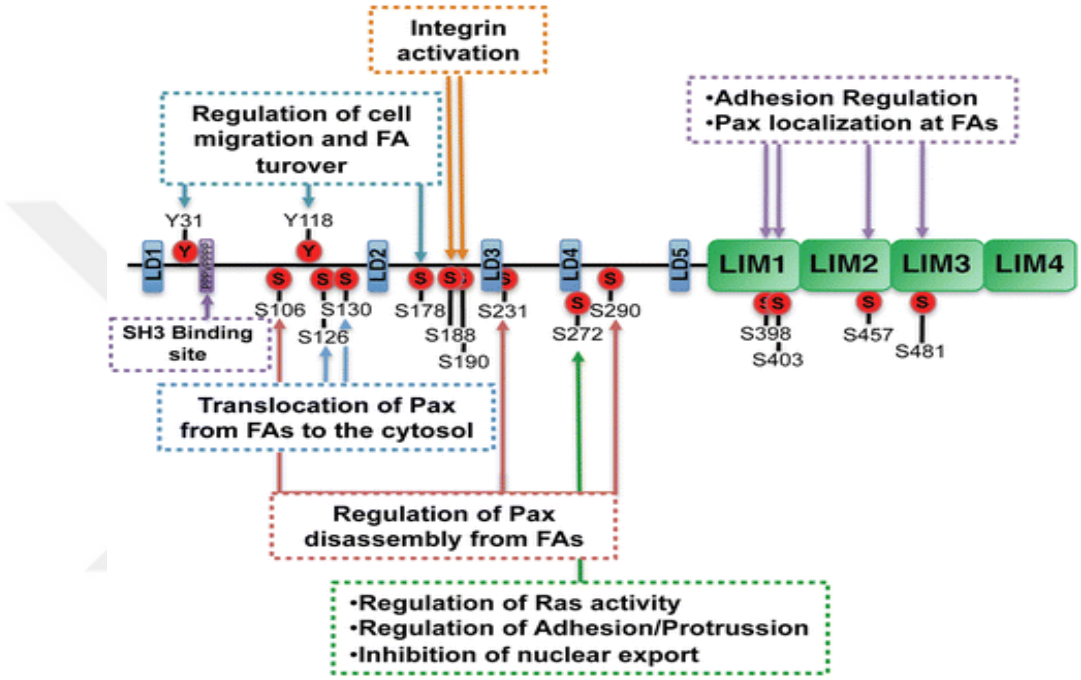

Figure 1.17 Structural and functional organization of paxillin. It is encoded by 591 amino acids. Protein having SH3-domain can interact at the N terminal. LD domains are also important for relation with vinculin, FAK and Crk tyrosine kinases of Src family, and talin. LDLLXXLL motif is important for FAK connection and conserved evolutionary. The C-terminal of FAK possesses a ~150 amino acid region called as "focal adhesion targeting (FAT) region" for binding sequences for paxillin and talin. LIM domais presenting at the C end have the roles in focal adhesion targeting and association with cellular membrane (López-Colomé et al., 2017). (Permission is presented in Appendix G.)

Cytokines, cellular adhesion, and some growth factors lead to phosphorylation of paxillin protein (López-Colomé et al., 2017). Integrin interaction to the ECM stimulates the phosphorylation of paxillin, a protein involved in the formation of FAs. In response to adhesion or growth factor stimulation, tyrosine phosphorylation of paxillin generates a

scaffold for the recruitment and activation of tyrosine kinases such as FAK and Src. This causes external signals to be converted into cellular responses mediated by mitogen-activated protein kinases (MAPKs). Furthermore, tyrosine phosphorylation of paxillin by FAK has been proposed to facilitate the cytoskeleton remodeling required for cell motility (BELLIS et al., 1997; Zaidel-Bar et al., 2007).

Paxillin serine phosphorylation occurs during cell migration and affects paxillin turnover, including proteasome destruction(Abou Zeid et al., 2006a). Paxillin is phosphorylated at various serine/threonine sites by various kinases, influencing its location, cell adhesion, and cytoskeletal rearrangement. For example, it was shown that phosphorylation at Ser178 residue by JNK is necessary for migration capability of cells (Huang et al., 2008) . Some serine phosphorylation processes have been linked to cell mobility and migration regulation. Specifically, serine 250 residue is phosphorylated by SLK protein, and it is necessary for cell migration and focal adhesion turnover (Quizi et al., 2013b).

In conclusion, both tyrosine and serine phosphorylation of paxillin are important in controlling cell adhesion, migration, and cytoskeletal dynamics, with various phosphorylation events influencing different aspects of cellular responses and functions.

- **Paxillin in Cancer**

Paxillin is a protein that plays a role in cell motility, specifically in cancer formation and metastasis. It was discovered in cancer tissues and metastatic cancer cells with high levels of phosphorylated paxillin expression during the epithelial-mesenchymal transition (Deakin et al., 2012). Gain-of-function mutations in paxillin have been linked to the advancement of cancers such as breast, lung, prostate, melanoma, and colorectal cancer (Kanteti et al., 2016).

Overexpression of paxillin has been associated to tumor aggressiveness and poor survival in glioblastoma multiforme (GBM). Authors also evaluated the paxillin protein as a prognostic biomarker in glioblastoma patients (Sun et al., 2017). Paxillin mutations, particularly the A127T mutation, have been found in lung cancer tissues and cell lines to increase tumor development and invasion. Paxillin, which lacks the LD1 domain, appears to inhibit cancer cell migration (Jagadeeswaran et al., 2008; Tumbarello et al., 2005).

Maximum tyrosine phosphorylation of paxillin by Src and FAK is essential for metastatic cells to initiate anchorage-independent signal transduction and proliferation. Paxillin regulates directional migration by integrating physical and chemical motility inputs. Phosphorylation of certain sites in paxillin is thought to be a sign of metastasis (Sero et al., 2011).

Paxillin promotes breast cancer cell migration via estrogen signaling, and retinoic acid has been demonstrated to disrupt this pathway and prevent breast cancer cell migration. RA (retinoic acid) inhibits cell migration of breast cancer cells in this pathway by regulating Moesin expression and inhibiting Src, FAK, and paxillin activity downstream, offering novel mechanistic clues for the creation of new cancer treatments (Sanchez et al., 2016). In aggressive breast cancer, it is also increased and phosphorylated by HER2 signaling. Paxillin is being identified as a marker of aggressive breast cancer as well as a promoter of neoplastic development and invasion, implying that it could be used as a biomarker or pharmaceutical target since its overexpression especially in breast cancer (Short et al., 2007). The Rho/ROCK signaling system controls cell motility and focal adhesions (FAs). ROCK inhibition with calyculin A enhances FA assembly and phosphorylation of paxillin and FAK, implying anticancer potential. The interplay of Paxillin/FAK/RhoA signaling with Rho GTPases and the tumor suppressor DLC1 is developmentally controlled (Leopoldt et al., 2001) (Kaushik et al., 2014).

MELK, a kinase that activates RhoA and phosphorylates FAK and paxillin, promotes cell migration and invasion. PTEN, a tumor suppressor, inhibits cell invasion and motility in colon cancer cells by downregulating paxillin expression (L.-L. Zhang et al., 2015). Paxillin cleavage by calpain results in the formation of a carboxy-terminal fragment that functions as an antagonist of endogenous paxillin and may restrict cancer cell migration (Cortesio et al., 2011). PKA activation and the loss of paxillin from FAs hinder migration and FA turnover in pancreatic cancer cells (Burdyga et al., 2013). HGF-induced c-Met signaling, mediated by PKC, promotes paxillin phosphorylation at Ser178 in hepatocellular carcinoma (HCC), enhancing cell motility, invasion, and metastasis (Hu et al., 2015).

Overall, paxillin appears to be a key participant in cell migration and cancer progression, suggesting that it could be used as a diagnostic and therapeutic target in cancer treatment. In the Figure 1.19, it is clearly seen that high paxillin expression in glioblastoma cases cause lower survival of the patients.

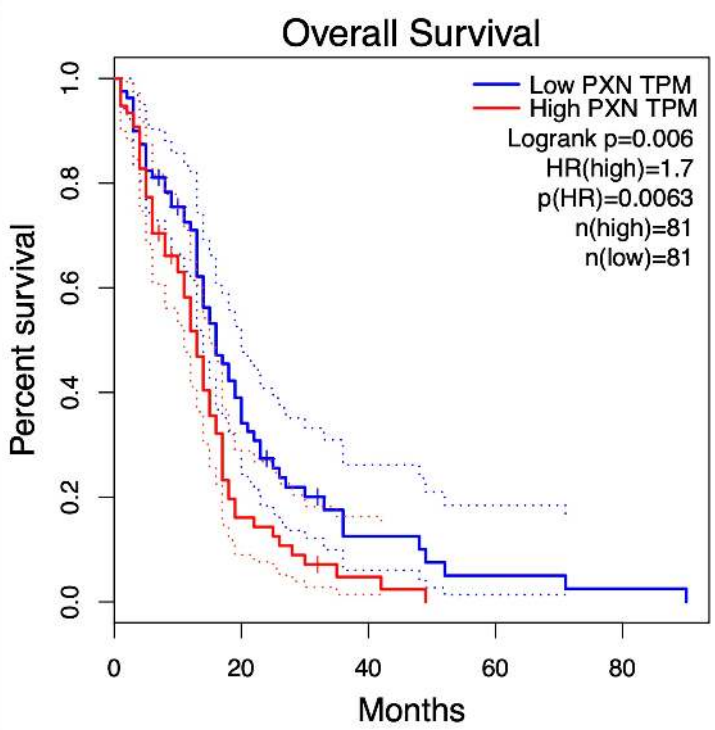

Figure 1.18 Paxillin expression level has an important effect in overall survival rate of GBM patients. Data was taken from GMB dataset in GEPIA online web server (Http://Gepia.Cancer-Pku.Cn/Detail.Php?Gene=PXN).

Chapter 2:
AIM OF THE THESIS

The purpose of the study is to thoroughly investigate the place and importance of SLK, a kinase associated with cancer cell migration and invasion, in autophagy pathways in the pediatric glioma (p-GM) in vitro cell culture model. Relation OF SLK protein with ATG5 was explored in comprehensive mass spectroscopy analysis under starvation condition which promote autophagic pathway. The result of that analysis is presented in "Results" section. Also, upregulation of SLK in gliomas were discovered in the literature.

In line with all these examinations, thesis's objectives can be listed as follows:

- Illuminating the role of a kinase not previously associated with autophagy mechanisms.
- Confirming the relationship of SLK kinase with ATG5 under endogenous conditions and elucidating its control with autophagy stimulation.
- Detailed examination of the functions of SLK and kinase activity through the generation of stable p-GM cell lines expressing wild-type or with SLK gene deletion.
- Establishing the effects of SLK kinase on autophagy activation, autophagosome distribution, and autolysosome formation.
- Investigating the effects of SLK on ATG5 and other autophagy components.
- Uncovering the autophagy-related role of SLK kinase in focal adhesion (FA) regulation.
- Obtaining new and valuable insights into fundamental autophagy mechanisms and their control through the project's research.
- Obtaining valuable information about the role of SLK and autophagy in this lethal disease by selecting the p-GM cell model, which represents tumors with the lowest treatment success among pediatric tumors, as part of the project studies.

Chapter 3:
MATERIALS AND METHODS

3.1 SILAC Labelling

HeLa cells overexpressing flag-tagged ATG5-expressing was treated with SILAC medium (DMEM without L-lysine and L- arginine (Thermo Fisher Scientific, 89985) containing penicillin/ streptomycin (100 units/ml, 100 µg/ml; PAN Biotech, 06-07100), L-glutamine (PAN Biotech, P04- 80100), and 10% dialyzed fetal calf serum (Gibco, 26400- 044)). 42 µg/ml L-arginine-13C6 15N4-hydrochloride (Arg-10) (Sigma-Isotec, 608033) and 40 µg/ml L-lysine-13C6 15N2- hydrochloride (Lys-8) (Sigma-Isotec, 608041) was used for was utilized for heavy labeling. Addition of 42 µg/ml L-arginine-13C6-hydrochloride (Arg-6) (Cambridge Isotope Laboratories Inc., Andover MA., CLM-2265) and 40 µg/m L-lysine- 4,4,5,5-d4-hydrochloride (Lys-4) (Sigma- Isotec, 616192) was performed for media labeling. For light labeling, non-labeled amino acids L-arginine (Sigma, 11039) and L-lysine (Sigma, L8662) were used. 112 µg/ml L-proline (Fluka, 81709) was exploited for all media type. Doubling of cells has passed 5 times during labeling process.

3.2 Sample Preparation for LC-MS/MS

Cells were lysed with RIPA buffer (50mM Tris, pH 7.5, 150mM NaCl, 1% Nonidet P-40, and 0.25% sodium deoxycholate) supplemented with protease inhibitors (Roche, 04693131001) and 1 mM phenylmethylsulphonyl fluoride (Sigma-Aldrich, P7626). Bradford assay was performed for measurement of protein concentration. 2.5 mg of total cell lysate were loaded onto an anti-FLAG M2 affinity gel (Sigma, A2220) for immunoprecipitating flag tagged ATG5 protein. Samples were firstly incubated for 30 minutes at 75°C with Laemmli buffer with 1 mM DTT. For alkylation and reduction, further incubated at room temperature for 30 mins upon 5.5 mM iodoacetamide addition. SDS-PAGE was performed with 4–12% Bis-Tris gels (NuPAGE®Novex, NP0335) and using 20x MOPS-SDS running buffer (NuPAGE®Novex, NP001) with 0.07% antioxidant supplement (NuPAGE®Novex, NP0005). Upon 10 minutes treatment in gel fixing solution, protein bands were visualized with NuPAGE®Novex Stainer solutions

(NuPAGE®Novex, 46-7015 and 46-7016). Proteins were extracted from gel and concentrated by Seçil Erbil according to standard lab protocol.

3.3 LC-MS/MS

Agilent 1200 or an Eksigent NanoLCultra system, connected inline to an LTQ-Orbitrap XL mass spectrometer were utilized for Nanoscale HPLC. A fused silica emitter microcolumn, measuring 15 cm in length and packed in-house with ReproSil-Pur C18-A Q beads (3.5 μm in size, 20 μm inner diameter) from Dr. Maisch, was used for peptide separation. A linear gradient of 10-30% acetonitrile in 0.5% acetic acid was applied, with a flow rate of 250 nl/min. The FT-MS part of the mass spectrometer performed full-scan acquisition within the m/z range of 350-2000, using an automatic gain control target value of 106 and a resolution of 60,000 at m/z 400. The AGC target value was set to 5000, ion selection thresholds were set at 1000 counts, and a maximum fill time of 100 ms was used to perform MS/MS analysis on the five most intense ions in the full scan (Top5) in a data-dependent mode with the LTQ. Wide band activation was enabled, applying an activation q= 0.25 for 30 ms at a normalized collision energy of 35%. Unassigned or single charged ions were excluded from MS/MS analysis, and dynamic exclusion was implemented to reject ions from repeated MS/MS selection for a period of 45 s.

The provided data was analyzed using MaxQuant version 1.4.0.8 with standard settings and the UniProt human database. MaxQuant was employed to eliminate identifications with a false discovery rate of less than 1% for peptides, sites, and proteins using forward-decoy searching. Match between runs was also activated during the analysis.

3.4 Cell Culture and Transfection

HEK293T human embryonic kidney and HeLa cells were growth in DMEM (Dulbecco's modified Eagle's medium; Sigma, D5671 supplemented with 10% (v/v) fetal bovine serum (FBS; PAN, P30-3302) and antibiotics (100 units/mL penicillin and 100 μg/mL streptomycin; Biological Industries, BI03-031-1B) and 1% L-glutamine (Biological Industries, BI03- 020-1B) in a 5% CO_2 humidified incubator at 37°C. Pediatric human glioblastoma SF188 were cultured in DMEM-F12 Ham's Medium which is completed with 10% (v/v) fetal bovine serum (FBS; PAN, P30-3302) and antibiotics

(100 units/mL penicillin and 100 μg/mL streptomycin; Biological Industries, BI03-031-1B) and 1% L-glutamine (Biological Industries, BI03- 020-1B). Calcium phosphate precipitation method was utilized to transiently transfect HEK293T and HeLa cells according to standard protocol. Knockdown experiments were performed by using non-targetin siRNA (siCNT) (Dharmacon SiGENOME, D-001210-01-20) and siRNA targeting SLK (Dharmacon SiGENOME, M-003850-02-0005)

In order to promote autophagy chemically, cells were treated for 3 hours with media with Torin1 (250 nM, Tocris, catalog no. 4247) dissolved in DMSO (Sigma D2650). Cells were also starved with EBSS for 4 hours to induce autophagy.

3.5 Plasmid constructs

Flag and GFP tagged human SLK (HG15999-NF, HG15999-ACG) plasmids were purchased from Sino Biological. hATG5 vector was a kind present from Noboru Mizushima. pGEX-4T-1-3xFLAG (129570) bacterial expression vector, lentiCRISPR V2 (52961), and pLenti CMV GFP Puro (658-5) lentiviral mammalian expression vector were purchased from Addgene.

3.6 Immunoblotting and Antibodies

Cells were lysed with RIPA lysis buffer (50 mM TRIS-HCl, pH 7.4, 150 mM NaCl, 1% NP40, 0.25% Na-deoxycholate) complemented with protease inhibitor cocktail (Roche, 04693131001) and 1 mM phenylmethylsulphonyl fluoride (Sigma-Aldrich, P7626). For detecting phosphorylated proteins, total protein was extracted with RIPA buffer was supplemented with protease inhibitor cocktail (Roche, 04693131001), 1 mM phenylmethylsulphonyl fluoride (Sigma-Aldrich, P7626), and 100 nM okadaic acid, 1 μM cyclosporine A, 1 mM NaF, 50 mM β-glycerophosphate. After centrifugation at 13.200g for 15 minutes total protein concentration was measured through Bradford assay as per manufacturer's instructions (Sigma-Aldrich, B6916). 30-100 ug protein was loaded and separated into 10-15% SDS-polyacrylamide gel and transferred to PVDF membranes. Following blocking application with 5% (w/v) non-fat milk powder (Biorad, 1706404) in 1X PBS-T (PBS and 0.05% Tween 20, pH 7.4) or 3% BSA (w/v) (Sigma-Aldrich, A3059) in 1X TBS-T (TBS and 0.05% Tween 20, pH 7.4) for phosphorylated proteins, membranes were incubated overnight at cold room with 3% BSA PBST including

primary antibodies. Then, following three washes membranes were treated for one hour at room temperature with appropriate secondary antibodies in blocking solution. Protein bands were visualized by using ChemiDoc MP Imaging systems (Bio-Rad). Band intensity were auentified with ImageLab software and normalized to intensities of ß-actin bands (phosphorylated proteins were normalized to total level of interested protein)

Following primary antibodies were used: anti-SLK (Abcam, ab226986, 1:1000), anti-phospho ezrin (Thr567)/ radixin(Thr564)/ moesin(Thr558) (Cell Signaling Technology, 3141S, 1:1000), anti-phospho paxillin (Ser272) (Invitrogen, PA5-114617), anti-ezrin (Cell Signaling Technology, 3145S, 1:1000), anti-ß-actin (Sigma-Aldrich, A5441, 1:10.000), anti-ATG5 (Sigma Aldrich, A0856, 1:1000), anti-LC3 (Cell Signaling Technology, 2775, 1:1000), anti-p62 (Abnova, H00008878-M01, 1:1000), anti-GST (Cell Signaling Technology, 2622S, 1:1000), anti-NBR1 (Novus Biologicals, H00004077-M05) anti-polyhistidine (Sigma- Aldrich, 062M4809, 1:1000). Secondary antibodies coupled to horseradish peroxidase were used: Jackson Immunoresearch Laboratories, anti-mouse-HRP 115035003 and anti-rabbit-HRP 111035144, dilutions 1:10.000.

3.7 Co-immunoprecipitation

For immunoprecipitation experiment with *SLK* overexpressed extracts, 1-1.500.000 HEK293T cells were seeded into 10 cm^2 plates and transfected with pcDNA3 as a negative control, flag tagged SLK and hATG5 plasmids. Cells were harvested after 48 hours after transfection with ice-cold PBS and total protein was extracted according to standard protocol. Following determination of total protein concentration, 1 mg of protein extract were loaded onto anti-Flag M2 Affinity Gel beads (Sigma, #A2220).

For detecting the interaction of proteins in endogeneous level, SF188 cells were cultured in 15 cm^2 plates. After 48 hours, cells were treated with EBSS and Torin 1 for 3 hours to induce autophagy. Following protein extraction and concentration analysis, 2 mg of protein extract was loaded onto protein A magnetic beads (Thermo Fisher Scientific, 100D) that have already coupled with ATG5 antibody for 6 hours at cold room. Beads were incubated with total lysate overnight at cold room on rotator. After overnight incubation, beads were centrifugated and washed with PBS a couple times, denaturated

with appropriate volume of 3X protein loading buffer and separated into 10% polyacrylamide gel. SDS-PAGE and Western blotting steps were performed in described previous section.

3.8 RNA Isolation and Real Time qPCR

Total RNA was isolated by using TRIzol reagent (Invitrogen, 15596018) from Sf188 pediatric glioma cells according to manufacturer's instructions. Briefly, cells were lysed with TRIzol reagent, nucleic acids were separated by chloroform addition. RNA containing part was taken into new tubes and precipitated with isopropanol. Extracted RNA pellet was resuspended within adequate amount of DEPC water. Concentration and purity of RNA samples was measured with Nanodrop (Thermo Scientific ND 2000C). cDNA was obtained via reverse transcription reaction with random hexamers (Invitrogen, 48190011) and RevertAid Reverse transcriptase (Thermo Scientific, EP0441) following DNase treatment. Quantitative PCR was performed with SYBER Green reaction mix (Roche, 04913914001) in Roche Light Cycler 480 device. Expression level of *SLK* was normalized to *GAPDH* and fold change was calculated with $1.8^{-\Delta\Delta Ct}$ method.

Table 3-1 Primer sequences used in qPCR

Gene	Direction	Sequence
SLK	Forward	5'- CAGAGGCGAAGGCTGAAGTA-'3
	Reverse	5'- AAGGTCAGAAGATGCACGCT-'3
GAPDH	Forward	5'- AGCCACATCGCTCAGACAC- 3'
	Reverse	5'- GCCCAATACGACCAAATCC- 3'

3.9 Establishment of SLK KO cell lines

HEK293T, HeLa, and SF188 cells were knocked out for *SLK* gene by CRISPR-Cas9 system. Four different guide RNAs (gRNA) were designed by an online tool that is CHOPCHOP. First, pLenti CRISPR V2 vector was digested with BsmBI restriction enzyme Thermo, (ER0451) and cut vector was extacted from agarose gel. gRNAs were annealed to each other according to standard lab protocol. After that annealed gRNAs ligated into digested CRISPR-Cas9 lentiviral vector. Confirmation was made by Sanger

sequencing by MCLAB. For construction of lentiviral particles, CRISPR-Cas9 vector encoding SLK targeting gRNAs and Cas9 protein were cotransfected into HEK293T cells with pmD2.G (Addgene, 12259) and psPAX2 (Addgene, 12260) vectors. GFP lentivirus was created as control cell lines with pLenti CMV GFP Puro lentiviral vector. HEK293T cells were cotransfected with pmD2.G, psPAX2, and pLenti CMV GFP Puro plasmids. Success of lentivirus construction was checked under fluorescence microscope. Virus particles were collected from culture media, filtered through 0.22 µM sterile filters, and aliquoted at -80°C for longer storage.

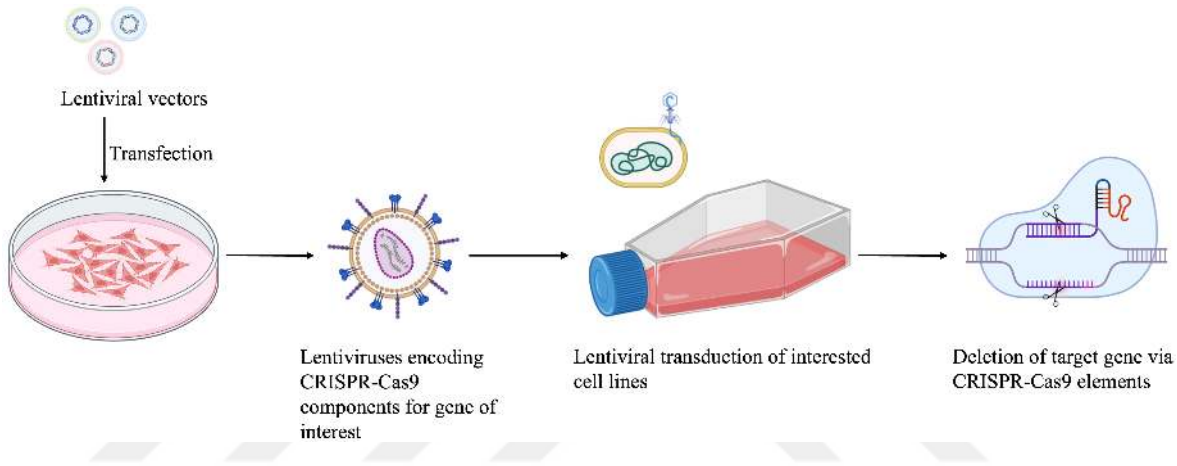

Figure 3.1 Representation of construction of SLK KO cell lines.

HEK293T, HeLa, and SF188 cells were transduced by newly formed lentivirus containing media with Polybrene (5 µg/ml) (Sigma, H9268). Two separated infections with the same gRNAs were performed for obtaining distinct polyclonal cell lines. (1:3, 1:1, virus containing media/fresh media). Following 48 hours incubation, antibiotic selection was applied with puromycin (1 µg/ml). Each polyclonal cell line was verified by immunoblotting after 1 week and 3 weeks later. Polyclonal knock-out cells were named as *SLK* KO polyclone1.1 and *SLK* KO polyclone1.2. These polyclones were created with the same gRNA (gRNA1). HeLa cells have 3 polyclones with gRNA1. HeLa CTL polyclone (GFP virus), HeLa *SLK* KO Polyclone1.1, HEK293T *SLK* KO Polyclone1.1, and HEK293T *SLK* KO Polyclone1.2 were mycoplasma positive so, they were treated with 1X Ciproflaxin for 14 days. Then, according to further mycoplasma testing there was no contamination. For obtaining monoclonal knock-out cell lines, cells were seeded into 96-well plates as individual cells and single clones were maintained and stored.

Table 3-2 Sequences of SLK gRNAs cloned into CRISPR vector

Gene	Direction	Sequence
SLK gRNA1	Forward	5'- CACCGGCAGTACGAACACGTGAAGA- '3
(exon1)	Reverse	5'- AAACTCTTCACGTGTTCGTACTGCC- '3
SLK gRNA2	Forward	5'- CACCGATTATAGGAGAACTGGGCGA- '3
(exon1)	Reverse	5'- AAACTCGCCCAGTTCTCCTATAATC- '3
SLK gRNA3	Forward	5' CACCGCACCTGCACAAAATTCAATG '3
(exon3)	Reverse	5' AAACCATTGAATTTTGTGCAGGTGC '3
SLK gRNA4	Forward	5' CACCGAACTGGGCGACGGAGCCTTT '3
(exon1)	Reverse	5' AAACAAAGGCTCCGTCGCCCAGTTC '3

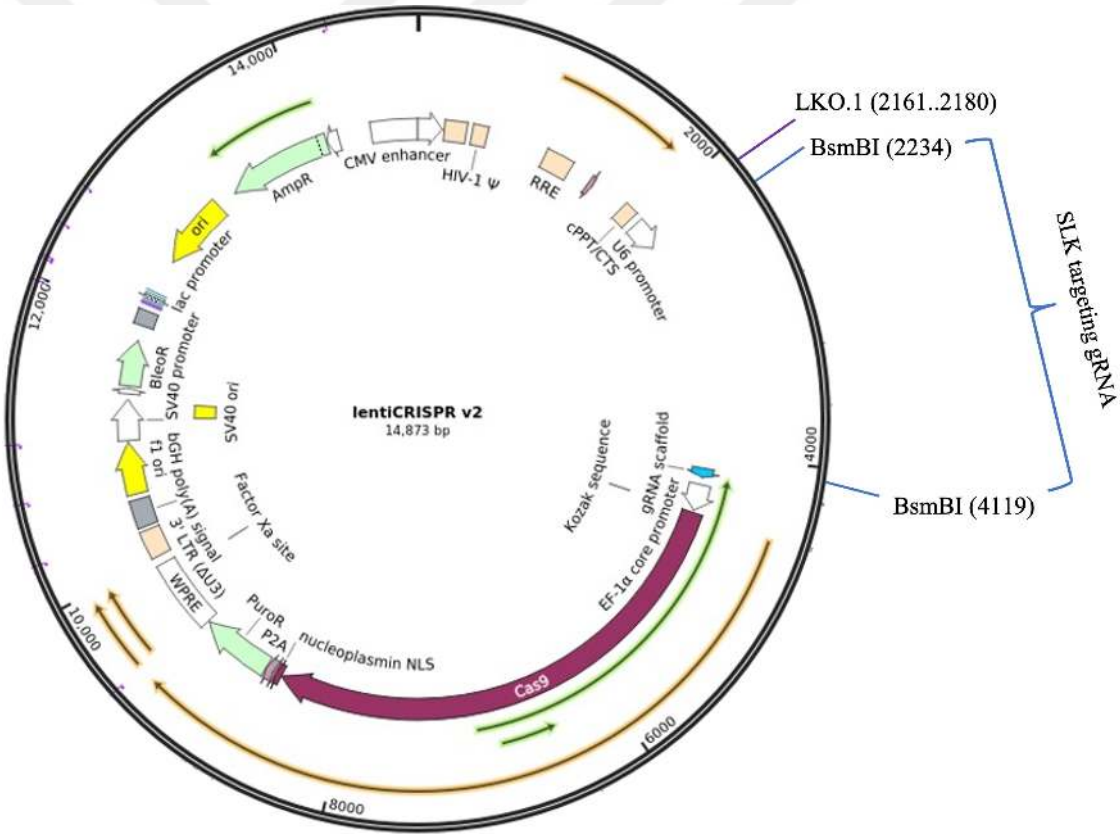

Figure 3.2 LentiCRISPR v2 vector mapping and SLK targeting CRISPR vector cloning strategy. Vector was cut with BsmBI and SLK gRNA oligos were ligated into this region. Ligated vector with SLK targeting gRNAs were sequenced with LKO.1 primer for verification.

3.10 Immunofluorescence

Cells were seeded on sterilized cover glass, 48 hours later required treatments were applied for inducing autophagic flux as described in the first section. Firstly, cells were fixed with ice-cold 4% PFA solution. Then cells were blocked and permeabilized for one hour at room temperature with 0.1% BSA and 0.1% Saponin (Sigma-Aldrich, 84510) in PBS. Following incubation with SLK (1:100) and ATG5 (Santa Cruz, SC-133158, 1:100) antibody overnight at 4°C, secondary antibody incubation was performed with anti-rabbit IgG Alexa-Flour-488 (Invitrogen, A11008, 1:500) and anti-mouse IgG Alexa-Flour-568 (Invitrogen, A11004, (1:500) for 1 hour at room temperature. Imaging was performed by 63×/1.4 oil immersion DIC Plan Apo objective with confocal microscopes (LSM710; Carl Zeiss, Inc., Germany, or Leica Microsystems, DMI8 SP8 DLS/CS). TIFF format of fluorescence images were acquired and proceed with ImageJ Java 1.8.0_172 (64 bit)

3.11 Cytotoxicity Assay

Effects of different chemotherapeutics on WT and SLK KO SF188 cells were evaluated by MTT 3-(4,5-dimethylthiazol-2-yl)-2,5-diphenyl tetrazolium bromide Assay. Cells were first seeded into 96-well plates with 10.000 cells in each well. After 24 hours, chemotherapeutic drugs were applied in certain concentrations. Cells were incubated for 48 hours with media, including drugs. 10 uL of MTT (5 mg/mL) was added to each well. After 6 hours, media was discarded, precipitates dissolved in DMSO, and absorbance was measured at 570 nm.

3.12 Transwell Migration Assay

Migration capability of WT and *SLK* KO Sf188 pediatric brain tumor cells was investigated in 24-well plates with 8 µm pores. (Sarstedt, TC insert, Germany). Appropriate number of cells were seeded into upper chamber in medium without FBS and lower chamber was filled with medium with 10% FBS as a chemo-attractant. Following 16 hours incubation at 37°C, medium in both upper and lower chamber was discarded, cells were fixed with ice-cold 4% PFA, permeabilized with ice-cold methanol. Migrated cell population was stained with crystal violet dye for 15 mins. After removing

the non-migrated cells by cotton swabs, visualized under a light microscope. Intensity of staining of the migrated cells were measured with ImageJ software.

3.13 Wound Healing Assay

Wound healing assay was performed with wild type and *SLK* KO SF188 cells for observing the effect of SLK protein on cellular migration. Firstly, cells were seeded into 12-well plates as 350.000 cells/well for almost full confluency. 16 hours later, cell layer was scraped in a straight line using a 200 µL pipette tip. Wounded cell layer was incubated for 12 and 24 hours in DMEM-F12 containing 3% FBS. After 12- and 24-hour incubation, cells were visualized under a light microscope. Wound closure was measured with ImageJ software.

3.14 Cloning of Catalytic Domain of SLK protein

pGEX-4T-1-3xFLAG bacterial expression vector was digested with EcoRI (Thermo Fisher Scientific, ER0271) and NotI (Thermo Fisher Scientific, ER0595) enzymes sequentially. Firstly, 1 ug plasmid DNA was incubated at 37°C for 4 hours in EcoRI buffer (Thermo Fisher Scientific, B12). Then, digested sample was run at 1% agarose gel at 100V for 45 mins and digested plasmid DNA was extracted with agarose gel extraction kit (Macherey-Nagel, MANA740609.50) according to manufacturer's protocol. Extracted plasmid DNA secondly was exposed to NotI restriction enzyme for 4 hours at 37°C. Again, restricted plasmid DNA run into and extracted from agarose gel. Because 1-338 aminoacids form catalytic domain of SLK protein, this region (1014 bp) was multiplied with PCR. For a flawless PCR, reaction was performed with Phusion High Fidelity DNA Polymerase (Thermo Fisher Scientific, F530S) by using flag tagged SLK plasmid as a template. The primer couple used for this cloning can limit the beginning and the end of the active domain and the recognition sequences of EcoRI and NotI enzymes. Therefore, sticky ends yielding a more effective ligation reaction can be achieved on both insert DNA and vector DNA.

Table 3-3 Primers used for amplification of different domains of SLK protein. Sequences in red color indicates the recognition site of restriction enzymes used for digestion of PCR products for making sticky ends. Sequences in green color indicates the stop codon in required position of transcription.

Domain	Direction	Sequence
Kinase	Forward	5'- AAAAGAATTCTCCTTCTTCAATTTCCGT- '3
	Reverse	5'- AAAGCGGCCGCTCAACGCTTACTTGCAGG -'3
Coiled-coil	Forward	5'- AAGAATTCGCATCTTCTGACCTTAGTA -'3
	Reverse	5'- GCGGCCGCTCATTGTCTTCTTGTTTCTTGTAA- '3
ATH	Forward	5'- GAATTCAAGAAAACATTGAAGAAAACA- '3
	Reverse	5'- AAAAGCGGCCGCTCATGATCCGGTGGA -'3

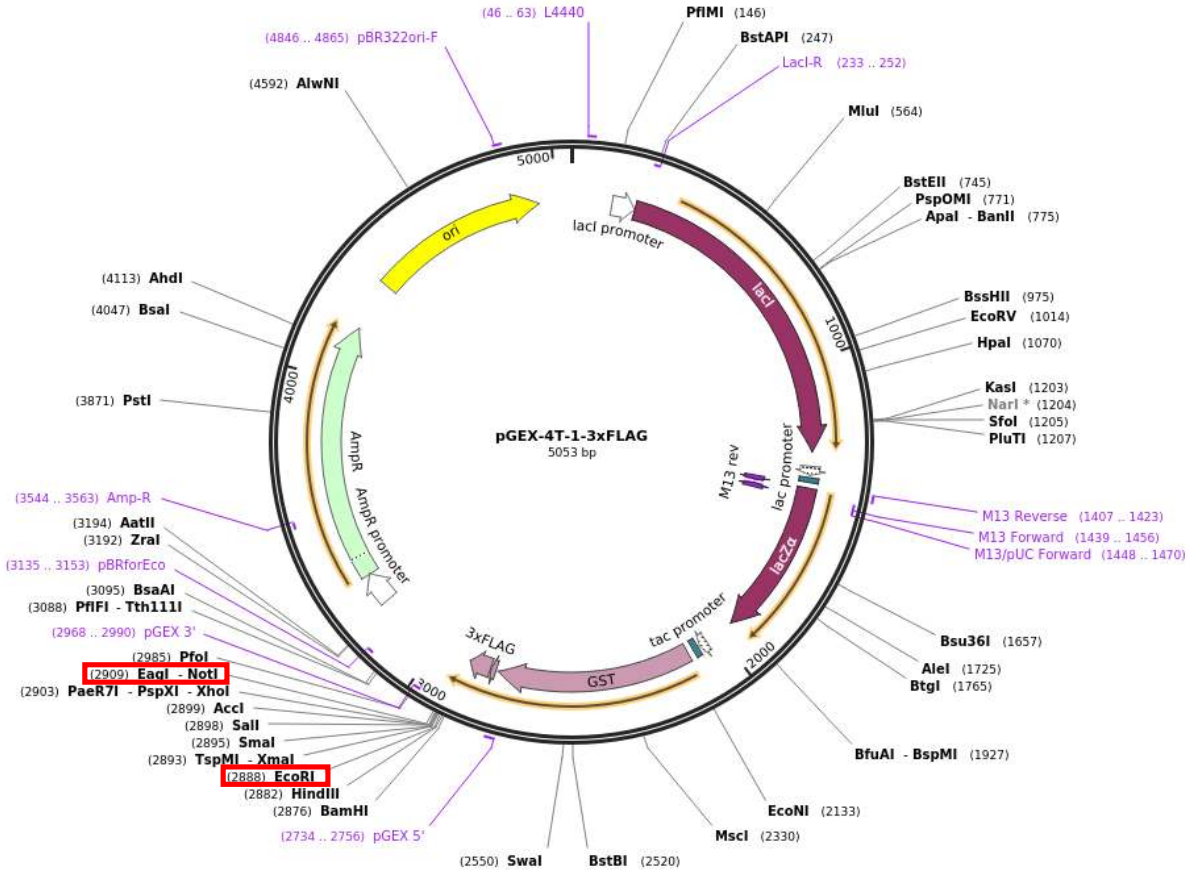

Figure 3.3 Structure of pGEX-4T-1-3xFLAG bacterial expression plasmid. Vector was digested with EcoRI and NotI enzymes. Kinase encoding region of SLK was amplified

via PCR reaction and inserted into this bacterial expression vector. See the details of cloning strategy in Section 2.14.

After amplification of kinase domain and restriction digestion of vector plasmid and PCR products, ligation reaction was performed with T4 DNA Ligase (Thermo Fisher Scientific, M0202) overnight at 16°C. New plasmid sequence was verified with Sanger sequencing by MCLAB.

3.15 Production and Purification of Recombinant Kinase Domain of SLK Protein

Following the verification of the new sequence, plasmid vector encoding the kinase part of SLK was transformed into BL21 for production of recombinant GST-SLK Kinase protein. As an additional control, BL21 strain was also transformed with original pGEX-4T-1-3xFLAG vector. After overnight incubation at 37°C on ampicillin including agar plates, each single colony was picked and growth in LB Broth overnight. When OD600 value reached between 0.3 and 0.5 bacteria suspension was divided into 2 different Erlenmeyer flasks. 0.5 mM isopropyl β-d-1 thiogalactopyranoside (IPTG) was added into one of each two bacteria culture to induce GST-fusion protein expression and bacteria were grown at 20°C for 24 hours. Following the protein production, bacteria was centrifuged, and pellets were firstly resuspended with appropriate volume of lysis buffer (500 mM NaCl, 50 mM Tris-HCl pH:8.0, 2 mM EDTA and, protease and phosphatase inhibitors) including 1% Sarcosyl. Following sonication of each bacteria lysate for 4 minutes at 37% amplitude. (2 seconds on, 5 seconds off), centrifugation was performed at 3000G for 1 hour at 4°C. Some volume of supernatant including recombinant proteins was completed with 3X SDS loading dye, while pellets were resuspended with 1X SDS loading dye with the volume as much as supernatant part. Equal volume of supernatant and pellet was further denaturated at 95°C for 10 mins and separated into 12% polyacrylamide gel. Gel, then was fixed with fixing solution (50% methanol, 10% glacial acetic acid) and stained with Coomassie Blue to observe the protein bands.

For purification of GST protein itself and GST tagged kinase domain of SLK, glutathione Sepharose 4B (GE Healthcare, 17-0756-01) beads was used. 25 uL bead solution was washed with bacteria lysis buffer including protease inhibitor and PMSF for removal of storage solution and equilibration of beads. Then, bacteria lysate was loaded onto beads and incubated overnight at cold room on a rotator. Afterward, beads coupled

with GST and GST tagged protein were treated with adequate amount of pull-down buffer (20 mM L-Reduced Glutathione (Fluka Analytical, 49750) 50 mM Tris HCI pH: 8.0, 5% glycerol, final pH:8.0) for 30 minutes while rotating at RT. Samples were run into polyacrylamide gel and analyzed by staining Coomassie Blue again to see if the purification and elution was successful.

3.16 Site-directed in Vitro Mutagenesis

Lys-63 residue of SLK was mutated through QuikChange site-directed mutagenesis kit (Agilent Technologies, 200524) by utilizing 20 ng flag-SLK plasmid DNA to obtain a kinases-dead protein according to manufacturer's recommendations. The following primers were used for this mutagenesis reaction:

Table 3-4 Primers used for site-directed mutagenesis.

Name	**Sequence**
SLK K63R	5'AGTGTTTTAGCTGCTGCAAGAGTGATTGACACTAAATCTG-'3
SLK K63R	5'CAGATTTAGTGTCAATCACTCTTGCAGCAGCTAAAACACT -'3

Lysine is encoding by AAA codon in flag-SLK plasmid. For mutated the lysine-63 residue we converted the codon from AAA to AGA. Following the treatment of PCR with DpnI, obtained plasmid DNA was transformed into XL Blue supercompotent cells. Kinase-dead SLK encoding plasmid DNA was extracted from bacteria culture, concentration and purity of the extracted plasmid was measured with Nanodrop (Thermo Scientific ND 2000C) and sequenced for verification of the mutation.

3.17 Construction of Lentiviral SLK Overexpression Plasmid

For obtaining stable SLK overexpressing cell lines, we cloned SLK open reading frame region into lentiviral mammalian expression vector.

pLenti-CMV-GFP-Puro, donor vector, was digested with BamHI (ThermoScientific, ER0051) and XbaI (ThermoScientific, ER00681) restriction enzymes in 2X Tango Buffer (Thermo Scientific, BY5) at 37°C. At the same time, for obtaining SLK open reading frame flag tagged SLK plasmid was treated with KpnI (ThermoScientific, ER0521) and NotI (ThermoScientific, ER0591) enzymes at 37°C. Size of the expected fragments was verified with agarose gel electrophoresis. Frangments were extracted with agarose gel

extaction kit mentioned before. Digested fragments were treated with Klenow Fragment (Thermo Scientific, EP0051) to make blunt ended fragments for 15 mins at 37°C and then incubated for 10 mins at 75°C for ending the reaction. After Klenow treatments, insert and donor vector were incubated with 1 unit Calf Intestinal Alkaline Phosphatase (CIAP) (Thermo Scientific, 18009019) for 1 hour at 50 °C. Then, reaction was ended with EDTA (Thermo Scientific, R1021) addition and incubation at 65°C for 15 mins. Following these steps, two DNA fragments were ligated with T4 DNA Ligase with the standard protocol previously mentioned.

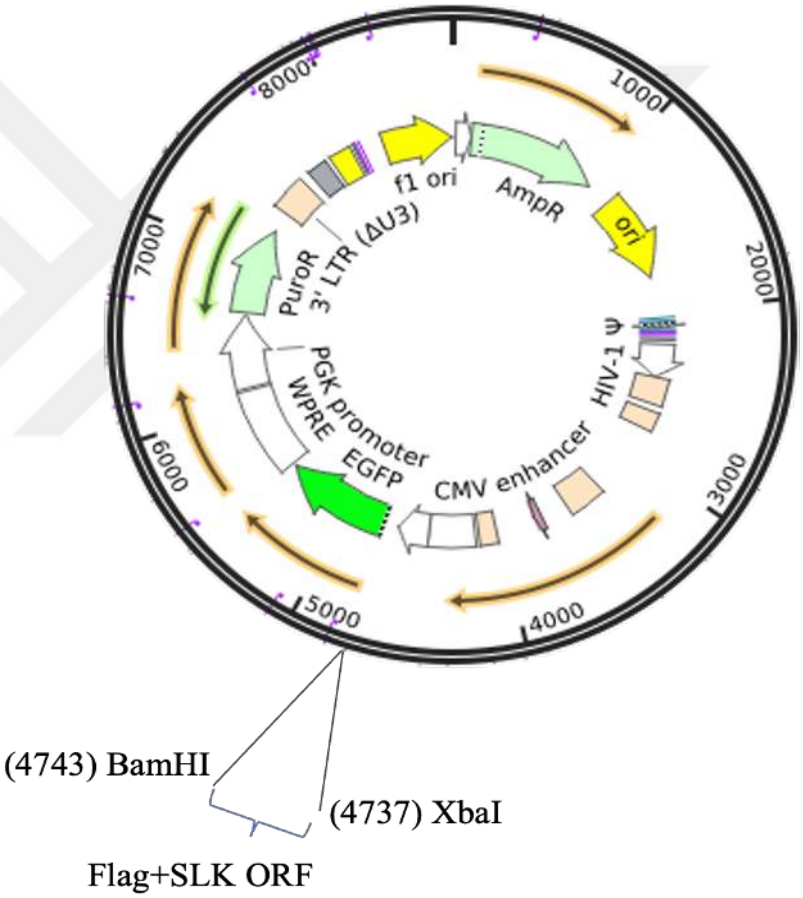

Figure 3.4 pLenti-CMV-GFP-Puro plasmid and overexpression vector cloning strategy.Vector was cut with BamHI and XbaI enzymes and SLK open reading frame (ORF) followed by flag tag was inserted. Blunt ends was obtained with Klenow fragment before ligation. (see Materials and Methods section for details).

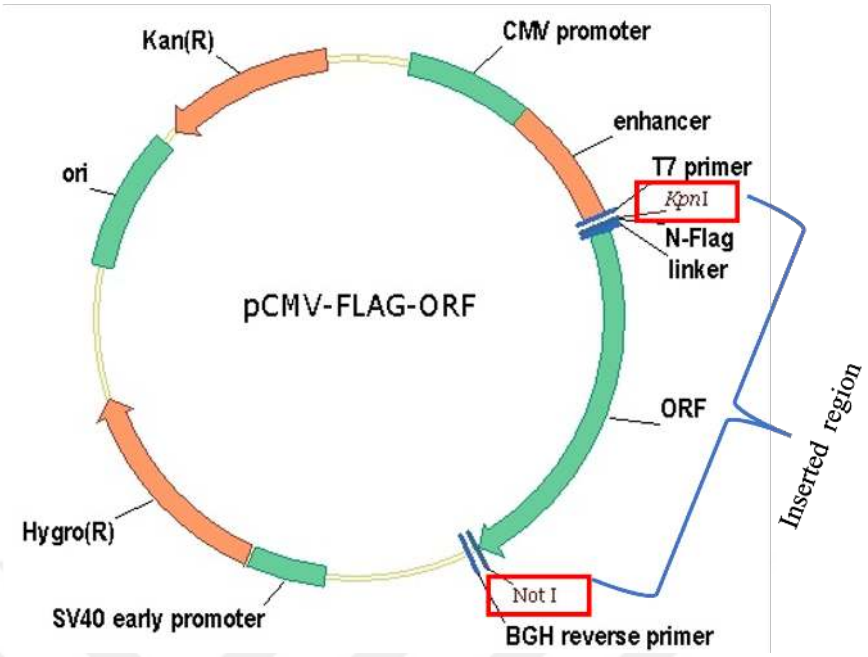

Figure 3.5 flag-tagged SLK vector. Vector was digested with KpnI and NotI vector for obtaining SLK open reading frame (ORF) with flag tag treated with Klenow fragments for obtaining blunt ends.

3.18 Ethical Approval

This study was approved by the Biomedical Researches Ethics Committee of Koç University (No: 2020.413.IRB2.113). All procedures were carried out in accordance with the ethical rules and the principles of the Declaration of Helsinki. An opt-out approach was used when obtaining consent from the patients before the study participation.

Chapter 4:
RESULTS

4.1 Analysis of ATG5-SLK Interaction under Autophagy- inducing Conditions

Interaction between ATG5 and SLK protein was detected with Tri-SILAC labelling and LC-MS/MS method following immunoprecipitation of flag-tagged ATG5 protein. Results of ATG5-SLK interaction fold change was represented in figure 3.1.1

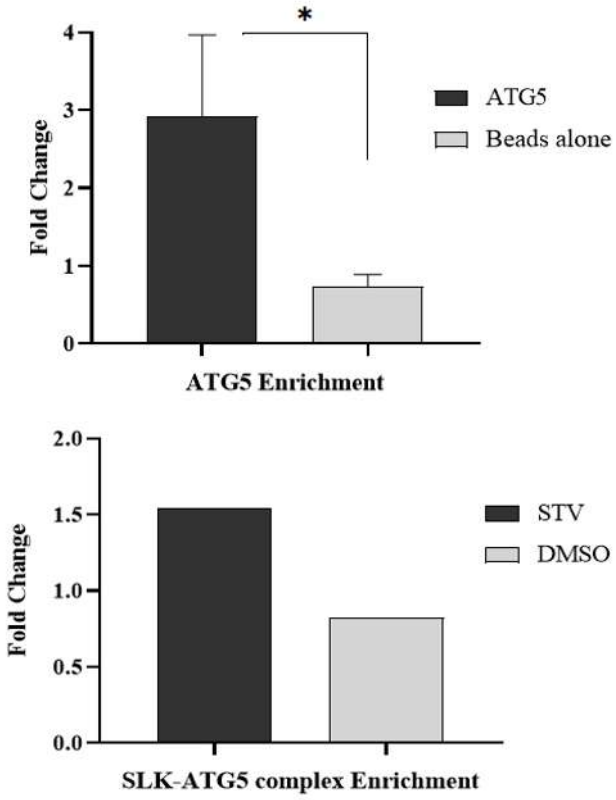

Figure 4.1 Tri-SILAC LC-MS/MS Analysis. ATG5 enrichment compared with beads alone (upper panel); SLK-ATG5 enrichment under starvation induced condition compared with DMSO treated as control. (lower panel) (n=3, *, $p \leq 0.05$) (Seçil Erbil)

4.2 SLK Expression Analysis in Non-tumor, Tumor Brain Samples and Cell Lines

We checked the Human Protein Atlas resource to see the tissues mostly expressing SLK protein. According to this map, SLK is especially expressed in brain, kidney, and some glandular parts of the human body. Also, we know that SLK have significant roles in neurogenerative diseases, neuronal differentiation, and synaptic plasticity. Besides,

SLK is abundant in gastrointestinal tract, liver, and kidney and it contributes the homeostasis by regulating CNS activity on these organs.

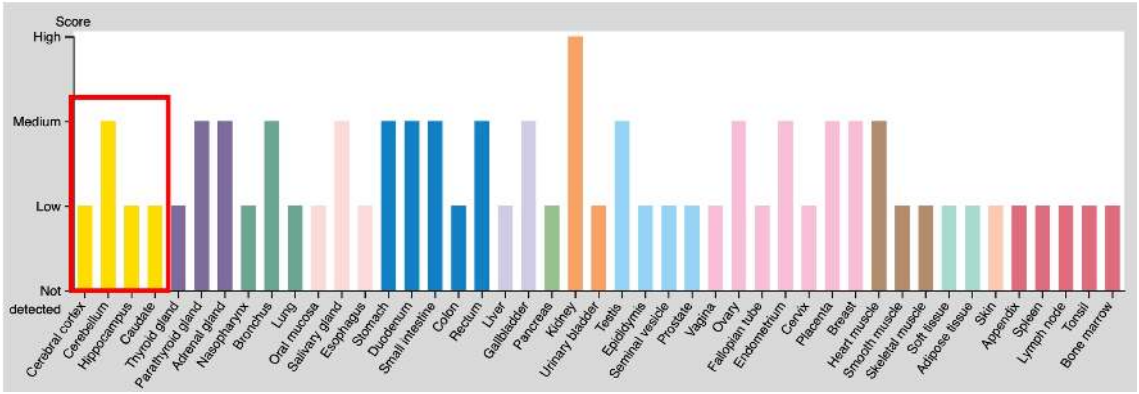

Figure 4.2 Protein expression data according to tissues. Each color-code corresponds to certain tissue groups. (Human Protein Atlas)

According to human protein atlas cerebellum of the brain is a region where SLK is mostly expressed. So, we analyzed the expression level in brain tumor samples. To confirm that the expression of SLK is higher in tumor tissues than in non-tumor tissues, we investigated the expression of SLK in tissues obtained after Koç University Ethics Committee approval and patient consent. qPCR analysis was performed with tissue samples from non-tumor brain and pediatric to see the SLK level. According to this result, we saw that SLK expression is higher in tumor tissue according to non-tumor brain tissue as shown in Figure 3.3.

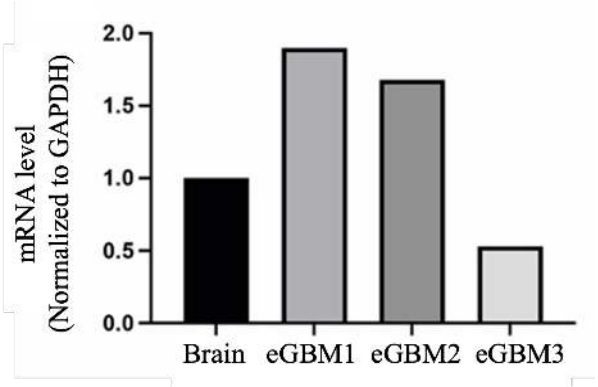

Figure 4.3 Expression level of SLK mRNA in non-tumor brain and glioblastoma samples (Peker, Gozuacik et al. unpublished).

We examined established glioma cell lines including medulloblastoma and glioblastoma. As a result, SLK protein was highly expressed in almost all adult glioma lines. Also, SLK expression level in SF-188 pediatric glioma cell line was highly similar to level of adult glioma lines as shown in Figure 3.4.

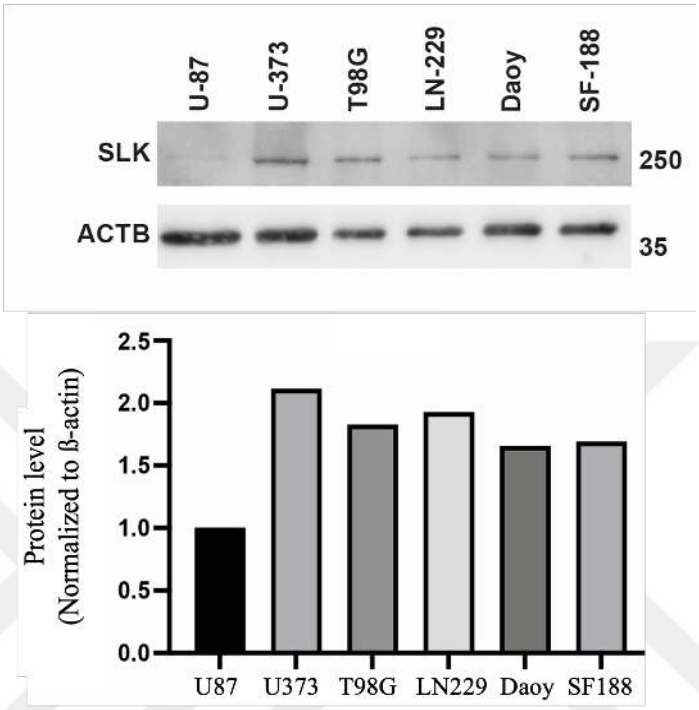

Figure 4.4 SLK is expressed in pediatric glioblastoma comparable level to adult glioblastoma and medulloblastoma cell lines (Peker, Gozuacik et al. unpublished).

Immunohistochemical analysis displays SLK expression in glioma cells around blood vessels in Figure 3.5. Considering the roles of SLK in the invasion and migration

capability of cells, it is important that the expression of the protein is seen in the invaded perivascular area.

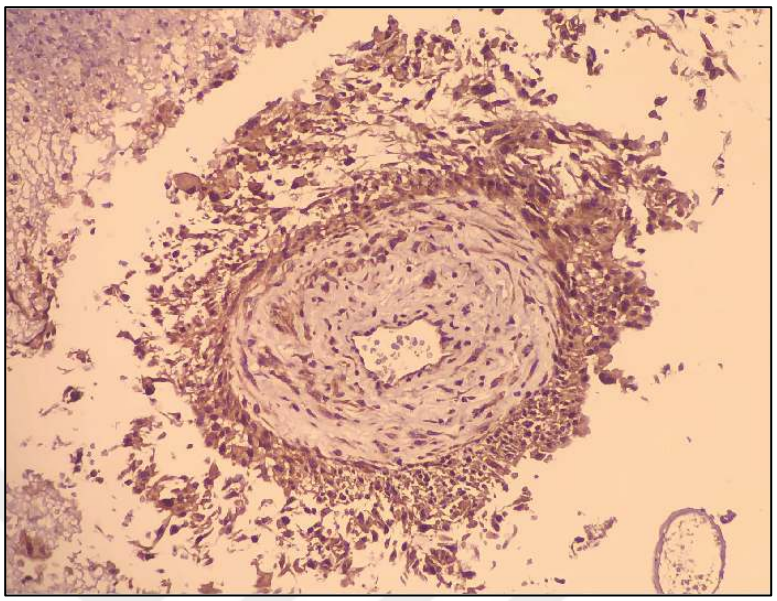

Figure 4.5 Immunohistochemical demonstration of SLK protein expression in adult glioblastoma sections. tumor cells are located around the blood vessel at the center (Assoc. Prof İbrahim Kulaç, MD)

4.3 Confirmation of ATG5-SLK Interaction

In the section 3.1 we demonstrated the SLK-ATG5 interaction via mass spectroscopy analysis. We planned various experiment to confirm the interactions between these two proteins. For verification of interaction of SLK with ATG5 protein, firstly correlation data between these two proteins case was obtained from The Cancer Genome Atlas (TCGA) from GEPIA interaction web server. According to this analysis, in GBM cases there is a statistically significant correlation between ATG5 and SLK as shown in Figure 3.6.

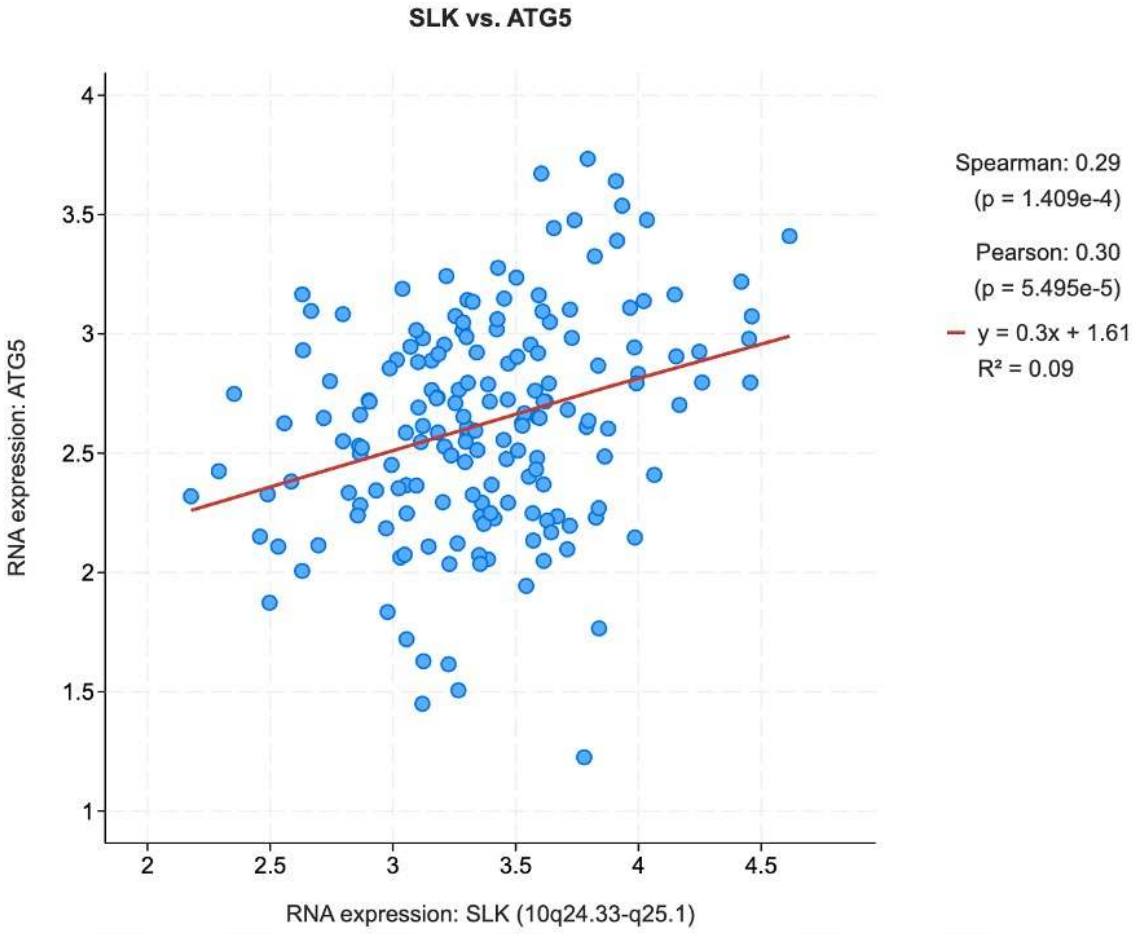

Figure 4.6 SLK and ATG5 expression is positively correlated in pediatric brain cancer cases. Data was created in cBioPortal online tool. Dataset is formed by 190 tumor sample from 174 patients (Petralia et al., 2020b) (*CBioPortal*, n.d.).

For further confirmation of ATG5-SLK interaction, coimmunoprecipitation experiment was implemented with HEK 293T cells overexpressing SLK and ATG5 prtoein following the transfection of cells. Flag immunoprecipitation was performed and ATG5 co-immunoprecipitation was detected in HEK293T cells. The western blot result is shown in Figure 3.7

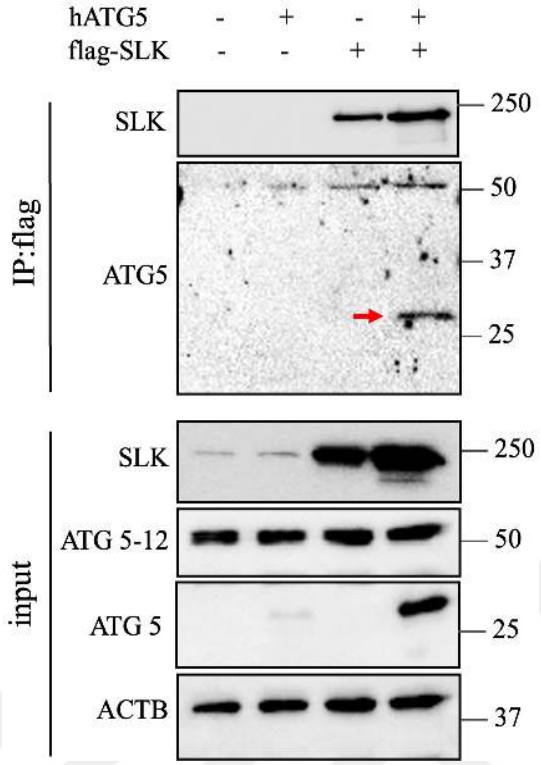

Figure 4.7 Co-IP in HEK293T cells confirms the interaction between SLK and ATG5 in exogeneous level. Flag-SLK IP was carried out with HEK293T cells and interaction of protein in exogeneous level was analysed. Input, 50 µg of total cell lysate. Molecular mass of proteins is shown in kDa. ACTB, as loading contol. n=3, representative result was obtained on 04.06.2023. Red arrow shows the expected band of ATG5 protein.

For observation of SLK-ATG5 interaction in endogeneous level, SF188 pediatric glioma cells were used upon on autophagy stimulated conditions. The result is shown in Figure 3.8. Also, we see the raise in SLK level in starvation and Torin1-treated condition.

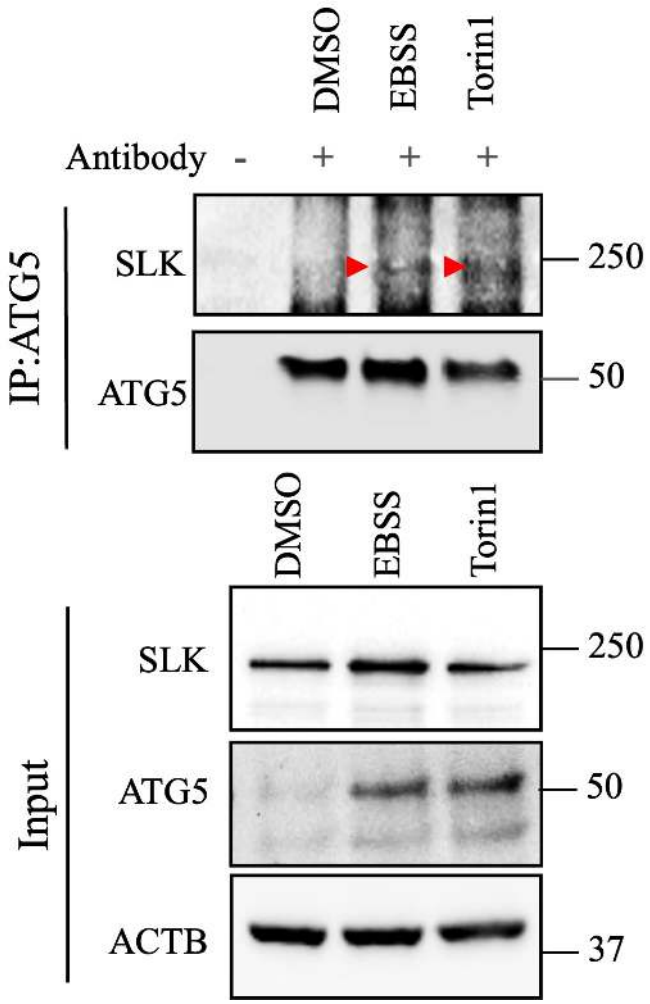

Figure 4.8 Co-IP assay confirms the SLK-ATG5 interaction in starved and Torin1-treated SF188 cells in endogeneous level. Endogeneous IP was performed with SF188 cell line. Cells treated with Torin1 (3 hour) or starved with EBSS (4 hour). n=3, representative result was obtained on 13.05.2023

To see the intracellular localization of SLK and ATG5 protein, immunofluorescence analysis was performed by confocal microscopy upon autophagy stimulation with starvation and Torin1 treatments of SF188 cells. Indeed, closer localization of the proteins can be seen in Figure 3.9.

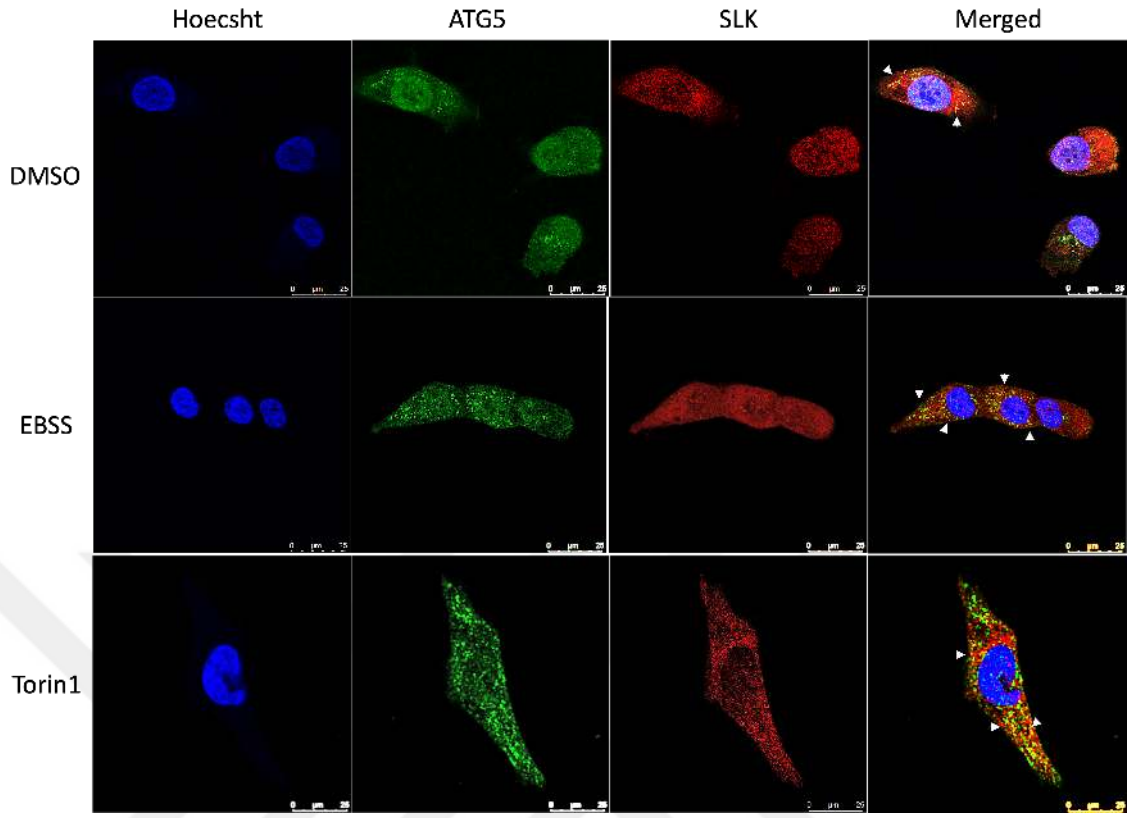

Figure 4.9 Confocal analysis for ATG5-SLK colocalization in SF188 cells. Cells were treated with Torin1 (250 nM, 3 hour) and starved with EBSS (4 hour). DMSO is control condition. White arrows indicate the yellow signals with ATG5 and SLK colocalization. n=1 on 10.05.2023.

For cloning of catalytic domain od SLK protein, firstly 3 different domains of SLK protein were multiplied with PCR by using flag tagged human SLK plasmid. PCR products were analyzed according to DNA size with agarose gel electrophoresis. The recognition sites of the EcoRI and NotI restriction enzyme was coupled on 5' end of forward primer and 3' end of reverse primer respectively. Therefore, PCR product was digested with these enzymes, and we had a DNA insert having sticky ends for ligation to vector plasmid. At the same time bacterial expression vector was digested with the EcoRI and NotI and after digestion separated into agarose gel. All DNA fragments were obtained at expected size and quality. Results of agarose gel electrophoresis is shown in Figure 3.10A and Figure 3.10B.

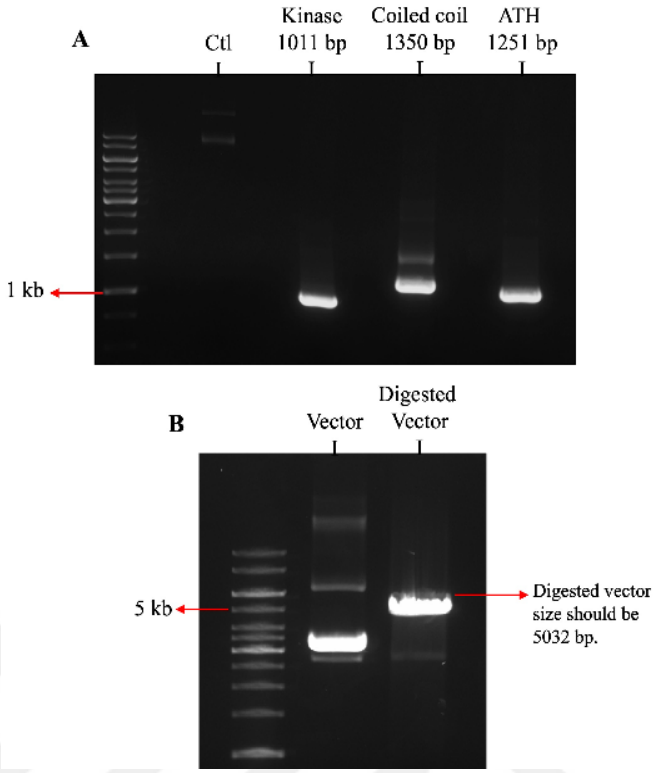

Figure 4.10 Agarose Gel electrophoresis results of (A) SLK domains multiplied with PCR (ctl, unprocessed flag-SLK plasmid) and (B) undigested and digested pGex-4T-1-3X-flag bacterial expression vector with EcoRI and NotI. Exp. Date: 10.08.2022.

Following overnight ligation of the kinase domain into vector plasmid, the new cloning vector was transformed into BL21 bacteria strain, and protein production was performed upon IPTG induction. In the first experiment, to see whether the cloning step is successful recombinant p38 protein with GST tag previously produced by Yunus Akkoç was used as a positive control. Following the production and extraction of recombinant proteins from bacteria, the total protein extract was analyzed with SDS-polyacrylamide gel electrophoresis. After protein extraction, samples from both supernatant and pellet were loaded into gel to see if the protein resides in the soluble or insoluble form. Protein bands were visualized with Coomassie staining as shown in Figure 3.11

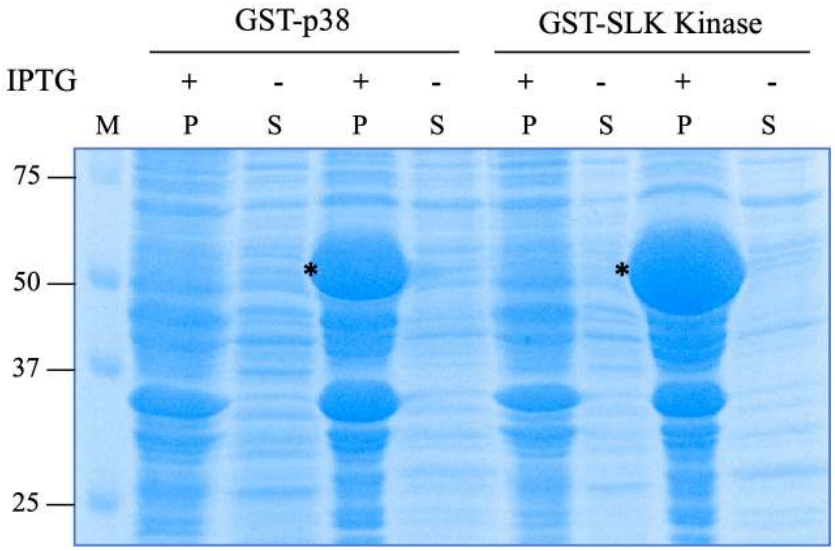

Figure 4.11 SDS-PAGE analysis of recombinant proteins produced in E.coli with Coomassie staining. M, protein marker; P, pellet; S, supernatant. *, bands of produced recombinant protein 29.09.2022, IPTG, Isopropyl β- d-1-thiogalactopyranoside is used for inducing protein expression where the gene is under the control of the lac operator.

P38 protein has a mass of approximately 64 kDa with a GST tag. The calculated molecular mass of the kinase domain of SLK is 63.18 kDa. Considering these calculated values, the produced protein was acquired upon IPTG induction and expected molecular mass (kDa). However, the kinase domain was obtained insoluble phase, making it difficult to purify the protein. To solubilize the recombinant protein, bacteria cells were lysed with a lysis buffer containing 1% Sarcosyl which is an ionic detergent. Extracted lysate again analyzed with SDS-PAGE and Coomassie staining. This time free GST protein was expressed by transforming the pGex-4T-1-3x-flag vector as negative control. Both free GST and recombinant kinase domain of the protein were obtained in soluble form at adequate amount.

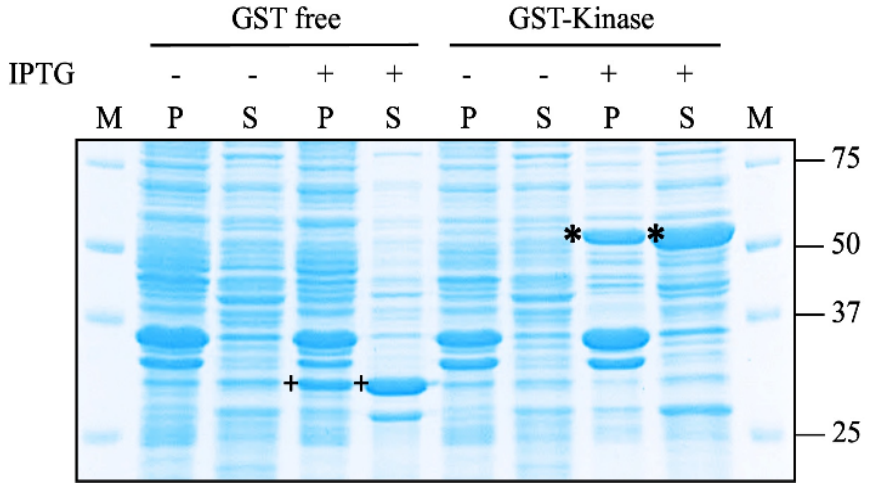

Figure 4.12 SDS-PAGE analysis of solubilized recombinant proteins in E.Coli with Coomassie staining. * designates the produced kinase domain. # designates free GST protein. M, marker; P, pellet; S, supernatant. For further analysis this extract was used.

To purify the GST protein and GST tagged SLK kinase domain, adequate amount of lysate was used for pull-down with glutathione sepharose beads. Purification experiment was mentioned with more details in 2.14th part of materials and methods chapter. Eluted protein samples were analyzed with Coomassie staining and specific antibodies as shown in Figure 3.13A and Figure 3.12B. Recombinant GST, and GST-SLK kinase proteins were successfully identified with anti-GST antibody.

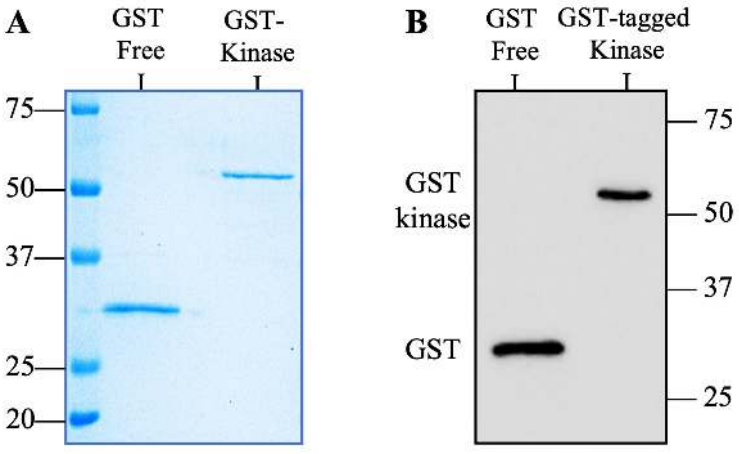

Figure 4.13 Coomassie staining (A) and immunoblotting assay (B) shows the purified recombinant GST and GST-SLK Kinase. Proteins were detected with anti-GST antibody. (15.06.2023 and 24.06.2023).

To investigate whether catalytic domain of SLK protein is crucial for the interaction with ATG5 protein, pull down assay was performed. GST-SLK kinase was pulled down with GST Sepharose beads and recombinant His-ATG5 protein was checked. Result was shown in Figure 3.14

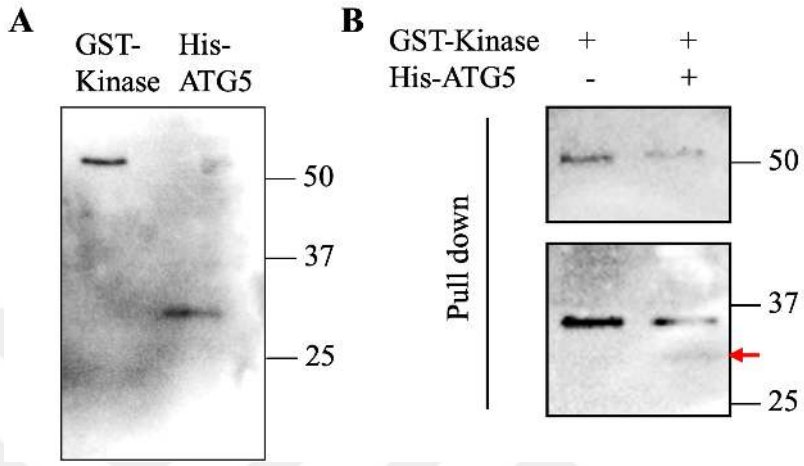

Figure 4.14 Pull down assay may show the direct interaction between catalytic domain of SLK and ATG5 protein. GST Pulldown Assay (A) Immunoblotting of recombinant GST-tagged SLK kinase domain and His-tagged ATG5 protein. Membrane was treated with anti-GST and anti-His antibodies. (B) Pulldown assay Membrane was treated with anti-GST and anti-His antibodies. (n=1, 24.06.2023)

4.4 Upregulation of SLK upon Autophagy Induction

To observe any change on the expression level of SLK protein, autophagy was induced in SF188 cells with starvation and torin1 treatment. Also, hydroxychloquine was added upon 3 hours starvation for inhibition of autophagic degradation and to see whether SLK is a autophagy target. Protein level was analyzed with immunoblot analysis that shown in Figure 3.10

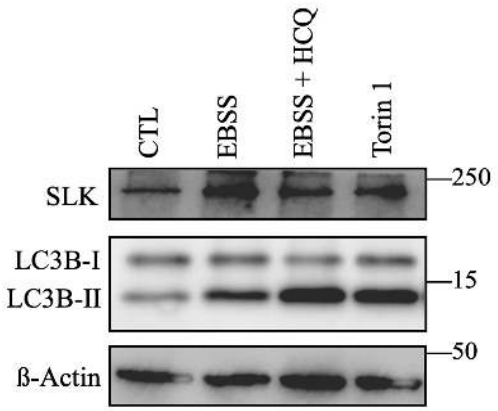

Figure 4.15 Western blot analysis of SLK protein following the autohagy inducing treatments on SF188 cells. Expression level was represented on graph (left panel). ß-actin was used as loading control. (n=1, Peker, gozuacik et al. unplished).

qPCR analysis was carried out to check if the increase in SLK protein seen in western blot analysis is transcriptional. We observed that SLK expression increased with 6 hours of starvation. The significance value (p-value) for 6 hours of starvation is calculated as 0.09, so more repeats of this experiment and more successful treatments may improve the result and represent upregulation of the protein. Compared to torin1 treatment, starvation-induced autophagy affects SLK expression in SF188 cells more.

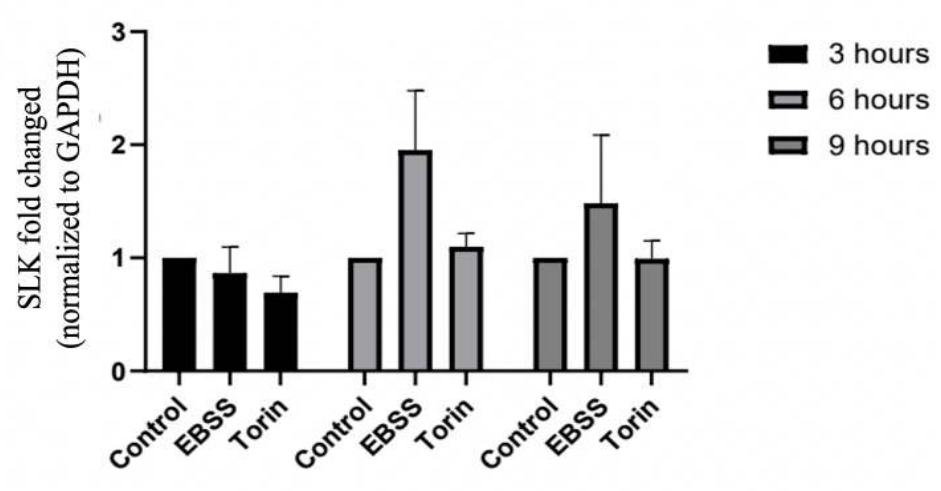

Figure 4.16 SLK is upregulated with autophagic induction. qPCR analysis of SF188 cells. Cells were treated with torin1 and starved with EBSS for 3,6, and 9 hours. n=3. (20.12.2022).

4.5 Investigation of the Effect of SLK on Autophagic Flux

One of the most important indicators of autophagic activation is the lipidation of LC3B protein. In normal conditions, LC3B protein is the cytoplasmic form called LC3B-I. When autophagy is activated in cells, LC3B-II is lipidated and located on membranes of autophagosomes. We can easily detect these two forms of autophagy by the immunoblotting method. That is why LC3 shift was investigated upon autophagic induction in SLK overexpressing HEK293T cells. As shown in Figure 3.16, excess SLK protein leads to augmentation on LC3 shift from form 1 to form II. Although the change is noticeable, this increase was not detected as significant based on statistical tests. It is known that SLK has an essential role in apoptosis. Indeed, SLK overexpressing HEK293T cells have lower viability. The effect of SLK on cellular survival was confirmed with a Trypan Blue staining done by Şüheda Duran. This change in cell survival can cause dramatic fluctuations in western blot analysis, and it can cause the result is not statistically significant. More repeats of this experiment and optimization of SLK expression can improve the outcome.

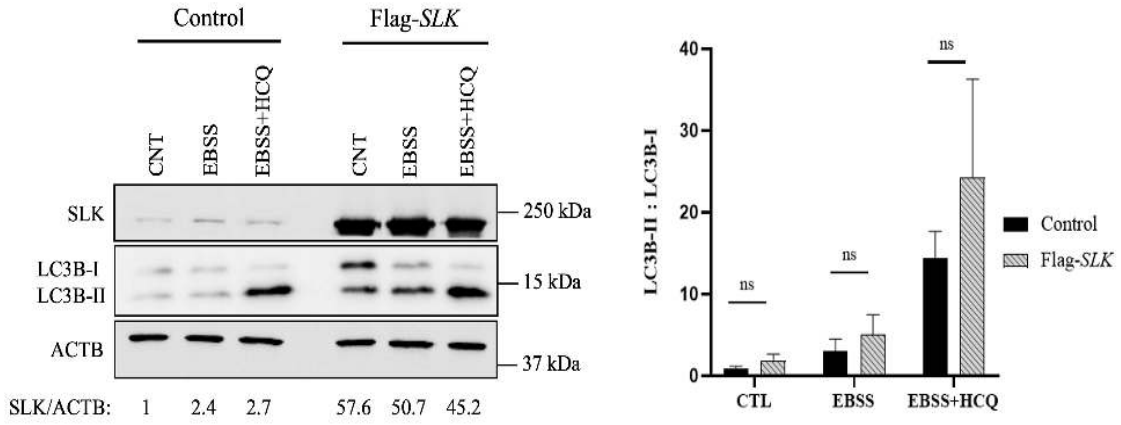

Figure 4.17 SLK overexpression causes increase in lipidation of LC3 protein in starvation induced autophagy and hydroxychloroquine treatment. Immunoblot analysis with normal and SLK overexpressing HEK293T cells (left) and graphical representation of the ratio of LC3BII to LC3BI (right). pcDNA3.1 was used to transfect HEK293T cell as control. n=3. Representative data was obtained on 29.03.2023.

We also confirmed the effect of SLK on LC3 shift, *SLK* expression was repressed in HEK293T cells with *SLK* targeting siRNA. Cells were transfected with siRNAs and

starved to promote autophagy. As expected, the shift from LC3BI to LC3BII decreased in knockdown condition as shown in Figure 3.17.

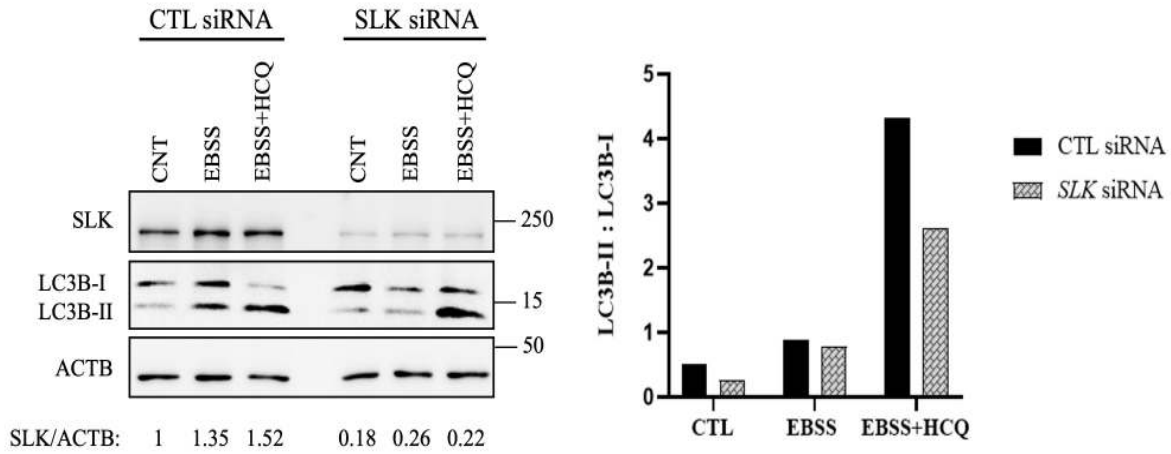

Figure 4.18 Knockdown of *SLK* gene leads to decrease of lipidation of LC3 protein especially in hydroxychloroquine treatment combined with starvation. Immunoblot analysis with wild-type and SLK knockdown HEK293T cells (left) and graphical representation of the ratio of LC3BII to LC3BI (right). Non-targeting siRNA was used as control. n=1, data from 28.03.2023.

4.6 Creation of SLK KO cell lines by using CRISPR-Cas9 method

After cloning of SLK targeting gRNAs into lentiviral CRISPR-Cas9 vector, produced lentiviral particles was applied to interested cell lines and selected transduced cell with puromycin application. Lentiviruses with the GFP gene were also constructed and used to check the success of lentivirus production and the efficiency of viral infection. Firstly, HEK293T cells treated with GFP lentiviruses were visualized under a. fluorescence microscope, and successful virus infection was confirmed as Shown in Figure 3.18.

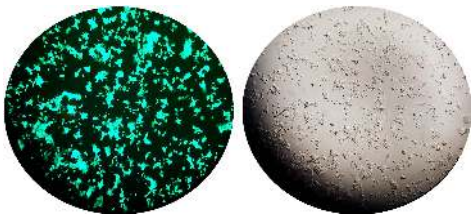

Figure 4.19 HEK293T cells transduced with GFP encoding lentiviruses. Fluorescence image (left), bright field image (right). 28.01.2023.

First confirmation for knock out was made 14 days after antibiotic selection. As shown in Figure 3.19 while gRNA1 efficiently delete *SLK* gene, gRNA2 cannot successfully target the gene.

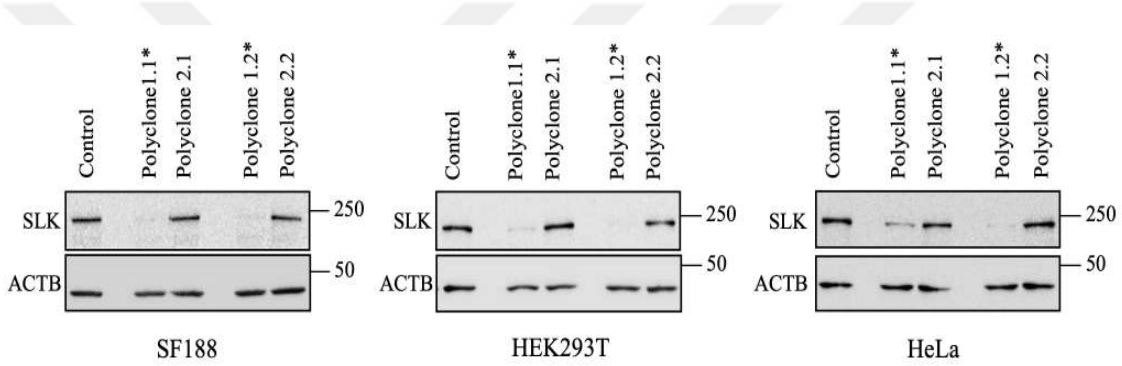

Figure 4.20 Immunoblotting upon 14 days of antibiotic selection. Two separate infection was performed with each gRNA for having different polyclones. Polyclone1.1, first infection of lentiviruses carrying SLK gRNA1. Vector was named as pLenti-cripr-v2-SLK_gRNA1. Polyclone1.2, second infection of lentiviruses with gRNA1. Polyclone2.1, first infection of lentiviruses carrying SLK gRNA2. Vector was named as pLenti-cripr-v2-SLK_gRNA2. Polyclone2.2, first infection of lentiviruses with gRNA2. Control, GFP lentivirus. 27.05.2023. Further experiments were performed with polyclone 1.2 cells.

Since each second infection was made with more virus-containing media, polyclone1.2 was the most efficient. That is why monoclonal cells were obtained from *SLK* KO SF188 polyclone1.2. Following the completion of 21 days with antibiotic selection, another verification was made by immunoblotting with SF188 cells. Also, monoclonal knockout cells were obtained and checked with immunoblotting, as shown in Figure 3.20. In polyclonal cells, phospho-ERM protein was also checked, and we can see that polyclone1.2 cells have a significant decrease in phospho-ERM proteins. We can

comment that even a small amount of SLK protein is sufficient for the phosphorylation of ERM proteins.

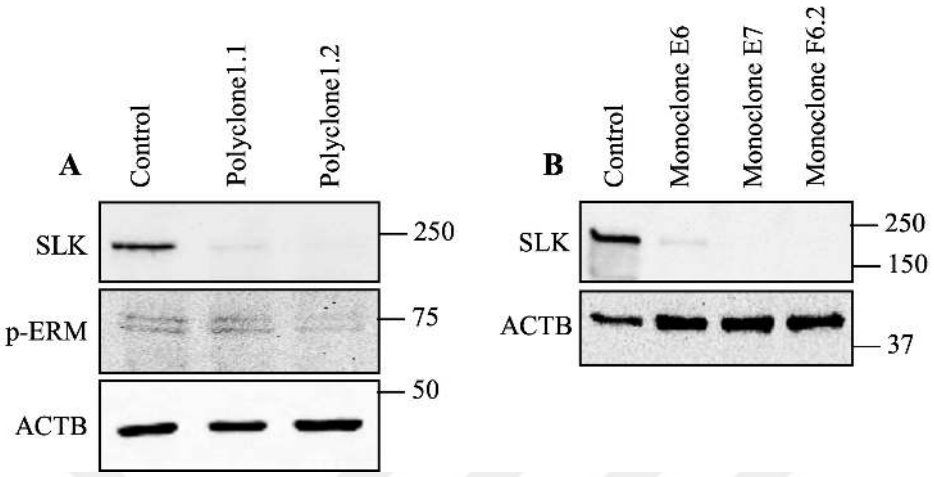

Figure 4.21 Immunoblot analysis to confirm polyclonal (A) and monoclonal (B) knockout cells after antibiotic selection. (A) 20.04.2023, (B) 27.05.2023

For further examination of the effect of SLK on autophagic mechanism, we induced autophagy in wild type and *SLK* KO SF188 cells and checked autophagy marker and receptor proteins. Strikingly, the shift of LC3B protein from cytosolic form to membrane-bond form is decreased in knockout cells. Also, accumulation of selective autophagy receptor proteins is observed as displayed in Figure 3.21.

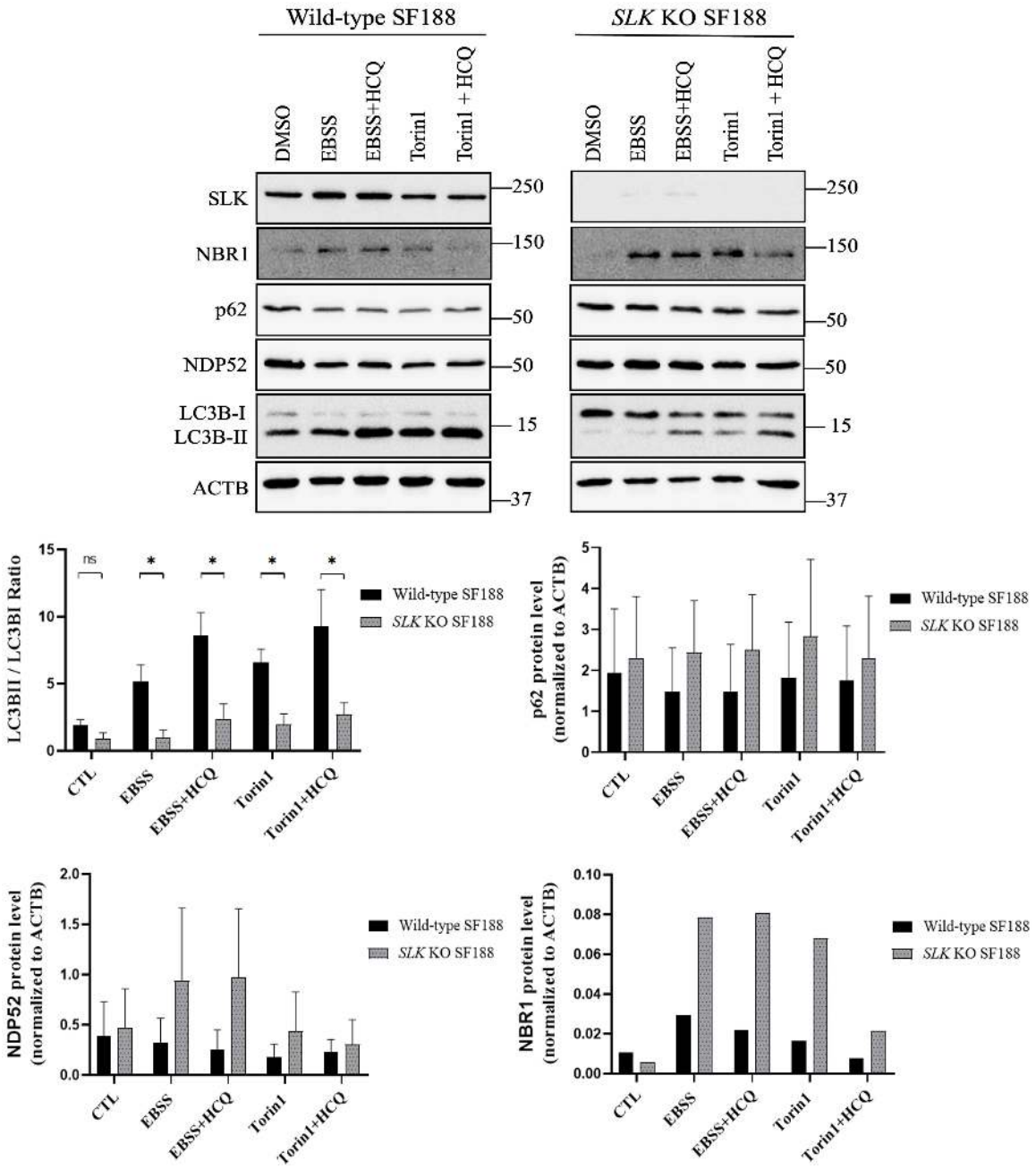

Figure 4.22 Immunoblot analysis of autophagy markers. Experiment was performed with wild-type and SLK KO SF188 cells. Each protein band for one protein was visualized in the same exposure time. Quantitave analysis of protein level was represented with graphs below.

4.7 The Effect of SLK on actin cytoskeleton

There are studies showing the effect of SLK on cytoskeleton rearrangement. So, we showed that SLK cause dissolution of actin fibers. Because SF188 cells are not transfectable, we overexpressed SLK protein in HeLa cells by transfecting the cells. Consequently, transfected cells cannot be stained by phalloidin staining as shown in Figure 3.22.

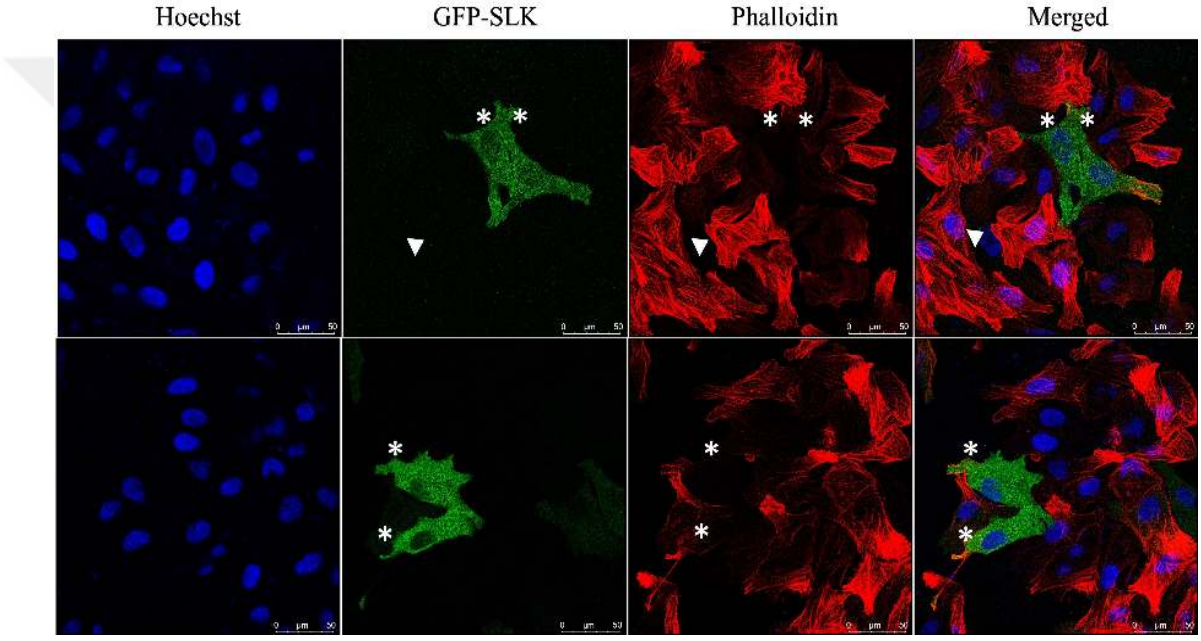

Figure 4.23 SLK overexpression cause depolymerization of actin stress fibers. Phalloidin staining of HeLa cells 48 hours after transfection with GFP-SLK plasmid. Alexa-Fluor 546 Phalloidin was used for staining of actin fibers. Asteriks (*) indicates transfected cells with no staining. Arrowhead shows non-transfected cells with actin fibers. 20.06.2023.

We performed phalloidin staining with wild-type and *SLK* KO SF188 pediatric glioblastoma cells to see the effect of SLK loss on cytoskeleton and adherence of cells. Indeed, we observe certainly higher phalloidin signals with *SLK* KO cells. Also, cell-cell connection was clearly observable compared to wild-type cells.

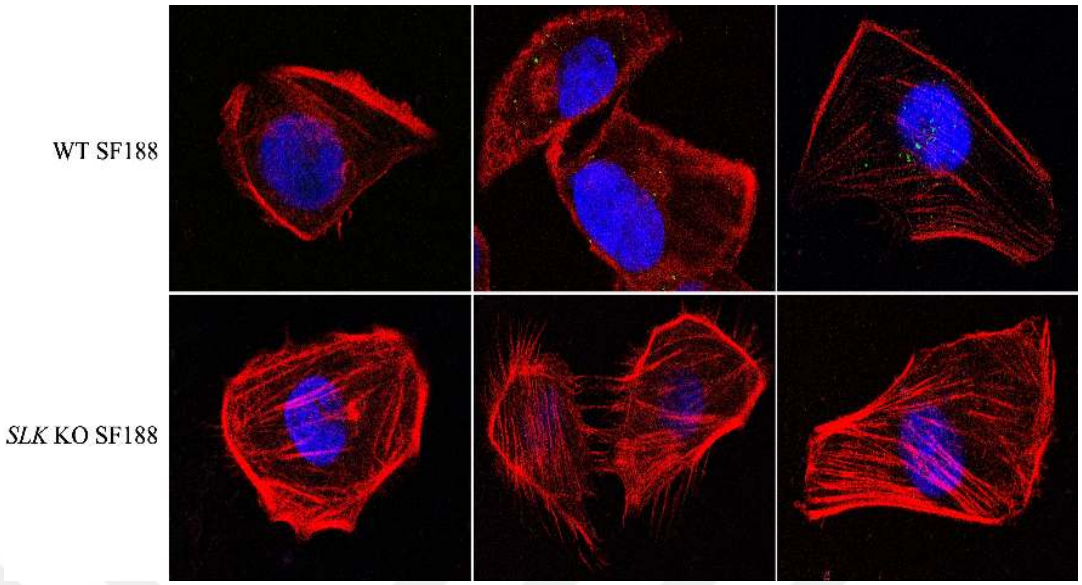

Figure 4.24 In SLK KO SF188 cells phalloidin staining of actin stress fiber is higher that wild-type SF188 cells. Red, Alexa-Fluor 546; Blue, Hoechst. SLK KO polyclone 1.2 cells were used for this experiment. n=1. (Duran, Gozuacik et al., unpublished.)

Modulation on cytoskeleton dynamics, intracellular adhesion, interaction of cytoskeleton components with extracellular matrix has important roles in cellular mobility. Cellular movement primarily driven polarization of cell and rearrangement of actin fibers. We know that SLK is localized leading edge of the migrating cells and interact with microtubule network. To investigate the effect of *SLK* on cellular movement and migration capability, we performed wound healing assay and transwell migration test. In both experiments we showed that SLK knockout cells have lower migration capacity as shown in Figure 2.34.

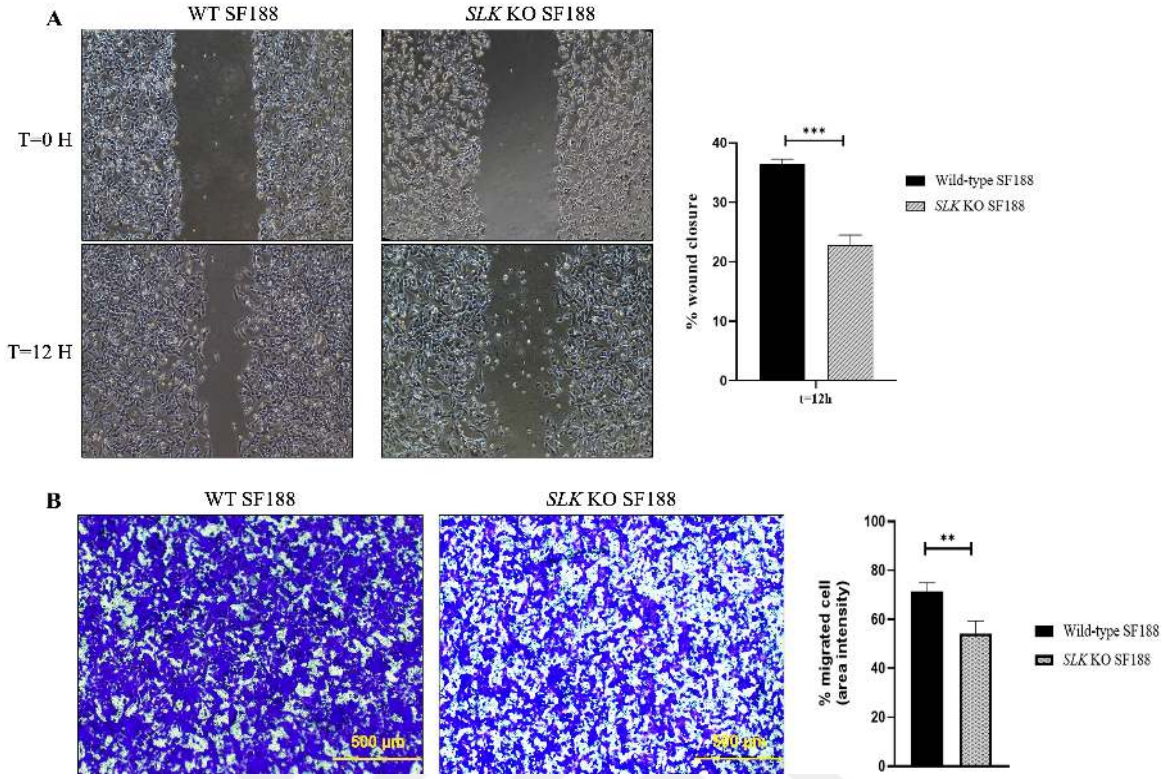

Figure 4.25 Deletion of *SLK* causes significant decrease in migration ability of SF188 pHGG cells. (A) scratch assay and quantitative representation. Images were taken 12 and 24 hours after scratch formation. n=6, p value=0.000026 for 12 h, p value=0.000208 for 24 h. Representative data from 23.05.2023. (B) Transwell migration assay and quantitative representation. Migrated cells were imaged at 16th hour. n=3, p-value=0.008. Representative data from 13.6.23.

4.8 Investigation of SLK activity on the phosphorylation of paxillin and ERM proteins

Significant variation in cellular motility with the absence of SLK protein encouraged us to investigate the cytoskeleton and adhesion-related molecules. So, we checked the phosphorylation status of ERM proteins and paxillin. Since ezrin protein is upregulated in some metastatic cancers and it is phosphorylated by SLK, ERM molecules are the most attractive candidate for observing the action of SLK. Moreover, paxillin, a FA molecule, is the second candidate for us because it is phosphorylated by SLK and degraded by autophagy. As shown in Figure 3.24, ERM molecules are phosphorylated by SLK overexpression in HEK293T cells, and their phosphorylation is relatively decreased upon

SLK knockdown by using siRNA targeting SLK. We cannot see an apparent change in phospho-paxillin level, which is unsurprising because we know that paxillin is phosphorylated at ser-250 residue by SLK. However, there is no commercial antibody specific to that residue. Nonetheless, we tried an antibody similar as much as the specific one. As a result, there is not specific change in paxillin phosphorylation.

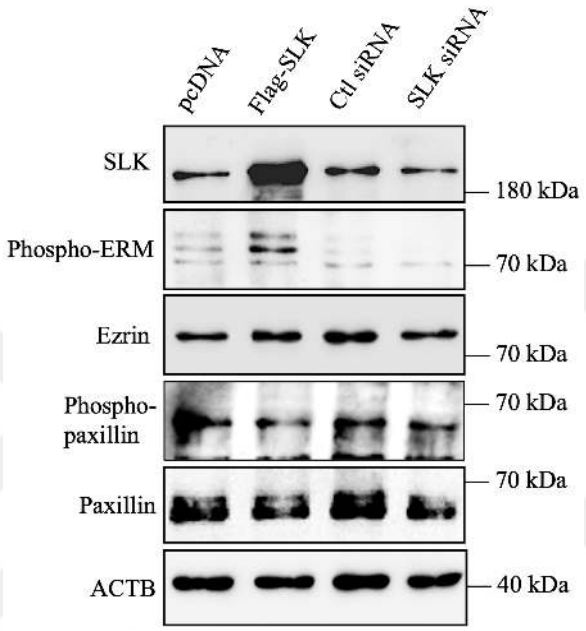

Figure 4.26 SLK is responsible for phosphorylation of ERM proteins (Phospho-Ezrin (Thr567)/Radixin (Thr564)/Moesin (Thr558)). n=1 20.09.2022. Phospho paxillin antibody is specific to Ser272 residue.

We further checked the phosphorylation level of ERM proteins by manipulating the SLK expression and autophagy induction. As shown in Figure 3.26, the phosphorylation level of phosphorylated ERM molecules is increased in SLK overexpressing HEK293T cells. Also, when we starve HEK293T cells to promote autophagy, the phosphorylation level is higher than normal SLK level conditions.

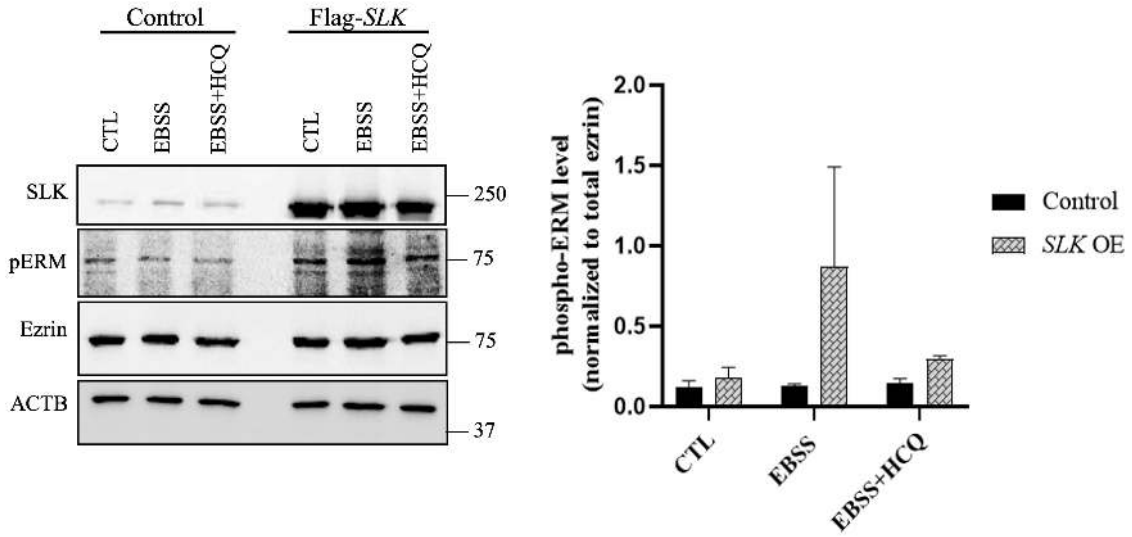

Figure 4.27 Phospho-ERM level in starvation conditions in SLK overexpressing HEK293T cells. Immunoblot analysis of phospho-ERM protein (left panel) and graphical presentation (right). Overexpression was occurred via transfection with flag-SLK vector. pcDNA3.1 vector was used as control. n=2, representative figure was obtained on 28.03.2023.

We also tried to specify further the phosphorylation activity of SLK on pERM protein in both control and autophagy-induced conditions. After the repression of SLK level in HEK293T and deletion of SLK in SF188 cells, we could not see significant attenuation in phospho-ERM molecules, as shown in Figure 3.26 and Figure 3.27. The phosphorylation level is not entirely zero based on just SLK because ERM proteins are not target of SLK only. This reminds us of the phenomenon of several kinase proteins regulating modifications of ERM molecules. For example, Rho-A or FAK activity can compensate impairment of the SLK effect on ERM molecules.

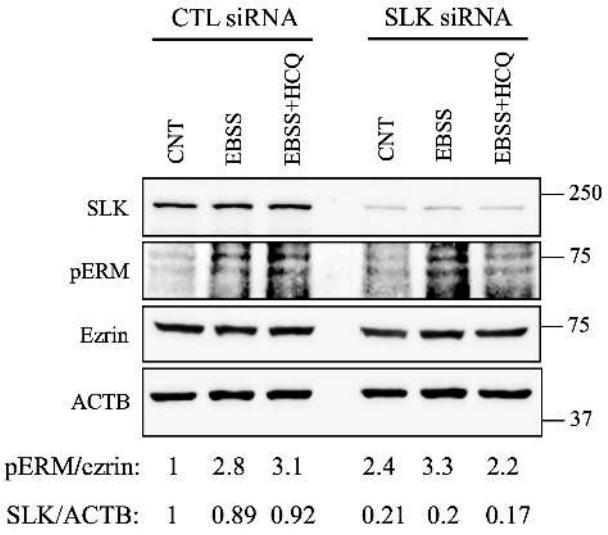

Figure 4.28 Immunoblot analysis of phospho-ERM molecules after SLK knockdown and starvation-induced autophagy. Non-targeting siRNA was used as control. SLK targeting siRNA was transfected into HEK293T cells for knockdown n=3, p-value >0.05 for pERM/ezrin ratio. Representative figure was obtained on 01.06.2023.

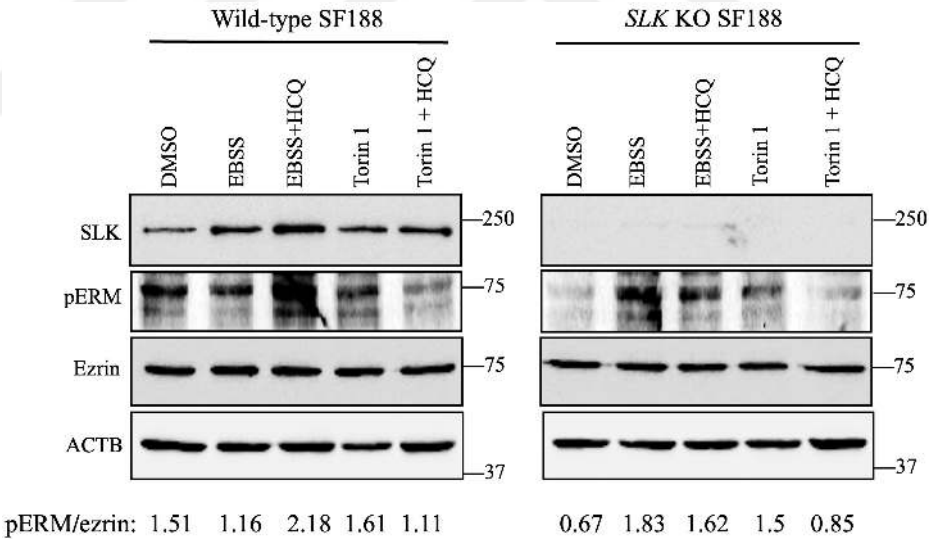

Figure 4.29 In SLK KO SF188 cells phospho-ERM levels and the ratio of LC3II/LC3I is decreased. Immunoblot analysis of phosho-ERM molecules in wild-type and SLK KO SF188 cells and starvation-induced autophagy conditions. n=3, p-value >0.05 for pERM/ezrin ratio. Representative figure was obtained on 16.06.2023.

Lastly, we investigated K63R mutant of SLK protein on phosphorylation of Erm molecules. Too observe this, immunoblot analysis was performed with HEK293T cells transfected with pcDNA3.1 as control, flag-SLK^{K63R}, and flag-SLK plasmids. According

to the result presented on Figure 3.28, phosphorylation level is slightly decreased with kinase-dead mutant type of SLK, and obvious increase can be observed on phospho-ERM level with SLK overexpression.

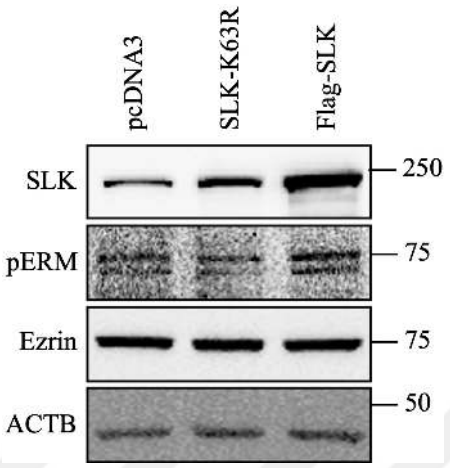

Figure 4.30 K63R mutation prevent the phosphorylation of ERM proteins by SLK. Site-directed mutagenesis was performed with flag-tagged SLK plasmid. HEK293T cells were transfected with control plasmid, kinase-dead SLK and flag-SLK plasmids. 18.05.2023.

4.9 Could Ezrin and Paxillin proteins be an autophagic target?

We analyzed SLK, paxillin and ezrin level under autophagy stimulating conditions to see whether these proteins are among autophagy targets. As it can be seen in Figure 3.28, level all these molecules are increasing upon starvation induction compared to control and torin1-treated conditions. Also as expected suppression of autophagy by hydroxychloroquine increases paxillin level. Considered LC3 and FA relation and the effect of autophagy on FA turnover explains this result.

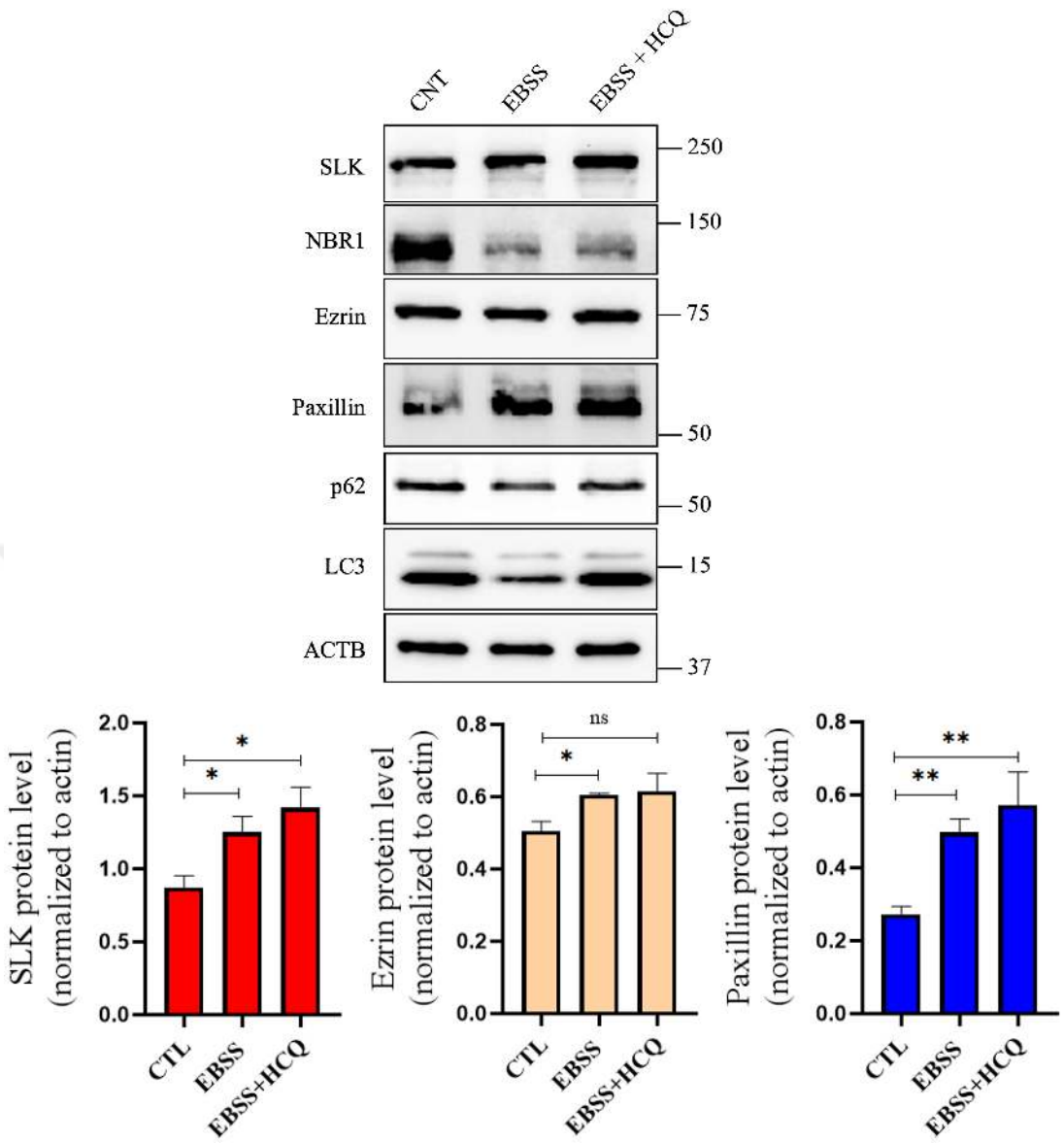

Figure 4.31 Immunoblot analysis of paxillin and ezrin protein level under autohagy stimulating conditions. Graphs represents SLK, ezrin and paxillin protein level normalized to ß-actin level. n=3; ns, p-value >0.05; *, p-value <0.05; **, p-value <0.005 representative figure from 09.02.2023.

4.10 Analysis of New Drug Candidates on SLK Activity and Cell Migration

There are a number of chemotherapeutic drugs to target the activity of various kinase protein to cope with highly proliferative and metastatic characteristics of tumor cells. In pediatric brain tumor cases, struggling with cellular migration and metastasis can be a great adjuvant therapy opportunity. Accordingly, we determined several candidates that

can target SLK protein and impair migration capability of tumor cells. Candidates are listed in Table 3.1.

Table 4-1 SLK Inhibitor candidate drugs. IC50 values were obtained from manufacturers.

Chemical	IC50	Reference
Erlotinib	830 nM	(Seto et al., 2014)
GSK3037619A	199 nM	(Elkins et al., 2016)
SB-633825	66 nM	(Elkins et al., 2016)
Danusertib	61 nM	(Carpinelli et al., 2007)
RN486	21 nM	(D. Xu et al., 2012)
K-00546	8.9	(Fedorov et al., 2011)
SCHEMBL21067926	*	(Pike et al., 2008b)

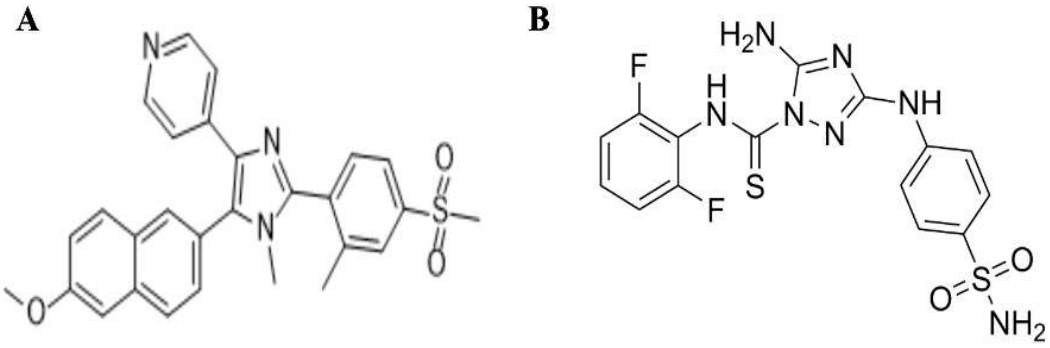

Figure 4.32 Chemical structure of (A) SB-633825 and (B) K00546 inhibitors.

As a result of our examinations, drugs named SB-633825 and K-00545 were selected as the most promising choice based on their chemical structure and results from reference studies. Firstly, we checked ERM proteins' phosphorylation level to determine when it can be considered as SLK is inhibited. According to the analysis of phosphorylation of ERM proteins shown in Figure 3.29A, both inhibitors are efficient at 30 mins and 1 hour of treatment. SB-633825 drug was used for continued experiments for its higher efficiency and lower toxicity for SF188 cells. To point out the effect of the inhibitor on SLK protein, it was applied to SLK overexpressing HEK293T cells. Result is presented in figure 3.29B.

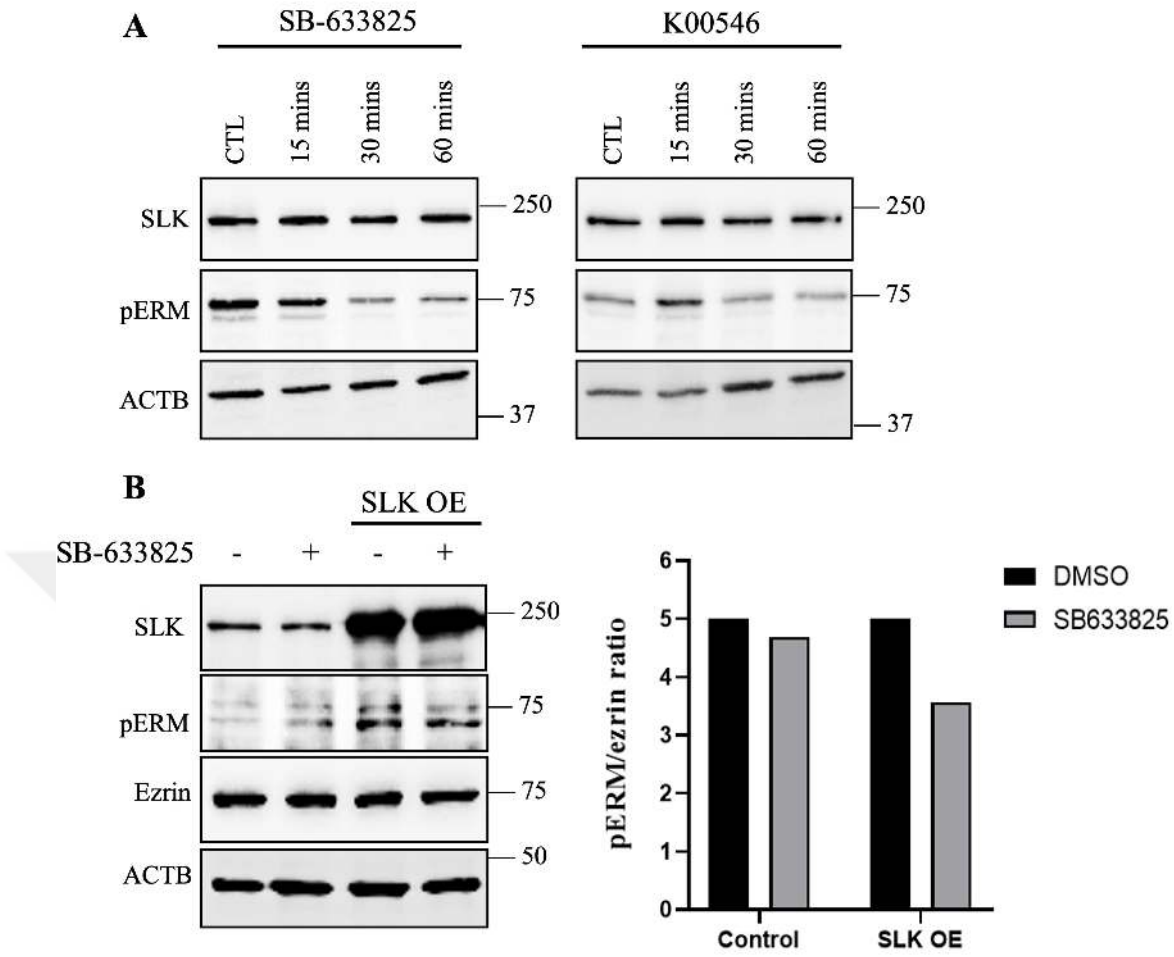

Figure 4.33 SLK inhibition by SB-633825 reduced the phospho-ERM level especially in SLK overexpression condition. 1 µM SB-633825 and K-00546 was applied to wild-type and SLK overexpressing HEK293T cells. (A) IB analysis upon the ttreatment of HEK293T at different time scales n=2, Representative figure from 2.1.23. (B) SB-633825 was applied to transfected HEK293T cells with flag-SLK plasmid. n=1 23.06.2023.

Our first aim in this study is targeting the migration capability of cells and promising candidates for the treatment of pediatric glioblastoma. Consequently, drugs were analyzed to check whether they affected the migration capability of SF188 cells. We performed a scratch test with SB-633825-treated SF188 cells. There was no significant change in the wound closure ratio, as shown in Figure 3.30

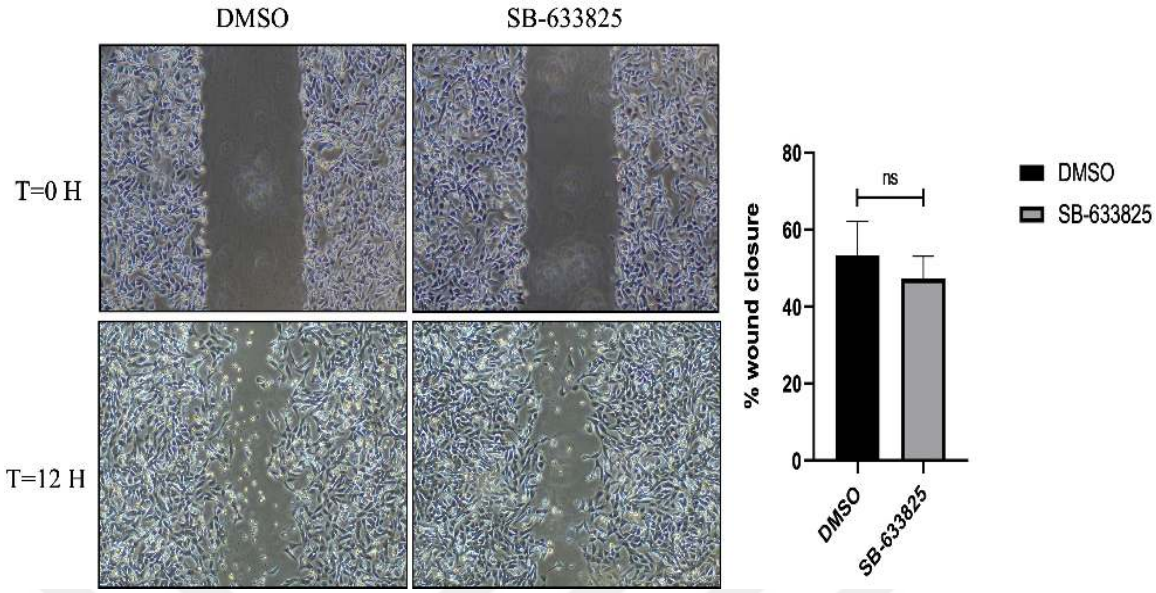

Figure 4.34 Wound healing ratio was not affected by SLK inhibitor drug. SF188 cells were incubated with 1 µM SB-633825 drug. DMSO was applied as control condition. n=3, p-value >0.05. Representative image from 24.05.2023.

4.11 Investigation of the Effect of SLK on Cellular Viability and Drug Resistance

MTT assay was performed to detect whether SLK protein has a potential contribution to pediatric glioblastoma chemotherapy drug resistance. The most common drugs were applied on wild-type and SLK KO cells at different concentrations. Significant changes were detected in cellular survival against carboplatin and etoposide treatment. Interestingly, a decrease in lower concentrations is higher despite it is not statistically significant.

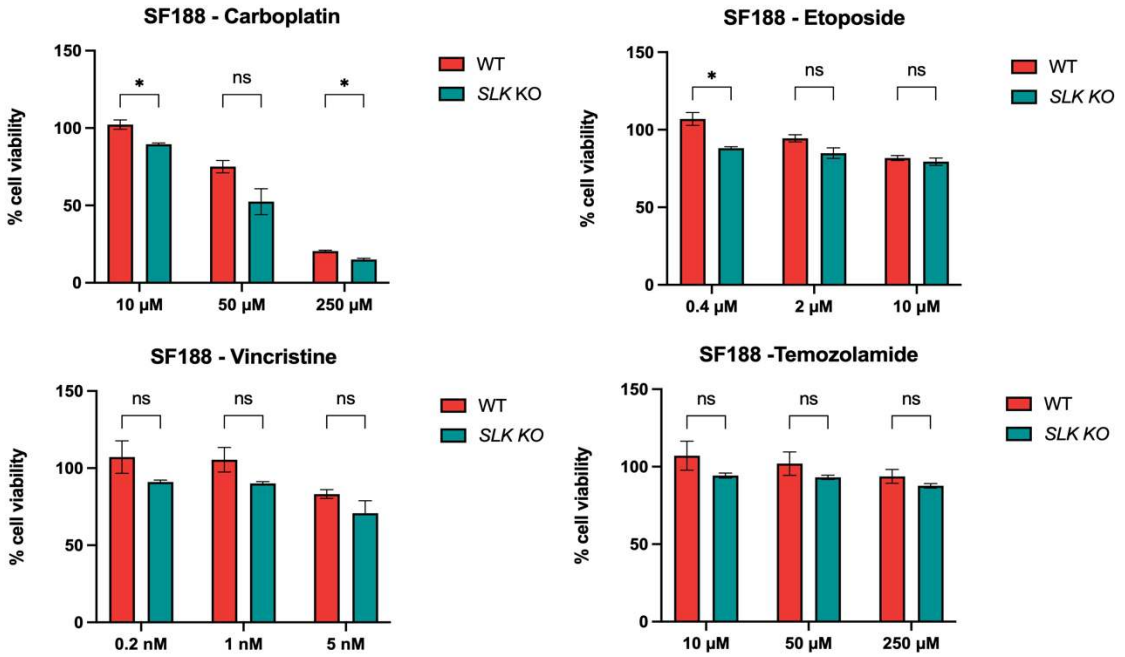

Figure 4.35 MTT assay is performed with wild-type and SLK KO SF188 cells. Cells were incubated with related drug for 48 hours. n=3. ns, p-value >0.05, *, p-value <0.05. 04-07.06.2023.

Moreover, conventional chemotherapeutic drugs were applied to SF188 cell in combined with SB-633825 and K-00546 to see whether there is any change in cellular survival. Relative inhibition of SLK did not affect the resistance of pediatric glioblastoma cells against cancer drug. Conversely, SB-633825 treatment resulted in higher survival compared to control condition. However, K-00546 cause toxicity on SF188 cells. All results were showed in Figure 3.32 and Figure 3.33.

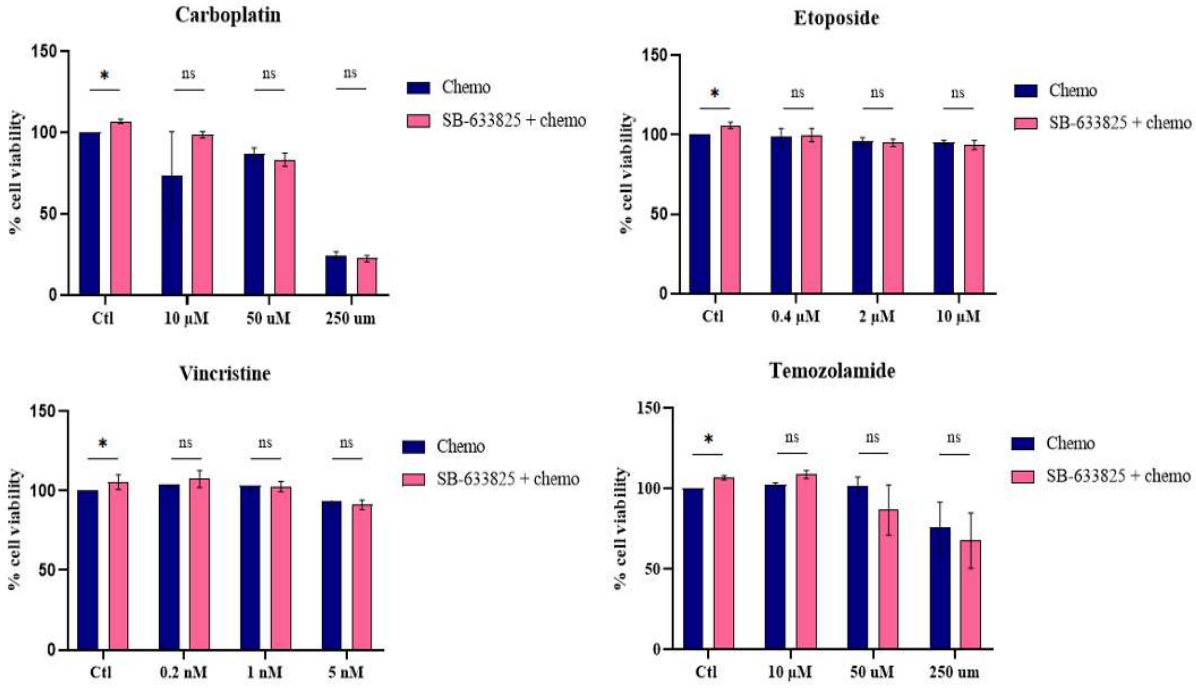

Figure 4.36 MTT assay was performed with chemotherapies alone and combined with SB-633825 as an SLK inhibitor molecule. DMSO was used as control condition alone and combined with SB-633825. Cells were incubated with related drugs for 48 hours. n=3, ns, p-value >0.05; *, p-value <0.05. 16.4.2023-07.05.2023.

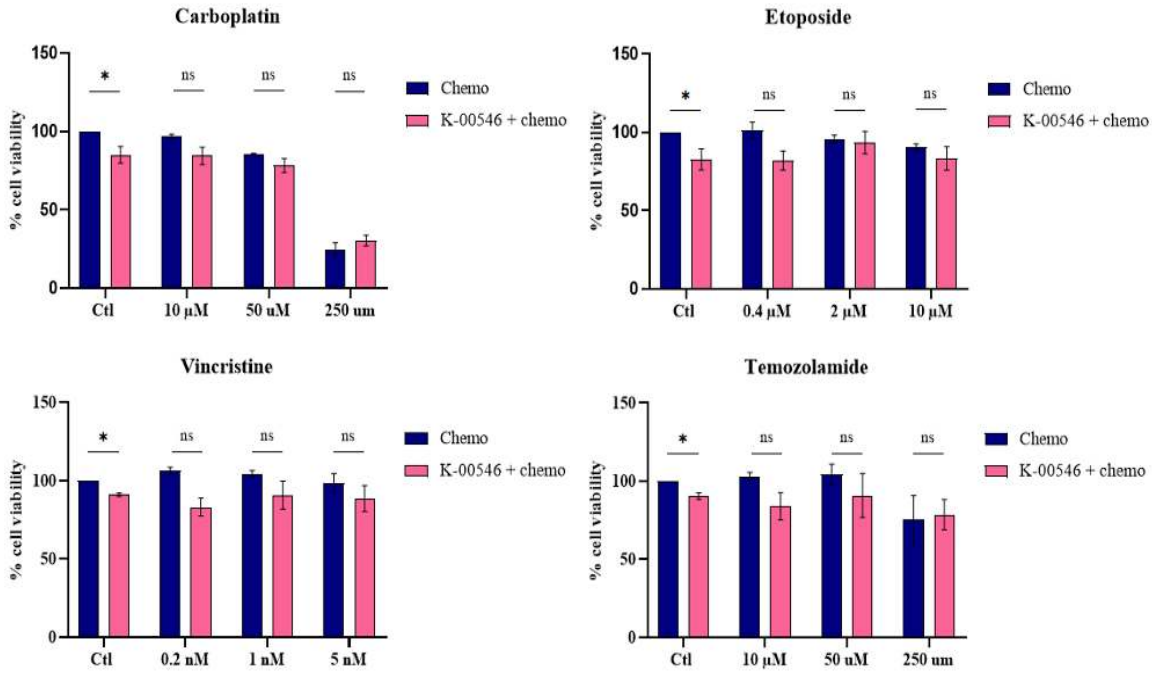

Figure 4.37 MTT assay was performed with chemotherapies alone and combined with K-00546 as an SLK inhibitor molecule. DMSO was used as control condition alone and combined with K-00546. Cells were incubated with related drugs for 48 hours. n=3, ns, p-value >0.05; *, p-value <0.05. 16.4.2023-07.05.2023.

Chapter 5:
DISCUSSION

Glioblastoma is a highly lethal and aggressive tumor type. The extreme infiltrative and invasive nature of tumor cells can be considered the main factor of poor prognosis. The studies showing the contribution of SLK in cellular motility encouraged scientists to investigate whether this kinase has a role in glioma invasiveness. The requirement of SLK in cellular migration and focal adhesion turnover was revealed by various studies (Wagner et al., 2008). It is also shown that SLK is upregulated in glioma cells and postoperative survival of glioma patients is altered with SLK expression level (K. Wang et al., 2018). We also observed high expression of SLK in pediatric glioblastoma and its effect on cellular migration. Therefore, our results suggest that SLK can be a drug target for restricting invasion capability of pHGG tumors. The epithelial-mesenchymal transition has been linked to cancer development and imparts metastatic qualities on cancer cells by increasing motility, invasion, and defense against apoptotic stimulation (Mittal, 2018). Since SLK target proteins have important roles in EMT as we mentioned in Chapter 1, EMT promoted by SLK-related proteins can also be investigated in pediatric glioblastoma. The roles of SLK in developmental stages could also support this idea.

The proteomic analysis performed in control and starvation conditions with HeLa cells shows an interaction between SLK and ATG5 proteins. In our experiments, we can see these proteins' interaction and close localization in coIP and confocal analysis. However, in pulldown assay we encountered a stickiness issue with His-ATG5 on Sepharose bead. We tried to overcome this with more washing steps. Even though the protein band was observed as faint, the experiment should be repeated for a more precise result. Pulldown assay performed with recombinant GST-Kinase of SLK and ATG5 can give foresight to detect the interaction site of the proteins. Further analysis can be performed with various mutant protein versions and bioinformatic methods like molecular docking.

The effect of SLK on LC3 lipidation was displayed with many repeats during this study. However, SLK also dramatically affects especially HEK293T cells, causing detachment of cells from the surface and decreased survival. In the culture, the cells transfected with pcDNA3.1 as control were observed in usual morphology while SLK transfected cells appeared in a rounder morphology and detached from surface extreme

easily. On the other hand, concentration of SLK plasmid should be enough to see the phosphorylation of ERM proteins. That is why, immunoblotting analysis performed with SLK overexpressing HEK293T cells has higher variance. Since these fluctuations affect the error bar levels, differences were calculated as statistically nonsignificant in several results in which we can see the difference clearly. Also, to see the SLK effect on pediatric glioblastoma cells we constructed lentiviral vector containing SLK open reading frame. Nevertheless, because of this apoptosis inducing action of SLK, construction of an inducible overexpression vector was decided. Therefore, overexpression of SLK protein can be restricted easily, and the survival of the cells can be improved. In addition, immunoblotting analysis showing the elevation of LC3 lipidation is a good starting point. However, the effect of SLK must be further explained. For example, this difference in LC3 lipidation upon SLK overexpression may cause by a transcriptional increase of LC3. qPCR analysis can be performed to reply to this interrogation. Also, confocal analysis can be beneficial to see the distribution of LC3-II with hydroxychloroquine treatment upon autophagy induction. We know that SLK has an essential role in cytoskeleton components. So, the confocal microscopy method with SLK overexpressing cells can observe the difference in autophagosome distribution dependent on cytoskeleton rearrangement.

Various kinase proteins, including FAK, RhoA, and LOK regulated phosphorylation ERM proteins. Also, ERM phosphorylation could depend on the location of proteins (Machicoane, de Frutos, Fink, Rocancourt, Lombardi, Garel, et al., 2014b; Viswanatha et al., 2012) Also, other regulating proteins can compensate for the effect of SLK. For example, in a study, LOK/SLK KO cell lines have elevated active RhoA protein that can cause phosphorylation of ERM (Zaman et al., 2021). That is why SLK knockdown and knockout models do not cause a dramatic decrease in the phospho-ERM level. Experiments with specific inhibitors affecting regulator proteins such as FAK and RhoA can be advantageous for the investigation of SLK more precise manner.

It was shown that SLK phosphorylates paxillin on Ser250 residue and this phosphorylation is required for cellular migration and turnover of focal adhesion molecules (Quizi et al., 2013b). Since an antibody specific to Ser250 residue is not obtained commercially, we purchased the most similar antibody possible. However, this antibody is not helpful for detecting the phosphorylated paxillin by SLK. Moreover, SLK is colocalized with adhesion molecules in the region close to cellular membrane (Quizi et

al., 2013b). For this reason, the phosphorylation activity of SLK on focal adhesion or ERM proteins may be dependent to localization into the cells. We checked phosphorylation level of total paxillin and ERM proteins in this study. However, immunofluorescence analysis with these phospho-antibodies can be more accurate approach. The relevance of paxillin and autophagy in pediatric glioblastoma has emerged as an attractive field of investigation in our research. Paxillin, a crucial regulator of cell migration and cancer progression, has been found as a predictive biomarker in glioblastoma, predicting poor survival. Furthermore, its overexpression has been associated with glioblastoma tumor aggressiveness, implying its potential as a therapeutic target for this highly aggressive central nervous system cancer (Sun et al., 2017). Autophagy, a cellular mechanism involved in the destruction and recycling of damaged organelles and proteins, on the other hand, has been linked to cancer progression and resistance to therapy (Karakaş & Gözüaçik, 2014). So, autophagy is an important target for the cancer treatments. It is shown that autophagy repression via ATG5 and ATG7 knockdown causes abnormalities in focal adhesions assembly in breast cancer cells. Disassembly of focal adhesions resulted an increase in size and number of FAs (Sharifi et al., 2016). Phosphorylation of paxillin has an important role in the turnover of the protein cell motility dependent on membrane dynamics. Although it is known that paxillin can be degraded by proteasome system (Abou Zeid et al., 2006b), autophagy is also responsible for paxillin degradation. This is supported by the ubiquitination of paxillin since autophagy receptor proteins such as NBR1 and p62 target ubiquitinated proteins for autophagic degradation (Rogov et al., 2014). Indeed, colocalization of paxillin with LC3 and accumulation upon Bafilomycin A treatment was observed in breast cancer cells was observed in mouse mammary tumor cells (Sharifi et al., 2016). Lastly, cell motility required autophagic breakdown of paxillin. However, we could not observe the degradation of paxillin upon starvation and autophagic inhibition via hydroxychloroquine followed by starvation conditions in pHGG cells. Conversely, we saw an increase in paxillin level upon starvation. However, paxillin degradation may require a longer time starvation for promoting focal adhesion turnover. Moreover, autophagy deficient in vitro models could be checked for paxillin dynamics. In conclusion, these experiments should be repeated for better results. Even though some aspects of paxillin was studied with adult glioblastoma, the interaction between paxillin and autophagy in pediatric glioblastoma is still mostly unknown.

SB-633825 and K00546 inhibitors were selected as SLK inhibitors by analyzing its chemical structure and literature review. SB-633825 is evaluated as a potent and ATP-competitive inhibitor of TIE2, LOK (STK10) and BRK. It can inhibit cancer cell growth and angiogenesis. In addition, K00546 is an inhibitor for CDK1, CDK2, CDK3 (Elkins et al., 2016). Although some changes were displayed upon treatments of these inhibitors, for evaluating the druggable feasibility, more specific chemicals should be utilized to investigate the role of SLK on focal adhesion and ERM molecules. Also, more specific inhibitor molecules for SLK would be essential in exploring the importance of kinase activity for the migration capability of pediatric glioblastoma cells.

Lastly, even though SLK depletion did not cause a striking change in overall cell, the most observable change was observed upon carboplatin and etoposide treatments. These two drugs affect DNA synthesis and entrance into further cell cycle stage. This result can point out the role of SLK on cell-cycle regulation.

We proposed a schematic model representing the role of SLK-mediated autophagy on paxillin focal adhesion turnover and cytoskeleton reorganization as shown in Figure 4.1

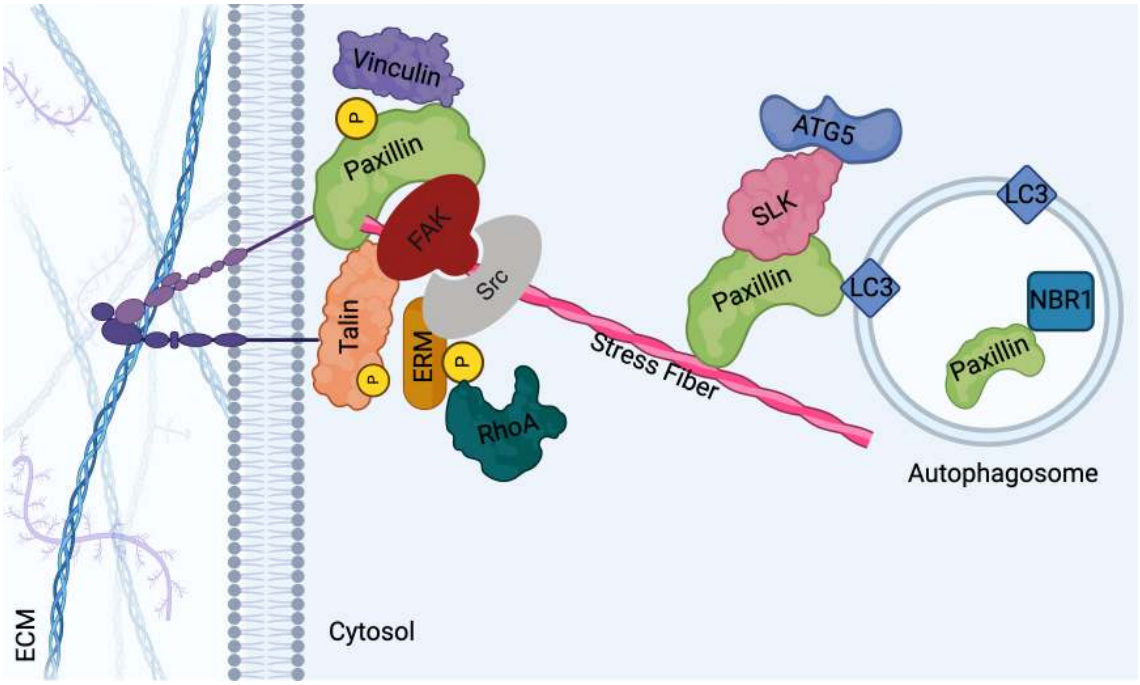

Figure 5.1 The role of SLK-mediated autophagy on paxillin turnover and cytoskeleton reorganization. Created by Biorender.

Chapter 6:
CONCLUSION AND FUTURE PROSPECTS

In this thesis, we showed the interaction between SLK and ATG5 protein under autophagy-stimulating conditions. The effect of SLK protein on autophagic flux and significant changes in LC3 lipidation, and relatively impaired degradation of autophagy receptors were detected. A recombinant protein containing the catalytic domain of SLK protein was produced. This recombinant protein will be used for in vitro kinase experiments. The phosphorylation level of ERM proteins and paxillin, one of the focal adhesion proteins, by SLK, was investigated under control and autophagy-promoting situations. Further studies will be on localized phosphorylation of the proteins, and interactions with other autophagic molecules will be investigated through microscopy methods.

Moreover, the effect of SLK protein on the migration capacity of pediatric glioblastoma was shown clearly. Further analysis to examine the kinase activity of SLK on cellular motility will be continued with more specific antibodies and inhibitor drug candidate molecules. Many unanswered questions exist about pediatric glioblastoma, SLK protein, and autophagy. Preliminary results and literature review suggest that SLK is a drug target for restricting the invasion capacity of pediatric glioblastoma cells, which is a helpful approach preoperative stage.

In considering the experimental results of our study, we aim to shed light on exciting possibilities and potential breakthroughs in our field. To investigate the functional role of SLK protein in the autophagy pathway, activation of various upstream and downstream molecules of autophagy will be checked with wild-type and SLK KO pHGG cell lines. For instance, we saw that SLK has an essential influence on LC3 lipidation. That is why autophagosome distribution and autophagosome and lysosome fusion could be analyzed by confocal microscopy. The SLK-dependent phosphorylation level of the paxillin protein should be examined more precisely. Also, the turnover of focal adhesion molecules should be investigated in autophagy-induced and autophagy-impaired cells to display the importance of autophagic degradation in the migration of pHGG cells. As we mentioned before, this turnover process may be dominant in the adhesion sites of leading edges. Therefore, microscopy analysis would be beneficial by examining the localization of autophagosomes, adhesion molecules, and ERM

molecules. In vitro, kinase assay could be performed to validate ERM and paxillin phosphorylation via SLK. Wild-type and SLK KO pHGG cells will be inserted in mouse models. Thus, infiltration and invasion capability will be observed. Moreover, the effect of the chemicals inhibiting the kinase activity of SLK will be evaluated as a chemotherapy drug. In conclusion, the SLK-autophagy relation and the effect of SLK on migration and invasion of pHGG cells in a cytoskeleton-related manner will be investigated more deeply,

BIBLIOGRAPHY

1. Abou Zeid, N., Vallés, A.-M., & Boyer, B. (2006a). Serine phosphorylation regulates paxillin turnover during cell migration. *Cell Communication and Signaling*, *4*(1), 8. https://doi.org/10.1186/1478-811X-4-8
2. Abou Zeid, N., Vallés, A.-M., & Boyer, B. (2006b). Serine phosphorylation regulates paxillin turnover during cell migration. *Cell Communication and Signaling*, *4*(1), 8. https://doi.org/10.1186/1478-811X-4-8
3. Aguilera, M. O., Berón, W., & Colombo, M. I. (2012). The actin cytoskeleton participates in the early events of autophagosome formation upon starvation induced autophagy. *Autophagy*, *8*(11), 1590–1603. https://doi.org/10.4161/auto.21459
4. Ahir, B. K., Engelhard, H. H., & Lakka, S. S. (2020). Tumor Development and Angiogenesis in Adult Brain Tumor: Glioblastoma. In *Molecular Neurobiology* (Vol. 57, Issue 5, pp. 2461–2478). Springer. https://doi.org/10.1007/s12035-020-01892-8
5. Ahmed, S., Pryce, B. R., Al-Zahrani, K. N., & Sabourin, L. A. (2018). The LIM domain binding protein 1, Ldb1, has distinct roles in Neu-induced mammary tumorigenesis. *Biochimica et Biophysica Acta - Molecular Cell Research*, *1865*(11), 1590–1597. https://doi.org/10.1016/j.bbamcr.2018.08.013
6. Akkoc, Y., Dalci, K., Karakas, H. E., Erbil-Bilir, S., Yalav, O., Sakman, G., Celik, F., Arikan, S., Zeybek, U., Ergin, M., Akkiz, H., Dilege, E., Dengjel, J., Dogan-Ekici, A. I., & Gozuacik, D. (2023). Tumor-derived CTF1 (cardiotrophin 1) is a critical mediator of stroma-assisted and autophagy-dependent breast cancer cell migration, invasion and metastasis. *Autophagy*, *19*(1), 306–323. https://doi.org/10.1080/15548627.2022.2090693
7. Al-Zahrani, K. N., Abou-Hamad, J., Cook, D. P., Pryce, B. R., Hodgins, J. J., Labrèche, C., Robineau-Charette, P., de Souza, C. T., Bell, J. C., Auer, R. C., Ardolino, M., Vanderhyden, B. C., & Sabourin, L. A. (2020). Loss of the Ste20-like kinase induces a basal/stem-like phenotype in HER2-positive breast cancers. *Oncogene*, *39*(23), 4592–4602. https://doi.org/10.1038/s41388-020-1315-3
8. Al-Zahrani, K. N., Sekhon, P., Tessier, D. R., Yockell-Lelievre, J., Pryce, B. R., Baron, K. D., Howe, G. A., Sriram, R. K., Daniel, K., Mckay, M., Lo, V., Quizi, J., Addison, C. L., Ee Gruslin, A., & Sabourin, L. A. (2013). *Essential Role for the SLK Protein Kinase in Embryogenesis and Placental Tissue Development*. https://doi.org/10.1002/dvdy
9. Aplin, A., Jasionowski, T., Tuttle, D. L., Lenk, S. E., & Dunn, W. A. (1992). Cytoskeletal elements are required for the formation and maturation of autophagic vacuoles. *Journal of Cellular Physiology*, *152*(3), 458–466. https://doi.org/10.1002/jcp.1041520304
10. Bagci, H., Sriskandarajah, N., Robert, A., Boulais, J., Elkholi, I. E., Tran, V., Lin, Z. Y., Thibault, M. P., Dubé, N., Faubert, D., Hipfner, D. R., Gingras, A. C., & Côté, J. F. (2020). Mapping the proximity interaction network of the Rho-family GTPases reveals signalling pathways and regulatory mechanisms. *Nature Cell Biology*, *22*(1), 120–134. https://doi.org/10.1038/s41556-019-0438-7

11. Baron, K. D., Al-Zahrani, K., Conway, J., Labrèche, C., Storbeck, C. J., Visvader, J. E., & Sabourin, L. A. (2015a). Recruitment and activation of SLK at the leading edge of migrating cells requires Src family kinase activity and the LIM-only protein 4. *Biochimica et Biophysica Acta (BBA) - Molecular Cell Research*, *1853*(7), 1683–1692. https://doi.org/https://doi.org/10.1016/j.bbamcr.2015.04.003
12. Baron, K. D., Al-Zahrani, K., Conway, J., Labrèche, C., Storbeck, C. J., Visvader, J. E., & Sabourin, L. A. (2015b). Recruitment and activation of SLK at the leading edge of migrating cells requires Src family kinase activity and the LIM-only protein 4. *Biochimica et Biophysica Acta - Molecular Cell Research*, *1853*(7), 1683–1692. https://doi.org/10.1016/j.bbamcr.2015.04.003
13. Bar-Peled, L., & Sabatini, D. M. (2014). Regulation of mTORC1 by amino acids. *Trends in Cell Biology*, *24*(7), 400–406. https://doi.org/10.1016/j.tcb.2014.03.003
14. BELLIS, S. L., PERROTTA, J. A., CURTIS, M. S., & TURNER, C. E. (1997). Adhesion of fibroblasts to fibronectin stimulates both serine and tyrosine phosphorylation of paxillin. *Biochemical Journal*, *325*(2), 375–381. https://doi.org/10.1042/bj3250375
15. Bershadsky, A., Chausovsky, A., Becker, E., Lyubimova, A., & Geiger, B. (1996). Involvement of microtubules in the control of adhesion-dependent signal transduction. *Current Biology*, *6*(10), 1279–1289. https://doi.org/10.1016/S0960-9822(02)70714-8
16. Bølge Tysnes, B., & Mahesparan, R. (2001). Biological Mechanisms of Glioma Invasion and Potential Therapeutic Targets. *Journal of Neuro-Oncology*, *53*(2), 129–147. https://doi.org/10.1023/A:1012249216117
17. Bourguignon, L. Y. W. (2008). Hyaluronan-mediated CD44 activation of RhoGTPase signaling and cytoskeleton function promotes tumor progression. *Seminars in Cancer Biology*, *18*(4), 251–259. https://doi.org/10.1016/j.semcancer.2008.03.007
18. Boyle, S., & Kopecki, Z. (2020). Mechanical Force and Actin Dynamics during Cutaneous Squamous Cell Carcinoma (cSCC) Progression: Opportunities for Novel Treatment Modalities. In *Squamous Cell Carcinoma - Hallmark and Treatment Modalities*. IntechOpen. https://doi.org/10.5772/intechopen.86041
19. Bredel, M., Pollack, I. F., Hamilton, R. L., & James, C. D. (1999). Epidermal growth factor receptor expression and gene amplification in high-grade non-brainstem gliomas of childhood. *Clinical Cancer Research : An Official Journal of the American Association for Cancer Research*, *5*(7), 1786–1792.
20. Broniscer, A. (2006). Past, present, and future strategies in the treatment of high-grade glioma in children. In *Cancer Investigation* (Vol. 24, Issue 1, pp. 77–81). https://doi.org/10.1080/07357900500449702
21. Burakov, A. V, Zhapparova, O. N., Kovalenko, O. V, Zinovkina, L. A., Potekhina, E. S., Shanina, N. A., Weiss, D. G., Kuznetsov, S. A., & Nadezhdina, E. S. (2008). Ste20-related protein kinase LOSK (SLK) controls microtubule radial array in interphase. *Molecular Biology of the Cell*, *19*(5), 1952–1961.
22. Burdyga, A., Conant, A., Haynes, L., Zhang, J., Jalink, K., Sutton, R., Neoptolemos, J., Costello, E., & Tepikin, A. (2013). cAMP inhibits migration, ruffling and paxillin

accumulation in focal adhesions of pancreatic ductal adenocarcinoma cells: Effects of PKA and EPAC. *Biochimica et Biophysica Acta (BBA) - Molecular Cell Research*, *1833*(12), 2664–2672. https://doi.org/https://doi.org/10.1016/j.bbamcr.2013.06.011

23. Caramia, M., Sforna, L., Franciolini, F., & Catacuzzeno, L. (2019). The Volume-Regulated Anion Channel in Glioblastoma. *Cancers*, *11*(3), 307. https://doi.org/10.3390/cancers11030307
24. Carpinelli, P., Ceruti, R., Giorgini, M. L., Cappella, P., Gianellini, L., Croci, V., Degrassi, A., Texido, G., Rocchetti, M., Vianello, P., Rusconi, L., Storici, P., Zugnoni, P., Arrigoni, C., Soncini, C., Alli, C., Patton, V., Marsiglio, A., Ballinari, D., … Moll, J. (2007). PHA-739358, a potent inhibitor of Aurora kinases with a selective target inhibition profile relevant to cancer. *Molecular Cancer Therapeutics*, *6*(12), 3158–3168. https://doi.org/10.1158/1535-7163.MCT-07-0444
25. Carreno, S., Kouranti, I., Glusman, E. S., Fuller, M. T., Echard, A., & Payre, F. (2008). Moesin and its activating kinase Slik are required for cortical stability and microtubule organization in mitotic cells. *Journal of Cell Biology*, *180*(4), 739–746. https://doi.org/10.1083/jcb.200709161
26. Cary, L. A. (1999). Focal adhesion kinase in integrin-mediated signaling. *Frontiers in Bioscience*, *4*(1–3), d102. https://doi.org/10.2741/Cary
27. Catacuzzeno, L., & Franciolini, F. (2018). Role of KCa3.1 Channels in Modulating Ca2+ Oscillations during Glioblastoma Cell Migration and Invasion. *International Journal of Molecular Sciences*, *19*(10), 2970. https://doi.org/10.3390/ijms19102970
28. Cavallaro, U., & Christofori, G. (2004). Cell adhesion and signalling by cadherins and Ig-CAMs in cancer. *Nature Reviews Cancer*, *4*(2), 118–132. https://doi.org/10.1038/nrc1276
29. *cBioPortal*. (n.d.).
30. Chaar, Z., O'Reilly, P., Gelman, I., & Sabourin, L. A. (2006). v-Src-dependent Down-regulation of the Ste20-like Kinase SLK by Casein Kinase II. *Journal of Biological Chemistry*, *281*(38), 28193–28199. https://doi.org/10.1074/jbc.M605665200
31. Chen, C.-Y., Chen, J., He, L., & Stiles, B. L. (2018). PTEN: Tumor Suppressor and Metabolic Regulator. *Frontiers in Endocrinology*, *9*. https://doi.org/10.3389/fendo.2018.00338
32. Conway, J., Al-Zahrani, K. N., Pryce, B. R., Abou-Hamad, J., & Sabourin, L. A. (2017). *Transforming growth factor β-induced epithelial to mesenchymal transition requires the Ste20-like kinase SLK independently of its catalytic activity*. www.impactjournals.com/oncotarget
33. Cortesio, C. L., Boateng, L. R., Piazza, T. M., Bennin, D. A., & Huttenlocher, A. (2011). Calpain-mediated Proteolysis of Paxillin Negatively Regulates Focal Adhesion Dynamics and Cell Migration. *Journal of Biological Chemistry*, *286*(12), 9998–10006. https://doi.org/10.1074/jbc.M110.187294
34. Cox, E. A., & Huttenlocher, A. (1998). Regulation of integrin-mediated adhesion during cell migration. *Microscopy Research and Technique*, *43*(5), 412–419. https://doi.org/10.1002/(SICI)1097-0029(19981201)43:5<412::AID-JEMT7>3.0.CO;2-F

35. Cuddapah, V. A., Robel, S., Watkins, S., & Sontheimer, H. (2014). A neurocentric perspective on glioma invasion. *Nature Reviews Neuroscience*, *15*(7), 455–465. https://doi.org/10.1038/nrn3765
36. Cybulsky, A. V., Papillon, J., Guillemette, J., Belkina, N., Patino-Lopez, G., & Torban, E. (2018). Ste20-like kinase, SLK, a novel mediator of podocyte integrity. *American Journal of Physiology - Renal Physiology*, *315*(1), F186–F198. https://doi.org/10.1152/ajprenal.00238.2017
37. Cybulsky, A. V, Takano, T., Papillon, J., Hao, W., Mancini, A., Di Battista, J. A., Cybulsky, M. I., & Battista, D. J. (2007). The 3-untranslated region of the Ste20-like kinase SLK regulates SLK expression. *Am J Physiol Renal Physiol*, *292*, 845–852. https://doi.org/10.1152/ajprenal.00234.2006.-Ste20-like
38. Dan, I., Watanabe, M. N., & Kusumi, A. (2001). The Ste20 group kinases as regulators of MAP kinase cascades. *Trends in Cell Biology*, *11*(5), 220–230.
39. de Gooijer, M. C., Guillén Navarro, M., Bernards, R., Wurdinger, T., & van Tellingen, O. (2018). An Experimenter's Guide to Glioblastoma Invasion Pathways. *Trends in Molecular Medicine*, *24*(9), 763–780. https://doi.org/10.1016/j.molmed.2018.07.003
40. De Jamblinne, C. V., Decelle, B., Dehghani, M., Joseph, M., Sriskandarajah, N., Leguay, K., Rambaud, B., Lemieux, S., Roux, P. P., Hipfner, D. R., & Carréno, S. (2020). STRIPAK regulates Slik localization to control mitotic morphogenesis and epithelial integrity. *Journal of Cell Biology*, *219*(11). https://doi.org/10.1083/JCB.201911035
41. Deakin, N. O., Pignatelli, J., & Turner, C. E. (2012). Diverse roles for the paxillin family of proteins in cancer. *Genes & Cancer*, *3*(5–6), 362–370. https://doi.org/10.1177/1947601912458582
42. Delarosa, S., Guillemette, J., Papillon, J., Han, Y.-S., Kristof, A. S., & Cybulsky, A. V. (2011). Activity of the Ste20-like kinase, SLK, is enhanced by homodimerization. *Am J Physiol Renal Physiol*, *301*, 554–564. https://doi.org/10.1152/ajprenal.00062.2011.-The
43. Desai, A., & Mitchison, T. J. (1997). MICROTUBULE POLYMERIZATION DYNAMICS. *Annual Review of Cell and Developmental Biology*, *13*(1), 83–117. https://doi.org/10.1146/annurev.cellbio.13.1.83
44. Diaz, A. K., & Baker, S. J. (2014). The genetic signatures of pediatric high-grade glioma: No longer a one-act play. In *Seminars in Radiation Oncology* (Vol. 24, Issue 4, pp. 240–247). W.B. Saunders. https://doi.org/10.1016/j.semradonc.2014.06.003
45. Donson, A. M., Addo-Yobo, S. O., Handler, M. H., Gore, L., & Foreman, N. K. (2007). MGMT promoter methylation correlates with survival benefit and sensitivity to temozolomide in pediatric glioblastoma. *Pediatric Blood & Cancer*, *48*(4), 403–407. https://doi.org/10.1002/pbc.20803
46. Elkins, J. M., Fedele, V., Szklarz, M., Abdul Azeez, K. R., Salah, E., Mikolajczyk, J., Romanov, S., Sepetov, N., Huang, X. P., Roth, B. L., Al Haj Zen, A., Fourches, D., Muratov, E., Tropsha, A., Morris, J., Teicher, B. A., Kunkel, M., Polley, E., Lackey, K. E., … Zuercher, W. J. (2016). Comprehensive characterization of the Published

Kinase Inhibitor Set. *Nature Biotechnology*, *34*(1), 95–103. https://doi.org/10.1038/nbt.3374

47. Ellinger-Ziegelbauer, H., Karasuyama, H., Yamada, E., Tsujikawa, K., Todokoro, K., & Nishida, E. (2000). Ste20-like kinase (SLK), a regulatory kinase for polo-like kinase (Plk) during the G2/M transition in somatic cells. Genes to cells : devoted to molecular & cellular mechanisms, 5(6), 491–498. https://doi.org/10.1046/j.1365-2443.2000.00337.x
48. Etienne-Manneville, S., & Hall, A. (2001). Integrin-Mediated Activation of Cdc42 Controls Cell Polarity in Migrating Astrocytes through PKCζ. *Cell*, *106*(4), 489–498. https://doi.org/10.1016/S0092-8674(01)00471-8
49. Fangusaro, J. (2009). Pediatric high-grade gliomas and diffuse intrinsic pontine gliomas. *Journal of Child Neurology*, *24*(11), 1409–1417. https://doi.org/10.1177/0883073809338960
50. Faury, D., Nantel, A., Dunn, S. E., Guiot, M. C., Haque, T., Hauser, P., Garami, M., Bognár, L., Hanzély, Z., Liberski, P. P., Lopez-Aguilar, E., Valera, E. T., Tone, L. G., Carret, A. S., Del Maestro, R. F., Gleave, M., Montes, J. L., Pietsch, T., Albrecht, S., & Jabado, N. (2007). Molecular profiling identifies prognostic subgroups of pediatric glioblastoma and shows increased YB-1 expression in tumors. *Journal of Clinical Oncology*, *25*(10), 1196–1208. https://doi.org/10.1200/JCO.2006.07.8626
51. Fedorov, O., Huber, K., Eisenreich, A., Filippakopoulos, P., King, O., Bullock, A. N., Szklarczyk, D., Jensen, L. J., Fabbro, D., Trappe, J., Rauch, U., Bracher, F., & Knapp, S. (2011). Specific CLK inhibitors from a novel chemotype for regulation of alternative splicing. *Chemistry and Biology*, *18*(1), 67–76. https://doi.org/10.1016/j.chembiol.2010.11.009
52. Fehon, R. G., McClatchey, A. I., & Bretscher, A. (2010). Organizing the cell cortex: The role of ERM proteins. In *Nature Reviews Molecular Cell Biology* (Vol. 11, Issue 4, pp. 276–287). https://doi.org/10.1038/nrm2866
53. Fievet, B. T., Gautreau, A., Roy, C., Del Maestro, L., Mangeat, P., Louvard, D., & Arpin, M. (2004). Phosphoinositide binding and phosphorylation act sequentially in the activation mechanism of ezrin. *Journal of Cell Biology*, *164*(5), 653–659. https://doi.org/10.1083/jcb.200307032
54. Friedl, P., & Alexander, S. (2011). Cancer Invasion and the Microenvironment: Plasticity and Reciprocity. *Cell*, *147*(5), 992–1009. https://doi.org/10.1016/j.cell.2011.11.016
55. Friedmann-Morvinski, D. (2014). Glioblastoma Heterogeneity and Cancer Cell Plasticity. In *Critical Reviews TM in Oncogenesis* (Vol. 19, Issue 5).
56. Fujita, N., Hayashi-Nishino, M., Fukumoto, H., Omori, H., Yamamoto, A., Noda, T., & Yoshimori, T. (2008). An Atg4B Mutant Hampers the Lipidation of LC3 Paralogues and Causes Defects in Autophagosome Closure. *Molecular Biology of the Cell*, *19*(11), 4651–4659. https://doi.org/10.1091/mbc.e08-03-0312
57. Gagnon, K. B., & Delpire, E. (2012). Molecular physiology of SPAK and OSR1: Two Ste20-related protein kinases regulating ion transport. *Physiological Reviews*, *92*(4), 1577–1617. https://doi.org/10.1152/physrev.00009.2012

58. Garland, B., Delisle, S., Al-Zahrani, K. N., Pryce, B. R., & Sabourin, L. A. (2021). The Ste20-like kinase – A Jack of all trades? In *Journal of Cell Science* (Vol. 134, Issue 9). Company of Biologists Ltd. https://doi.org/10.1242/jcs.258269
59. Gatto, F., Milletti, G., Carai, A., Mastronuzzi, A., & Nazio, F. (2021). Recent Advances in Understanding the Role of Autophagy in Paediatric Brain Tumours. *Diagnostics*, *11*(3), 481. https://doi.org/10.3390/diagnostics11030481
60. Geoerger, B., Hargrave, D., Thomas, F., Ndiaye, A., Frappaz, D., Andreiuolo, F., Varlet, P., Aerts, I., Riccardi, R., Jaspan, T., Chatelut, E., Le Deley, M. C., Paoletti, X., Saint-Rose, C., Leblond, P., Morland, B., Gentet, J. C., Méresse, V., & Vassal, G. (2011). Innovative therapies for children with cancer pediatric phase I study of erlotinib in brainstem glioma and relapsing/refractory brain tumors. *Neuro-Oncology*, *13*(1), 109–118. https://doi.org/10.1093/neuonc/noq141
61. Gerada, C., & Ryan, K. M. (2020). Autophagy, the innate immune response and cancer. *Molecular Oncology*, *14*(9), 1913–1929. https://doi.org/10.1002/1878-0261.12774
62. Goldbrunner, R. H., Bernstein, J. J., & Tonn, J.-C. (1999). Cell-Extracellular Matrix Interaction in Glioma Invasion. *Acta Neurochirurgica*, *141*(3), 295–305. https://doi.org/10.1007/s007010050301
63. González, A., & Hall, M. N. (2017). Nutrient sensing and TOR signaling in yeast and mammals. *The EMBO Journal*, *36*(4), 397–408. https://doi.org/10.15252/embj.201696010
64. Gozuacik, D., Akkoc, Y., Ozturk, D. G., & Kocak, M. (2017). Autophagy-Regulating microRNAs and Cancer. *Frontiers in Oncology*, *7*. https://doi.org/10.3389/fonc.2017.00065
65. Guilluy, C., Rolli-Derkinderen, M., Loufrani, L., Bourgá, A., Henrion, D., Sabourin, L., Loirand, G., & Pacaud, P. (2008). Ste20-related kinase SLK phosphorylates serl88 of RhoA to induce vasodilation in response to angiotensin II type 2 receptor activation. *Circulation Research*, *102*(10), 1265–1274. https://doi.org/10.1161/CIRCRESAHA.107.164764
66. Hamasaki, M., Shibutani, S. T., & Yoshimori, T. (2013). Up-to-date membrane biogenesis in the autophagosome formation. *Current Opinion in Cell Biology*, *25*(4), 455–460. https://doi.org/10.1016/j.ceb.2013.03.004
67. Hanif, F., Muzaffar, K., Perveen, K., Malhi, S. M., & Simjee, S. U. (2017). Glioblastoma multiforme: A review of its epidemiology and pathogenesis through clinical presentation and treatment. In *Asian Pacific Journal of Cancer Prevention* (Vol. 18, Issue 1, pp. 3–9). Asian Pacific Organization for Cancer Prevention. https://doi.org/10.22034/APJCP.2017.18.1.3
68. Hao, W., Takano, T., Guillemette, J., Papillon, J., Ren, G., & Cybulsky, A. V. (2006). Induction of apoptosis by the Ste20-like kinase SLK, a germinal center kinase that activates apoptosis signal-regulating kinase and p38. *Journal of Biological Chemistry*, *281*(6), 3075–3084. https://doi.org/10.1074/jbc.M511744200

69. Hemmings, B. A., & Restuccia, D. F. (2012). PI3K-PKB/Akt Pathway. *Cold Spring Harbor Perspectives in Biology*, *4*(9), a011189–a011189. https://doi.org/10.1101/cshperspect.a011189
70. Hipfner, D. R., & Cohen, S. M. (2003). The Drosophila sterile-20 kinase slik controls cell proliferation and apoptosis during imaginal disc development. *PLoS Biology*, *1*(2). https://doi.org/10.1371/journal.pbio.0000035
71. Hipfner, D. R., Keller, N., & Cohen, S. M. (2004). Slik Sterile-20 kinase regulates Moesin activity to promote epithelial integrity during tissue growth. *Genes and Development*, *18*(18), 2243–2248. https://doi.org/10.1101/gad.303304
72. Holland, D. O., Gotea, V., Fedkenheuer, K., Jaiswal, S. K., Baugher, C., Tan, H., Fedkenheuer, M., & Elnitski, L. (2022). Characterization and clustering of kinase isoform expression in metastatic melanoma. *PLOS Computational Biology*, *18*(5), e1010065. https://doi.org/10.1371/journal.pcbi.1010065
73. Horwitz, A. F. (1997). Integrins and Health. *Scientific American*, *276*(5), 68–75. https://doi.org/10.1038/scientificamerican0597-68
74. Hoshide, R., & Jandial, R. (2016). 2016 World Health Organization Classification of Central Nervous System Tumors: An Era of Molecular Biology. *World Neurosurgery*, *94*, 561–562. https://doi.org/10.1016/j.wneu.2016.07.082
75. Hosokawa, N., Hara, T., Kaizuka, T., Kishi, C., Takamura, A., Miura, Y., Iemura, S., Natsume, T., Takehana, K., Yamada, N., Guan, J.-L., Oshiro, N., & Mizushima, N. (2009). Nutrient-dependent mTORC1 Association with the ULK1–Atg13–FIP200 Complex Required for Autophagy. *Molecular Biology of the Cell*, *20*(7), 1981–1991. https://doi.org/10.1091/mbc.e08-12-1248
76. Howarth, A., Madureira, P. A., Lockwood, G., Storer, L. C. D., Grundy, R., Rahman, R., Pilkington, G. J., & Hill, R. (2019). Modulating autophagy as a therapeutic strategy for the treatment of paediatric high-grade glioma. *Brain Pathology*, *29*(6), 707–725. https://doi.org/10.1111/bpa.12729
77. *http://gepia.cancer-pku.cn/detail.php?gene=PXN*. (n.d.).
78. *http://gepia.cancer-pku.cn/detail.php?gene=SLK*. (n.d.).
79. *https://www.phosphosite.org/proteinAction.action?id=2519&showAllSites=true*. (n.d.).
80. *https://www.uniprot.org/uniprotkb/Q9H2G2/entry#structure*. (n.d.).
81. Hu, C.-T., Cheng, C.-C., Wu, J.-R., Pan, S.-M., & Wu, W.-S. (2015). PKCε-mediated c-Met endosomal processing directs fluctuant c-Met-JNK-paxillin signaling for tumor progression of HepG2. *Cellular Signalling*, *27*(7), 1544–1555. https://doi.org/10.1016/j.cellsig.2015.02.031
82. Huang, Z., Yan, D.-P., & Ge, B.-X. (2008). JNK regulates cell migration through promotion of tyrosine phosphorylation of paxillin. *Cellular Signalling*, *20*(11), 2002–2012. https://doi.org/10.1016/j.cellsig.2008.07.014
83. Hughes, S. C., & Fehon, R. G. (2006a). Phosphorylation and activity of the tumor suppressor Merlin and the ERM protein Moesin are coordinately regulated by the Slik kinase. *Journal of Cell Biology*, *175*(2), 305–313. https://doi.org/10.1083/jcb.200608009

84. Hughes, S. C., & Fehon, R. G. (2006b). Phosphorylation and activity of the tumor suppressor Merlin and the ERM protein Moesin are coordinately regulated by the Slik kinase. *Journal of Cell Biology*, *175*(2), 305–313. https://doi.org/10.1083/jcb.200608009
85. *Human Protein Atlas*. (n.d.). Consensus Dataset. https://www.proteinatlas.org/ENSG00000065613-SLK/tissue
86. Hunt, S. D., & Stephens, D. J. (2011). The role of motor proteins in endosomal sorting. *Biochemical Society Transactions*, *39*(5), 1179–1184. https://doi.org/10.1042/BST0391179
87. Hunter, K. W. (2004). Ezrin, a key component in tumor metastasis. *Trends in Molecular Medicine*, *10*(5), 201–204. https://doi.org/10.1016/j.molmed.2004.03.001
88. Iser, I. C., Pereira, M. B., Lenz, G., & Wink, M. R. (2017). The Epithelial-to-Mesenchymal Transition-Like Process in Glioblastoma: An Updated Systematic Review and In Silico Investigation. *Medicinal Research Reviews*, *37*(2), 271–313. https://doi.org/10.1002/med.21408
89. Ivetic, A., & Ridley, A. J. (2004). Ezrin/radixin/moesin proteins and Rho GTPase signalling in leucocytes. *Immunology*, *112*(2), 165–176. https://doi.org/10.1111/j.1365-2567.2004.01882.x
90. Jaberi, A., Hooker, E., Guillemette, J., Papillon, J., Kristof, A. S., & Cybulsky, A. V. (2015). Identification of Tpr and α-actinin-4 as two novel SLK-interacting proteins. *Biochimica et Biophysica Acta (BBA) - Molecular Cell Research*, *1853*(10), 2539–2552. https://doi.org/10.1016/j.bbamcr.2015.06.005
91. Jagadeeswaran, R., Surawska, H., Krishnaswamy, S., Janamanchi, V., Mackinnon, A. C., Seiwert, T. Y., Loganathan, S., Kanteti, R., Reichman, T., Nallasura, V., Schwartz, S., Faoro, L., Wang, Y.-C., Girard, L., Tretiakova, M. S., Ahmed, S., Zumba, O., Soulii, L., Bindokas, V. P., … Salgia, R. (2008). Paxillin Is a Target for Somatic Mutations in Lung Cancer: Implications for Cell Growth and Invasion. *Cancer Research*, *68*(1), 132–142. https://doi.org/10.1158/0008-5472.CAN-07-1998
92. Jahreiss, L., Menzies, F. M., & Rubinsztein, D. C. (2008). The Itinerary of Autophagosomes: From Peripheral Formation to Kiss-and-Run Fusion with Lysosomes. *Traffic*, *9*(4), 574–587. https://doi.org/10.1111/j.1600-0854.2008.00701.x
93. Johansen, T., & Lamark, T. (2020). Selective Autophagy: ATG8 Family Proteins, LIR Motifs and Cargo Receptors. *Journal of Molecular Biology*, *432*(1), 80–103. https://doi.org/10.1016/j.jmb.2019.07.016
94. Jordens, I., Fernandez-Borja, M., Marsman, M., Dusseljee, S., Janssen, L., Calafat, J., Janssen, H., Wubbolts, R., & Neefjes, J. (2001). The Rab7 effector protein RILP controls lysosomal transport by inducing the recruitment of dynein-dynactin motors. *Current Biology*, *11*(21), 1680–1685. https://doi.org/10.1016/S0960-9822(01)00531-0
95. Kalluri, R., & Weinberg, R. A. (2009). The basics of epithelial-mesenchymal transition. *Journal of Clinical Investigation*, *119*(6), 1420–1428. https://doi.org/10.1172/JCI39104

96. Kanteti, R., Batra, S. K., Lennon, F. E., & Salgia, R. (2016). FAK and paxillin, two potential targets in pancreatic cancer. *Oncotarget*, *7*(21), 31586–31601. https://doi.org/10.18632/oncotarget.8040
97. KARAKAŞ, H. E., & GÖZÜAÇIK, D. (2014). Autophagy and cancer. *TURKISH JOURNAL OF BIOLOGY*, *38*, 720–739. https://doi.org/10.3906/biy-1408-16
98. Karanasios, E., Stapleton, E., Manifava, M., Kaizuka, T., Mizushima, N., Walker, S. A., & Ktistakis, N. T. (2013). Dynamic association of the ULK1 complex with omegasomes during autophagy induction. *Journal of Cell Science*. https://doi.org/10.1242/jcs.132415
99. Kaushik, S., Ravi, A., Hameed, F. M., & Low, B. C. (2014). Concerted modulation of paxillin dynamics at focal adhesions by deleted in liver cancer-1 and focal adhesion kinase during early cell spreading. *Cytoskeleton*, *71*(12), 677–694. https://doi.org/10.1002/cm.21201
100. Kenific, C. M., Stehbens, S. J., Goldsmith, J., Leidal, A. M., Faure, N., Ye, J., Wittmann, T., & Debnath, J. (2016). NBR 1 enables autophagy-dependent focal adhesion turnover. *Journal of Cell Biology*, *212*(5), 577–590. https://doi.org/10.1083/jcb.201503075
101. Kim, Y. H., Baek, S. H., Kim, E. K., Ha, J. M., Jin, S. Y., Lee, H. S., Ha, H. K., Song, S. H., Kim, S. J., Shin, H. K., Yong, J., Kim, D.-H., Kim, C. D., & Bae, S. S. (2016). Uncoordinated 51-like kinase 2 signaling pathway regulates epithelial-mesenchymal transition in A549 lung cancer cells. *FEBS Letters*, *590*(9), 1365–1374. https://doi.org/10.1002/1873-3468.12172
102. Kimura, S., Noda, T., & Yoshimori, T. (2008). Dynein-dependent Movement of Autophagosomes Mediates Efficient Encounters with Lysosomes. *Cell Structure and Function*, *33*(1), 109–122. https://doi.org/10.1247/csf.08005
103. Knizhnik, A. V., Roos, W. P., Nikolova, T., Quiros, S., Tomaszowski, K.-H., Christmann, M., & Kaina, B. (2013). Survival and Death Strategies in Glioma Cells: Autophagy, Senescence and Apoptosis Triggered by a Single Type of Temozolomide-Induced DNA Damage. *PLoS ONE*, *8*(1), e55665. https://doi.org/10.1371/journal.pone.0055665
104. Köchl, R., Hu, X. W., Chan, E. Y. W., & Tooze, S. A. (2006). Microtubules Facilitate Autophagosome Formation and Fusion of Autophagosomes with Endosomes. *Traffic*, *7*(2), 129–145. https://doi.org/10.1111/j.1600-0854.2005.00368.x
105. Korolchuk, V. I., Saiki, S., Lichtenberg, M., Siddiqi, F. H., Roberts, E. A., Imarisio, S., Jahreiss, L., Sarkar, S., Futter, M., Menzies, F. M., O'Kane, C. J., Deretic, V., & Rubinsztein, D. C. (2011). Lysosomal positioning coordinates cellular nutrient responses. *Nature Cell Biology*, *13*(4), 453–460. https://doi.org/10.1038/ncb2204
106. Korshunov, A., Schrimpf, D., Ryzhova, M., Sturm, D., Chavez, L., Hovestadt, V., Sharma, T., Habel, A., Burford, A., Jones, C., Zheludkova, O., Kumirova, E., Kramm, C. M., Golanov, A., Capper, D., von Deimling, A., Pfister, S. M., & Jones, D. T. W. (2017). H3-/IDH-wild type pediatric glioblastoma is comprised of molecularly and

prognostically distinct subtypes with associated oncogenic drivers. *Acta Neuropathologica*, *134*(3), 507–516. https://doi.org/10.1007/s00401-017-1710-1

107. Krieg, J., & Hunter, T. (1992). Identification of the two major epidermal growth factor-induced tyrosine phosphorylation sites in the microvillar core protein ezrin. *The Journal of Biological Chemistry*, *267*(27), 19258–19265.
108. Leopoldt, D., Yee, H. F., & Rozengurt, E. (2001). Calyculin-A induces focal adhesion assembly and tyrosine phosphorylation of p125Fak, p130Cas, and paxillin in Swiss 3T3 cells. *Journal of Cellular Physiology*, *188*(1), 106–119. https://doi.org/10.1002/jcp.1102
109. Levine, B. (2007). Autophagy and cancer. *Nature*, *446*(7137), 745–747. https://doi.org/10.1038/446745a
110. Li, J., Wang, R., Gannon, O. J., Rezey, A. C., Jiang, S., Gerlach, B. D., Liao, G., & Tang, D. D. (2016). Polo-like kinase 1 regulates vimentin phosphorylation at Ser-56 and contraction in smooth muscle. *Journal of Biological Chemistry*, *291*(45), 23693–23703. https://doi.org/10.1074/jbc.M116.749341
111. Li, J., Zhu, S., Kozono, D., Ng, K., Futalan, D., Shen, Y., Akers, J. C., Steed, T., Kushwaha, D., Schlabach, M., Carter, B. S., Kwon, C.-H., Furnari, F., Cavenee, W., Elledge, S., & Chen, C. C. (n.d.). *Genome-wide shRNA screen revealed integrated mitogenic signaling between dopamine receptor D2 (DRD2) and epidermal growth factor receptor (EGFR) in glioblastoma* (Vol. 5, Issue 4). www.impactjournals.com/oncotarget
112. Li, Z., & Zhang, X. (2017). Kinases Involved in Both Autophagy and Mitosis. *International Journal of Molecular Sciences*, *18*(9), 1884. https://doi.org/10.3390/ijms18091884
113. Litan, A., & Langhans, S. A. (2015). Cancer as a channelopathy: ion channels and pumps in tumor development and progression. *Frontiers in Cellular Neuroscience*, *9*. https://doi.org/10.3389/fncel.2015.00086
114. Liu, M., Inoue, K., Leng, T., Guo, S., & Xiong, Z. (2014). TRPM7 channels regulate glioma stem cell through STAT3 and Notch signaling pathways. *Cellular Signalling*, *26*(12), 2773–2781. https://doi.org/10.1016/j.cellsig.2014.08.020
115. Liu, R., Zhi, X., & Zhong, Q. (2015). ATG14 controls SNARE-mediated autophagosome fusion with a lysosome. *Autophagy*, *11*(5), 847–849. https://doi.org/10.1080/15548627.2015.1037549
116. Lokker, N. A., Sullivan, C. M., Hollenbach, S. J., Israel, M. A., & Giese, N. A. (2002). Platelet-derived growth factor (PDGF) autocrine signaling regulates survival and mitogenic pathways in glioblastoma cells: evidence that the novel PDGF-C and PDGF-D ligands may play a role in the development of brain tumors. *Cancer Research*, *62*(13), 3729–3735.
117. López-Colomé, A. M., Lee-Rivera, I., Benavides-Hidalgo, R., & López, E. (2017). Paxillin: a crossroad in pathological cell migration. *Journal of Hematology & Oncology*, *10*(1), 50. https://doi.org/10.1186/s13045-017-0418-y
118. Louis, D. N., Ohgaki, H., Wiestler, O. D., Cavenee, W. K., Burger, P. C., Jouvet, A., Scheithauer, B. W., & Kleihues, P. (2007). The 2007 WHO classification of

tumours of the central nervous system. In *Acta Neuropathologica* (Vol. 114, Issue 2, pp. 97–109). https://doi.org/10.1007/s00401-007-0243-4

119. Luhovy, A. Y., Jaberi, A., Papillon, J., Guillemette, J., & Cybulsky, A. V. (2012a). Regulation of the Ste20-like kinase, SLK: Involvement of activation segment phosphorylation. *Journal of Biological Chemistry*, *287*(8), 5446–5458. https://doi.org/10.1074/jbc.M111.302018
120. Luhovy, A. Y., Jaberi, A., Papillon, J., Guillemette, J., & Cybulsky, A. V. (2012b). Regulation of the Ste20-like kinase, SLK: Involvement of activation segment phosphorylation. *Journal of Biological Chemistry*, *287*(8), 5446–5458. https://doi.org/10.1074/jbc.M111.302018
121. MacDonald, T. J., Aguilera, D., & Kramm, C. M. (2011). Treatment of high-grade glioma in children and adolescents. *Neuro-Oncology*, *13*(10), 1049–1058. https://doi.org/10.1093/neuonc/nor092
122. Machicoane, M., de Frutos, C. A., Fink, J., Rocancourt, M., Lombardi, Y., Gare, S., Piel, M., & Echard, A. (2014). SLK-dependent activation of ERMs controls LGN-NuMA localization and spindle orientation. *Journal of Cell Biology*, *205*(6), 791–799. https://doi.org/10.1083/jcb.201401049
123. Machicoane, M., de Frutos, C. A., Fink, J., Rocancourt, M., Lombardi, Y., Garel, S., Piel, M., & Echard, A. (2014a). SLK-dependent activation of ERMs controls LGN–NuMA localization and spindle orientation. *Journal of Cell Biology*, *205*(6), 791–799. https://doi.org/10.1083/jcb.201401049
124. Machicoane, M., de Frutos, C. A., Fink, J., Rocancourt, M., Lombardi, Y., Garel, S., Piel, M., & Echard, A. (2014b). SLK-dependent activation of ERMs controls LGN–NuMA localization and spindle orientation. *Journal of Cell Biology*, *205*(6), 791–799. https://doi.org/10.1083/jcb.201401049
125. Mahesparan, R., Read, T.-A., Lund-Johansen, M., Skaftnesmo, K., Bjerkvig, R., & Engebraaten, O. (2003). Expression of extracellular matrix components in a highly infiltrative in vivo glioma model. *Acta Neuropathologica*, *105*(1), 49–57. https://doi.org/10.1007/s00401-002-0610-0
126. Mathew, R., Karp, C. M., Beaudoin, B., Vuong, N., Chen, G., Chen, H.-Y., Bray, K., Reddy, A., Bhanot, G., Gelinas, C., DiPaola, R. S., Karantza-Wadsworth, V., & White, E. (2009). Autophagy Suppresses Tumorigenesis through Elimination of p62. *Cell*, *137*(6), 1062–1075. https://doi.org/10.1016/j.cell.2009.03.048
127. Matsui, T., Maeda, M., Doi, Y., Yonemura, S., Amano, M., Kaibuchi, K., Tsukita, S., & Tsukita, S. (1998). Rho-Kinase Phosphorylates COOH-terminal Threonines of Ezrin/Radixin/Moesin (ERM) Proteins and Regulates Their Head-to-Tail Association. *Journal of Cell Biology*, *140*(3), 647–657. https://doi.org/10.1083/jcb.140.3.647
128. Mazurek, M., Grochowski, C., Litak, J., Osuchowska, I., Maciejewski, R., & Kamieniak, P. (2020). Recent Trends of microRNA Significance in Pediatric Population Glioblastoma and Current Knowledge of Micro RNA Function in Glioblastoma Multiforme. *International Journal of Molecular Sciences*, *21*(9), 3046. https://doi.org/10.3390/ijms21093046

129. Miele, E., Buttarelli, F. R., Arcella, A., Begalli, F., Garg, N., Silvano, M., Po, A., Baldi, C., Carissimo, G., Antonelli, M., Spinelli, G. P., Capalbo, C., Donofrio, V., Morra, I., Nozza, P., Gulino, A., Giangaspero, F., & Ferretti, E. (2014). High-throughput microRNA profiling of pediatric high-grade gliomas. *Neuro-Oncology*, *16*(2), 228–240. https://doi.org/10.1093/neuonc/not215

130. Mitra, S. K., Hanson, D. A., & Schlaepfer, D. D. (2005). Focal adhesion kinase: In command and control of cell motility. In *Nature Reviews Molecular Cell Biology* (Vol. 6, Issue 1, pp. 56–68). https://doi.org/10.1038/nrm1549

131. Mittal, V. (2018). Epithelial Mesenchymal Transition in Tumor Metastasis. *Annual Review of Pathology: Mechanisms of Disease*, *13*(1), 395–412. https://doi.org/10.1146/annurev-pathol-020117-043854

132. Mizushima, N. (2007). Autophagy: Process and function. In *Genes and Development* (Vol. 21, Issue 22, pp. 2861–2873). https://doi.org/10.1101/gad.1599207

133. Mondal, C., Di Martino, J. S., & Bravo-Cordero, J. J. (2021). Chapter Three - Actin dynamics during tumor cell dissemination. In C. Thomas & L. Galluzzi (Eds.), *International Review of Cell and Molecular Biology* (Vol. 360, pp. 65–98). Academic Press. https://doi.org/https://doi.org/10.1016/bs.ircmb.2020.09.004

134. Nakamura, F., Amieva, M. R., & Furthmayr, H. (1995). Phosphorylation of Threonine 558 in the Carboxyl-terminal Actin-binding Domain of Moesin by Thrombin Activation of Human Platelets. *Journal of Biological Chemistry*, *270*(52), 31377–31385. https://doi.org/10.1074/jbc.270.52.31377

135. Nicholson-Dykstra, S., Higgs, H. N., & Harris, E. S. (2005). Actin Dynamics: Growth from Dendritic Branches. *Current Biology*, *15*(9), R346–R357. https://doi.org/10.1016/j.cub.2005.04.029

136. Nobes, C. D., & Hall, A. (1995). Rho, Rac, and Cdc42 GTPases Regulate the Assembly of Multimolecular Focal Complexes Associated with Actin Stress Fibers, Lamellipodia, and Filopodia. In *Cell* (Vol. 81).

137. O'Reilly, P. G., Wagner, S., Franks, D. J., Cailliau, K., Browaeys, E., Dissous, C., & Sabourin, L. A. (2005). The Ste20-like kinase SLK is required for cell cycle progression through G2. *Journal of Biological Chemistry*, *280*(51), 42383–42390. https://doi.org/10.1074/jbc.M510763200

138. Paugh, B. S., Zhu, X., Qu, C., Endersby, R., Diaz, A. K., Zhang, J., Bax, D. A., Carvalho, D., Reis, R. M., Onar-Thomas, A., Broniscer, A., Wetmore, C., Zhang, J., Jones, C., Ellison, D. W., & Baker, S. J. (2013). Novel oncogenic PDGFRA mutations in pediatric high-grade gliomas. *Cancer Research*, *73*(20), 6219–6229. https://doi.org/10.1158/0008-5472.CAN-13-1491

139. Peker, N., & Gozuacik, D. (2020). Autophagy as a Cellular Stress Response Mechanism in the Nervous System. In *Journal of Molecular Biology* (Vol. 432, Issue 8, pp. 2560–2588). Academic Press. https://doi.org/10.1016/j.jmb.2020.01.017

140. Petralia, F., Tignor, N., Reva, B., Koptyra, M., Chowdhury, S., Rykunov, D., Krek, A., Ma, W., Zhu, Y., Ji, J., Calinawan, A., Whiteaker, J. R., Colaprico, A., Stathias, V., Omelchenko, T., Song, X., Raman, P., Guo, Y., Brown, M. A., … Bocik,

W. E. (2020). Integrated Proteogenomic Characterization across Major Histological Types of Pediatric Brain Cancer. *Cell*, *183*(7), 1962-1985.e31. https://doi.org/10.1016/j.cell.2020.10.044

141. Pike, A. C. W., Rellos, P., Niesen, F. H., Turnbull, A., Oliver, A. W., Parker, S. A., Turk, B. E., Pearl, L. H., & Knapp, S. (2008a). Activation segment dimerization: A mechanism for kinase autophosphorylation of non-consensus sites. *EMBO Journal*, *27*(4), 704–714. https://doi.org/10.1038/emboj.2008.8
142. Pike, A. C. W., Rellos, P., Niesen, F. H., Turnbull, A., Oliver, A. W., Parker, S. A., Turk, B. E., Pearl, L. H., & Knapp, S. (2008b). Activation segment dimerization: A mechanism for kinase autophosphorylation of non-consensus sites. *EMBO Journal*, *27*(4), 704–714. https://doi.org/10.1038/emboj.2008.8
143. Pollack, I. F., Finkelstein, S. D., Woods, J., Burnham, J., Holmes, E. J., Hamilton, R. L., Yates, A. J., Boyett, J. M., Finlay, J. L., & Sposto, R. (2002). Expression of p53 and Prognosis in Children with Malignant Gliomas. *New England Journal of Medicine*, *346*(6), 420–427. https://doi.org/10.1056/NEJMoa012224
144. Pollack, I. F., Hamilton, R. L., Burger, P. C., Brat, D. J., Rosenblum, M. K., Murdoch, G. H., Nikiforova, M. N., Holmes, E. J., Zhou, T., Cohen, K. J., & Jakacki, R. I. (2010). Akt activation is a common event in pediatric malignant gliomas and a potential adverse prognostic marker: a report from the Children's Oncology Group. *Journal of Neuro-Oncology*, *99*(2), 155–163. https://doi.org/10.1007/s11060-010-0297-3
145. Prag, S., Lepekhin, E. A., Kolkova, K., Hartmann-Petersen, R., Kawa, A., Walmod, P. S., Belman, V., Gallagher, H. C., Berezin, V., Bock, E., & Pedersen, N. (2002). NCAM regulates cell motility. *Journal of Cell Science*, *115*(2), 283–292. https://doi.org/10.1242/jcs.115.2.283
146. Pranzini, E., Raugei, G., & Taddei, M. L. (2022). Metabolic Features of Tumor Dormancy: Possible Therapeutic Strategies. *Cancers*, *14*(3), 547. https://doi.org/10.3390/cancers14030547
147. Pryce, B. R., Al-Zahrani, K. N., Dufresne, S., Belkina, N., Labrèche, C., Patino-Lopez, G., Frenette, J., Shaw, S., & Sabourin, L. A. (2017). Deletion of the Ste20-like kinase SLK in skeletal muscle results in a progressive myopathy and muscle weakness. *Skeletal Muscle*, *7*(1). https://doi.org/10.1186/s13395-016-0119-1
148. Qiang, L., Zhao, B., Ming, M., Wang, N., He, T.-C., Hwang, S., Thorburn, A., & He, Y.-Y. (2014). Regulation of cell proliferation and migration by p62 through stabilization of Twist1. *Proceedings of the National Academy of Sciences of the United States of America*, *111*(25), 9241–9246. https://doi.org/10.1073/pnas.1322913111
149. Quizi, J. L., Baron, K., Al-Zahrani, K. N., O'Reilly, P., Sriram, R. K., Conway, J., Laurin, A. A., & Sabourin, L. A. (2013a). SLK-mediated phosphorylation of paxillin is required for focal adhesion turnover and cell migration. *Oncogene*, *32*(39), 4656–4663. https://doi.org/10.1038/onc.2012.488
150. Quizi, J. L., Baron, K., Al-Zahrani, K. N., O'Reilly, P., Sriram, R. K., Conway, J., Laurin, A. A., & Sabourin, L. A. (2013b). SLK-mediated phosphorylation of

paxillin is required for focal adhesion turnover and cell migration. *Oncogene*, *32*(39), 4656–4663. https://doi.org/10.1038/onc.2012.488

151. Ramirez, Y., Weatherbee, J., Wheelhouse, R., & Ross, A. (2013). Glioblastoma Multiforme Therapy and Mechanisms of Resistance. *Pharmaceuticals*, *6*(12), 1475–1506. https://doi.org/10.3390/ph6121475
152. Ranuncolo, S. M., Ladeda, V., Specterman, S., Varela, M., Lastiri, J., Morandi, A., Matos, E., De Kier Joffe, E. B., Puricelli, L., & Pallotta, M. G. (2002). CD44 expression in human gliomas. *Journal of Surgical Oncology*, *79*(1), 30–36. https://doi.org/10.1002/jso.10045
153. Ravikumar, B., Acevedo-Arozena, A., Imarisio, S., Berger, Z., Vacher, C., O'Kane, C. J., Brown, S. D. M., & Rubinsztein, D. C. (2005). Dynein mutations impair autophagic clearance of aggregate-prone proteins. *Nature Genetics*, *37*(7), 771–776. https://doi.org/10.1038/ng1591
154. Raymond, E., Brandes, A. A., Dittrich, C., Fumoleau, P., Coudert, B., Clement, P. M. J., Frenay, M., Rampling, R., Stupp, R., Kros, J. M., Heinrich, M. C., Gorlia, T., Lacombe, D., & Van Den Bent, M. J. (2008). Phase II study of imatinib in patients with recurrent gliomas of various histologies: A European organisation for research and treatment of cancer brain tumor group study. *Journal of Clinical Oncology*, *26*(28), 4659–4665. https://doi.org/10.1200/JCO.2008.16.9235
155. Reggiori, F., Monastyrska, I., Shintani, T., & Klionsky, D. J. (2005). The Actin Cytoskeleton Is Required for Selective Types of Autophagy, but Not Nonspecific Autophagy, in the Yeast *Saccharomyces cerevisiae*. *Molecular Biology of the Cell*, *16*(12), 5843–5856. https://doi.org/10.1091/mbc.e05-07-0629
156. Ren, L., Hong, S. H., Cassavaugh, J., Osborne, T., Chou, A. J., Kim, S. Y., Gorlick, R., Hewitt, S. M., & Khanna, C. (2009). The actin-cytoskeleton linker protein ezrin is regulated during osteosarcoma metastasis by PKC. *Oncogene*, *28*(6), 792–802. https://doi.org/10.1038/onc.2008.437
157. Rickert, C. H., Sträter, R., Kaatsch, P., Wassmann, H., Jürgens, H., Dockhorn-Dworniczak, B., & Paulus, W. (2001). Pediatric high-grade astrocytomas show chromosomal imbalances distinct from adult cases. The American journal of pathology, 158(4), 1525–1532. https://doi.org/10.1016/S0002-9440(10)64103-X
158. Rizzo, D., Ruggiero, A., Martini, M., Rizzo, V., Maurizi, P., & Riccardi, R. (2015). Molecular Biology in Pediatric High-Grade Glioma: Impact on Prognosis and Treatment. In *BioMed Research International* (Vol. 2015). Hindawi Publishing Corporation. https://doi.org/10.1155/2015/215135
159. Rogov, V., Dötsch, V., Johansen, T., & Kirkin, V. (2014). Interactions between Autophagy Receptors and Ubiquitin-like Proteins Form the Molecular Basis for Selective Autophagy. *Molecular Cell*, *53*(2), 167–178. https://doi.org/10.1016/j.molcel.2013.12.014
160. Roovers, K., Wagner, S., Storbeck, C. J., O'Reilly, P., Lo, V., Northey, J. J., Chmielecki, J., Muller, W. J., Siegel, P. M., & Sabourin, L. A. (2009). The Ste20-like kinase SLK is required for ErbB2-driven breast cancer cell motility. *Oncogene*, *28*(31), 2839–2848. https://doi.org/10.1038/onc.2009.146

161. Sabourin, L. A., & Rudnicki, M. A. (1999). Induction of apoptosis by SLK, a Ste20-related kinase. *Oncogene*, *18*(52), 7566–7575. https://doi.org/10.1038/sj.onc.1203119

162. Sabourin, L. A., Seale, P., Wagner, J., & Rudnicki, M. A. (2000). Caspase 3 Cleavage of the Ste20-Related Kinase SLK Releases and Activates an Apoptosis-Inducing Kinase Domain and an Actin-Disassembling Region. In *MOLECULAR AND CELLULAR BIOLOGY* (Vol. 20, Issue 2).

163. Sales, A., Beck, J., Schnell, O., Fung, C., Meyer, B., & Gempt, J. (2022). Surgical Treatment of Glioblastoma: State-of-the-Art and Future Trends. *Journal of Clinical Medicine*, *11*(18), 5354. https://doi.org/10.3390/jcm11185354

164. Sanchez, A. M., Shortrede, J. E., Vargas-Roig, L. M., & Flamini, M. I. (2016). Retinoic acid induces nuclear FAK translocation and reduces breast cancer cell adhesion through Moesin, FAK, and Paxillin. *Molecular and Cellular Endocrinology*, *430*, 1–11. https://doi.org/10.1016/j.mce.2016.04.021

165. Sardiello, M., Palmieri, M., di Ronza, A., Medina, D. L., Valenza, M., Gennarino, V. A., Di Malta, C., Donaudy, F., Embrione, V., Polishchuk, R. S., Banfi, S., Parenti, G., Cattaneo, E., & Ballabio, A. (2009). A Gene Network Regulating Lysosomal Biogenesis and Function. *Science*, *325*(5939), 473–477. https://doi.org/10.1126/science.1174447

166. Schwartzentruber, J., Korshunov, A., Liu, X. Y., Jones, D. T. W., Pfaff, E., Jacob, K., Sturm, D., Fontebasso, A. M., Quang, D. A. K., Tönjes, M., Hovestadt, V., Albrecht, S., Kool, M., Nantel, A., Konermann, C., Lindroth, A., Jäger, N., Rausch, T., Ryzhova, M., … Jabado, N. (2012). Driver mutations in histone H3.3 and chromatin remodelling genes in paediatric glioblastoma. *Nature*, *482*(7384), 226–231. https://doi.org/10.1038/nature10833

167. Seker-Polat, F., Pinarbasi Degirmenci, N., Solaroglu, I., & Bagci-Onder, T. (2022). Tumor Cell Infiltration into the Brain in Glioblastoma: From Mechanisms to Clinical Perspectives. *Cancers*, *14*(2), 443. https://doi.org/10.3390/cancers14020443

168. Sero, J. E., Thodeti, C. K., Mammoto, A., Bakal, C., Thomas, S., & Ingber, D. E. (2011). Paxillin Mediates Sensing of Physical Cues and Regulates Directional Cell Motility by Controlling Lamellipodia Positioning. *PLoS ONE*, *6*(12), e28303. https://doi.org/10.1371/journal.pone.0028303

169. Seto, T., Kato, T., Nishio, M., Goto, K., Atagi, S., Hosomi, Y., Yamamoto, N., Hida, T., Maemondo, M., Nakagawa, K., Nagase, S., Okamoto, I., Yamanaka, T., Tajima, K., Harada, R., Fukuoka, M., & Yamamoto, N. (2014). Erlotinib alone or with bevacizumab as first-line therapy in patients with advanced non-squamous non-small-cell lung cancer harbouring EGFR mutations (JO25567): An open-label, randomised, multicentre, phase 2 study. *The Lancet Oncology*, *15*(11), 1236–1244. https://doi.org/10.1016/S1470-2045(14)70381-X

170. Shah, S., Chu, Y., Cegielski, V., & Chu, X.-P. (2021). Acid-Sensing Ion Channel 1 Contributes to Weak Acid-Induced Migration of Human Malignant Glioma Cells. *Frontiers in Physiology*, *12*. https://doi.org/10.3389/fphys.2021.734418

171. Sharifi, M. N., Mowers, E. E., Drake, L. E., Collier, C., Chen, H., Zamora, M., Mui, S., & Macleod, K. F. (2016). Autophagy Promotes Focal Adhesion Disassembly and Cell Motility of Metastatic Tumor Cells through the Direct Interaction of Paxillin with LC3. *Cell Reports*, *15*(8), 1660–1672. https://doi.org/10.1016/j.celrep.2016.04.065

172. Short, S. M., Yoder, B. J., Tarr, S. M., Prescott, N. L., Laniauskas, S., Coleman, K. A., Downs-Kelly, E., Pettay, J. D., Choueiri, T. K., Crowe, J. P., Tubbs, R. R., Budd, T. G., & Hicks, D. G. (2007). The Expression of the Cytoskeletal Focal Adhesion Protein Paxillin in Breast Cancer Correlates with HER2 Overexpression and May Help Predict Response to Chemotherapy: A Retrospective Immunohistochemical Study. *The Breast Journal*, *13*(2), 130–139. https://doi.org/10.1111/j.1524-4741.2007.00389.x

173. Slobodkin, M. R., & Elazar, Z. (2013). The Atg8 family: multifunctional ubiquitin-like key regulators of autophagy. *Essays in Biochemistry*, *55*, 51–64. https://doi.org/10.1042/bse0550051

174. Søreng, K., Neufeld, T. P., & Simonsen, A. (2018). Chapter One - Membrane Trafficking in Autophagy. In L. Galluzzi (Ed.), *International Review of Cell and Molecular Biology* (Vol. 336, pp. 1–92). Academic Press. https://doi.org/https://doi.org/10.1016/bs.ircmb.2017.07.001

175. Storbeck, C. J., Al-Zahrani, K. N., Sriram, R., Kawesa, S., O'reilly, P., Daniel, K., Mckay, M., Kothary, R., Tsilfidis, C., & Sabourin, L. A. (2013). *Distinct roles for Ste20-like kinase SLK in muscle function and regeneration*. http://www.skeletalmusclejournal.com/content/3/1/16

176. Storbeck, C. J., Daniel, K., Zhang, Y. H., Lunde, J., Scime, A., Asakura, A., Jasmin, B., Korneluk, R. G., & Sabourin, L. A. (2004). STE20-like kinase SLK displays myofiber type specificity and is involved in C2C12 myoblast differentiation. *Muscle and Nerve*, *29*(4), 553–564. https://doi.org/10.1002/mus.20000

177. Storbeck, C. J., Wagner, S., O'Reilly, P., McKay, M., Parks, R. J., Westphal, H., & Sabourin, L. A. (2009). The Ldb1 and Ldb2 Transcriptional Cofactors Interact with the Ste20-like Kinase SLK and Regulate Cell Migration. *Molecular Biology of the Cell*, *20*(19), 4174–4182. https://doi.org/10.1091/mbc.e08-07-0707

178. Storbeck, C. J., Wagner, S., O'reilly, P., Mckay, M., Parks, R. J., Westphal, H., & Sabourin, L. A. (2009). The Ldb1 and Ldb2 Transcriptional Cofactors Interact with the Ste20-like Kinase SLK and Regulate Cell Migration. *Molecular Biology of the Cell*, *20*, 4174–4182. https://doi.org/10.1091/mbc.E08

179. STRING Interaction Network. (n.d.). *https://string-db.org/cgi/network?taskId=bJt08XKm8Etn&sessionId=bwtMpeRVa1Ou*.

180. Stupp, R., Mason, W. P., Van Den Bent, M. J., Weller, M., Fisher, B., Taphoorn, M. J. B., Belanger, K., Brandes, A. A., Marosi, C., Bogdahn, U., Curschmann, J., Janzer, R. C., Ludwin, S. K., Gorlia, T., Allgeier, A., Lacombe, D., Cairncross, J. G., Eisenhauer, E., & Mirimanoff, R. O. (n.d.). *Radiotherapy plus Concomitant and Adjuvant Temozolomide for Glioblastoma*. www.nejm.org

181. Sturm, D., Pfister, S. M., & Jones, D. T. W. (2017). JOURNAL OF CLINICAL ONCOLOGY Pediatric Gliomas: Current Concepts on Diagnosis, Biology, and Clinical Management. *J Clin Oncol*, *35*, 2370–2377. https://doi.org/10.1200/JCO.2017

182. Sun, L.-H., Yang, F.-Q., Zhang, C.-B., Wu, Y.-P., Liang, J.-S., Jin, S., Wang, Z., Wang, H.-J., Bao, Z.-S., Yang, Z.-X., & Jiang, T. (2017). Overexpression of Paxillin Correlates with Tumor Progression and Predicts Poor Survival in Glioblastoma. *CNS Neuroscience & Therapeutics*, *23*(1), 69–75. https://doi.org/10.1111/cns.12606

183. Tsoli, M., Liu, J., Franshaw, L., Shen, H., Cheng, C., Jung, M., Joshi, S., Ehteda, A., Khan, A., Montero-Carcabosso, A., Dilda, P. J., Hogg, P., & Ziegler, D. S. (2018). Dual targeting of mitochondrial function and mTOR pathway as a therapeutic strategy for diffuse intrinsic pontine glioma. *Oncotarget*, *9*(7), 7541–7556. https://doi.org/10.18632/oncotarget.24045

184. Tsukita, S., Yonemura, S., & Tsukita, S. (1997). ERM (ezrin/radixin/moesin) family: from cytoskeleton to signal transduction. *Current Opinion in Cell Biology*, *9*(1), 70–75. https://doi.org/10.1016/S0955-0674(97)80154-8

185. Tumbarello, D. A., Brown, M. C., Hetey, S. E., & Turner, C. E. (2005). Regulation of paxillin family members during epithelial-mesenchymal transformation: a putative role for paxillin δ. *Journal of Cell Science*, *118*(20), 4849–4863. https://doi.org/10.1242/jcs.02615

186. Tumbarello, D. A., Waxse, B. J., Arden, S. D., Bright, N. A., Kendrick-Jones, J., & Buss, F. (2012). Autophagy receptors link myosin VI to autophagosomes to mediate Tom1-dependent autophagosome maturation and fusion with the lysosome. *Nature Cell Biology*, *14*(10), 1024–1035. https://doi.org/10.1038/ncb2589

187. Turner, C. E. (2000). Paxillin and focal adhesion signalling. *Nature Cell Biology*, *2*(12), E231–E236. https://doi.org/10.1038/35046659

188. Vanan, M. I., & Eisenstat, D. D. (2014). Management of high-grade gliomas in the pediatric patient: Past, present, and future. *Neuro-Oncology Practice*, *1*(4), 145–157. https://doi.org/10.1093/nop/npu022

189. Vera-Ramirez, L., Vodnala, S. K., Nini, R., Hunter, K. W., & Green, J. E. (2018). Autophagy promotes the survival of dormant breast cancer cells and metastatic tumour recurrence. *Nature Communications*, *9*(1), 1944. https://doi.org/10.1038/s41467-018-04070-6

190. Viswanatha, R., Ohouo, P. Y., Smolka, M. B., & Bretscher, A. (2012). Local phosphocycling mediated by LOK/SLK restricts ezrin function to the apical aspect of epithelial cells. *Journal of Cell Biology*, *199*(6), 969–984. https://doi.org/10.1083/jcb.201207047

191. Wagner, S., Storbeck, C. J., Roovers, K., Chaar, Z. Y., Kolodziej, P., McKay, M., & Sabourin, L. A. (2008). FAK/src-family dependent activation of the Ste20-like kinase SLK is required for microtubule-dependent focal adhesion turnover and cell migration. *PLoS ONE*, *3*(4). https://doi.org/10.1371/journal.pone.0001868

192. Wang, H., Han, M., Whetsell, W., Wang, J., Rich, J., Hallahan, D., & Han, Z. (2014). Tax-interacting protein 1 coordinates the spatiotemporal activation of Rho

GTPases and regulates the infiltrative growth of human glioblastoma. *Oncogene*, *33*(12), 1558–1569. https://doi.org/10.1038/onc.2013.97

193. Wang, K., Hong, R. L., Lu, J. B., & Wang, D. L. (2018). Ste20-like kinase is upregulated in glioma and induces glioma invasion. *Neoplasma*, *65*(2), 185–191. https://doi.org/10.4149/neo_2018_170318N193
194. Wang, M., Wang, T., Liu, S., Yoshida, D., & Teramoto, A. (2003). The expression of matrix metalloproteinase-2 and-9 in human gliomas of different pathological grades. *Brain Tumor Pathology*, *20*(2), 65–72. https://doi.org/10.1007/BF02483449
195. Weiss, F., Lauffenburger, D., & Friedl, P. (2022). Towards targeting of shared mechanisms of cancer metastasis and therapy resistance. *Nature Reviews Cancer*, *22*(3), 157–173. https://doi.org/10.1038/s41568-021-00427-0
196. Whale, A. (2011). Signalling to cancer cell invasion through PAK family kinases. *Frontiers in Bioscience*, *16*(1), 849. https://doi.org/10.2741/3724
197. Wicki, A., Lehembre, F., Wick, N., Hantusch, B., Kerjaschki, D., & Christofori, G. (2006). Tumor invasion in the absence of epithelial-mesenchymal transition: Podoplanin-mediated remodeling of the actin cytoskeleton. *Cancer Cell*, *9*(4), 261–272. https://doi.org/10.1016/j.ccr.2006.03.010
198. Wijdeven, R. H., Janssen, H., Nahidiazar, L., Janssen, L., Jalink, K., Berlin, I., & Neefjes, J. (2016). Cholesterol and ORP1L-mediated ER contact sites control autophagosome transport and fusion with the endocytic pathway. *Nature Communications*, *7*(1), 11808. https://doi.org/10.1038/ncomms11808
199. Wolff, J. E. A., Driever, P. H., Erdlenbruch, B., Kortmann, R. D., Rutkowski, S., Pietsch, T., Parker, C., Metz, M. W., Gnekow, A., & Kramm, C. M. (2010). Intensive chemotherapy improves survival in pediatric high-grade glioma after gross total resection: Results of the HIT-gBM-c protocol. *Cancer*, *116*(3), 705–712. https://doi.org/10.1002/cncr.24730
200. Wyss, J., Frank, N. A., Soleman, J., & Scheinemann, K. (2022). Novel Pharmacological Treatment Options in Pediatric Glioblastoma—A Systematic Review. In *Cancers* (Vol. 14, Issue 11). MDPI. https://doi.org/10.3390/cancers14112814
201. Xu, D., Kim, Y., Postelnek, J., Vu, M. D., Hu, D. Q., Liao, C., Bradshaw, M., Hsu, J., Zhang, J., Pashine, A., Srinivasan, D., Woods, J., Levin, A., O'Mahony, A., Owens, T. D., Lou, Y., Hill, R. J., Narula, S., DeMartino, J., & Fine, J. S. (2012). RN486, a selective Bruton's tyrosine kinase inhibitor, abrogates immune hypersensitivity responses and arthritis in rodents. *Journal of Pharmacology and Experimental Therapeutics*, *341*(1), 90–103. https://doi.org/10.1124/jpet.111.187740
202. Xu, W., Yang, Z., & Lu, N. (2015). A new role for the PI3K/Akt signaling pathway in the epithelial-mesenchymal transition. *Cell Adhesion & Migration*, *9*(4), 317–324. https://doi.org/10.1080/19336918.2015.1016686
203. Yamada, E., Tsujikawa, K., Itoh, S., Kameda, Y., Kohama, Y., & Yamamoto, H. (2000). Molecular cloning and characterization of a novel human STE20-like kinase, hSLK1The nucleotide sequence reported in this paper has been submitted to the DDBJ/EMBL/GenBank with accession number AB002804.1. *Biochimica et*

Biophysica Acta (BBA) - Molecular Cell Research, *1495*(3), 250–262. https://doi.org/https://doi.org/10.1016/S0167-4889(99)00164-0

204. Yamaguchi, H., & Oikawa, T. (2010). Membrane lipids in invadopodia and podosomes: key structures for cancer invasion and metastasis. *Oncotarget*, *1*(5), 320–328. https://doi.org/10.18632/oncotarget.100907
205. Yang, H.-S., & Hinds, P. W. (2003). Increased Ezrin Expression and Activation by CDK5 Coincident with Acquisition of the Senescent Phenotype. *Molecular Cell*, *11*(5), 1163–1176. https://doi.org/10.1016/S1097-2765(03)00135-7
206. Yu, Q., & Stamenkovic, I. (2000). Cell surface-localized matrix metalloproteinase-9 proteolytically activates TGF-beta and promotes tumor invasion and angiogenesis. *Genes & Development*, *14*(2), 163–176.
207. Yuminamochi, T., Yatomi, Y., Osada, M., Ohmori, T., Ishii, Y., Nakazawa, K., Hosogaya, S., & Ozaki, Y. (2003). Expression of the LIM Proteins Paxillin and Hic-5 in Human Tissues. *Journal of Histochemistry & Cytochemistry*, *51*(4), 513–521. https://doi.org/10.1177/002215540305100413
208. Zaidel-Bar, R., Milo, R., Kam, Z., & Geiger, B. (2007). A paxillin tyrosine phosphorylation switch regulates the assembly and form of cell-matrix adhesions. *Journal of Cell Science*, *120*(1), 137–148. https://doi.org/10.1242/jcs.03314
209. Zaman, R., Lombardo, A., Sauvanet, C., Viswanatha, R., Awad, V., Bonomo, L. E.-R., McDermitt, D., & Bretscher, A. (2021). Effector-mediated ERM activation locally inhibits RhoA activity to shape the apical cell domain. *Journal of Cell Biology*, *220*(6). https://doi.org/10.1083/jcb.202007146
210. Zhang, L.-L., Mu, G.-G., Ding, Q.-S., Li, Y.-X., Shi, Y., Dai, J.-F., & Yu, H.-G. (2015). Phosphatase and Tensin Homolog (PTEN) Represses Colon Cancer Progression through Inhibiting Paxillin Transcription via PI3K/AKT/NF-κB Pathway. *Journal of Biological Chemistry*, *290*(24), 15018–15029. https://doi.org/10.1074/jbc.M115.641407
211. Zhang, Y.-H., Hume, K., Cadonic, R., Thompson, C., Hakim, A., Staines, W., & Sabourin, L. A. (2002). E xpression of the Ste20-like kinase SLK during embryonic development and in the murine adult central nervous system. In *Developmental Brain Research* (Vol. 139). www.elsevier.com/locate/devbrainres
212. Zhapparova, O. N., Fokin, A. I., Vorobyeva, N. E., Bryantseva, S. A., & Nadezhdina, E. S. (2013a). Ste20-like protein kinase SLK (LOSK) regulates microtubule organization by targeting dynactin to the centrosome. *Molecular Biology of the Cell*, *24*(20), 3205–3214. https://doi.org/10.1091/mbc.e13-03-0137
213. Zhapparova, O. N., Fokin, A. I., Vorobyeva, N. E., Bryantseva, S. A., & Nadezhdina, E. S. (2013b). Ste20-like protein kinase SLK (LOSK) regulates microtubule organization by targeting dynactin to the centrosome. *Molecular Biology of the Cell*, *24*(20), 3205–3214. https://doi.org/10.1091/mbc.E13-03-0137
214. Zhuo, C., Ji, Y., Chen, Z., Kitazato, K., Xiang, Y., Zhong, M., Wang, Q., Pei, Y., Ju, H., & Wang, Y. (2013). Proteomics analysis of autophagy-deficient Atg7−/− MEFs reveals a close relationship between F-actin and autophagy. *Biochemical and*

Biophysical Research Communications, *437*(3), 482–488. https://doi.org/10.1016/j.bbrc.2013.06.111

APPENDIX

Appendix A: full sequence of SLK isoform2 (shorter isoform). Transcript Variant: This variant (2) lacks an in-frame exon in the 3' coding region, compared to variant 1, and encodes a shorter isoform (2) compared to isoform 1.

>NM_001304743.2 Homo sapiens STE20 like kinase (SLK), transcript variant 2, mRNA
GGAGTCGGCGTCGGCGCGCGCTCCAGGCCGAGGCTGTGTGGGCTGGGGAGG
GAGACAGGCGGCGGCGGCGGCGCCCCAGACCCGAGGGGACGCGCGGGCC
TGCGCCGCGGGAGCGGACGGCGGCGGAGGAGACCCTAGGCTCGCGGCCCG
AGGCGGGAGGGCTCGGCTTCTCGACTGCCCGCCTCCGAGGCCGCCGGCCGC
TTCTCTCTCCCAGAGTGGCCGCCGCCCCTGGAGACTCGCCGTGACACGGGCC
TAAGCCGCCGCCGCGGGAGTCCTGACCGCTCGGACCCGTCGGATCAGGCCG
GGTGGGAGCGAGCTTGCGGGCAGGTGCCGCTCCCGGAGGGTGGGCCGGAG
GCGAGGCGCCCACCGCGCGGCTCGCGGGCCGGGCTCGGCGGAGGGGCCGCT
CGCGCAGCACCCCCACCGCGGGCCGGAGCCCGGGTCGCCGCCCCGCCTTCT
CCCGGGACCGCCCGGCCGGAGCTGCGGGGGCCGAGGGACGCCGCGCCCGC
CGCCGCCAGCCGGGCTCGCGCGGGAGAGCAGGGAAGAGAAACTTTGCCTTT
TATTGTTTTTAGTCCTTAAGTGCAAGGAACTCTGTGTTGGGAGGAAAAATGT
CCTTCTTCAATTTCCGTAAGATCTTCAAGTTGGGGAGCGAGAAGAAGAAGA
AGCAGTACGAACACGTGAAGAGGGACCTGAACCCCGAAGACTTTTGGGAG
ATTATAGGAGAACTGGGCGACGGAGCCTTTGGGAAAGTGTACAAGGCCCAG
AATAAAGAGACCAGTGTTTTAGCTGCTGCAAAAGTGATTGACACTAAATCT
GAAGAAGAACTTGAAGATTACATGGTAGAGATTGACATATTAGCATCTTGT
GATCACCCAAATATAGTCAAGCTTCTAGATGCCTTCTATTATGAGAACAATC
TTTGGATCCTCATTGAATTTTGTGCAGGTGGAGCAGTAGATGCTGTGATGCT
TGAACTTGAGAGACCATTAACTGAGTCCCAAATACAAGTAGTTTGCAAGCA
GACTTTAGATGCATTGAACTACTTACATGATAATAAGATCATCCACAGAGAT
CTGAAGGCTGGCAACATTCTCTTTACCTTAGATGGAGATATCAAATTGGCGG
ATTTTGGAGTATCAGCTAAAAACACGAGGACAATTCAAAGAAGAGATTCCT
TTATTGGTACACCATATTGGATGGCTCCTGAAGTAGTCATGTGTGAAACATC
TAAGGACAGACCCTATGACTACAAAGCTGATGTTTGGTCCCTGGGTATCACT
TTAATAGAAATGGCTGAGATAGAACCACCTCATCATGAATTAAATCCAATG
CGAGTGCTGCTAAAAATAGCAAAATCTGAGCCACCTACATTAGCACAGCCA
TCCAGATGGTCTTCAAATTTTAAGGACTTTCTAAAGAAATGCTTAGAAAAGA
ATGTGGATGCCAGGTGGACTACATCTCAGCTGCTGCAGCATCCCTTTGTTAC
TGTTGATTCCAACAAACCCATCCGAGAATTGATTGCAGAGGCGAAGGCTGA
AGTAACAGAAGAAGTTGAAGATGGCAAAGAGGAAGATGAAGAGGAGGAA
ACAGAAAATTCTCTGCCAATACCTGCAAGTAAGCGTGCATCTTCTGACCTTA
GTATCGCCAGCTCTGAAGAAGATAAACTTTCACAAAATGCTTGTATTTTGGA
GTCTGTCTCAGAAAAAACAGAACGTAGTAACTCTGAAGATAAACTCAACAG
CAAAATTCTTAATGAAAAACCCACCACTGATGAACCTGAAAAGGCTGTGGA
GGATATTAATGAACATATTACCGATGCTCAGTTAGAAGCAATGACTGAACT
CCATGACAGAACAGCAGTAATCAAGGAGAATGAAAGAGAGAAGAGGCCCA
AGCTTGAAAATCTGCCTGACACAGAAGACCAAGAAACTGTGGACATTAATT
CAGTCAGTGAAGGAAAAGAGAATAATATAATGATAACCTTAGAAACAAAT
ATTGAACATAATCTAAAATCTGAGGAAGAAAAGGATCAGGAAAAGCAACA

GATGTTTGAAAATAAGCTTATAAAATCTGAAGAAATTAAAGATACTATTTTG
CAAACAGTAGATTTAGTTTCTCAAGAGACTGGAGAAAAAGAGGCAAATATT
CAGGCAGTTGATAGTGAAGTTGGGCTTACAAAGGAAGACACCCAAGAGAA
ATTGGGGGAAGACGACAAAACTCAAAAAGATGTGATCAGCAATACAAGTG
ATGTGATAGGAACATGTGAGGCAGCAGATGTGGCTCAGAAAGTGGATGAA
GACAGTGCTGAGGATACGCAGAGTAATGATGGGAAAGAAGTGGTCGAAGT
AGGCCAGAAATTAATTAATAAGCCCATGGTGGGTCCTGAGGCTGGTGGTAC
TAAGGAAGTTCCTATTAAAGAAATAGTTGAAATGAATGAAATAGAAGAAGG
TAAAAATAAGGAACAAGCAATAAACAGTTCAGAGAACATAATGGACATCA
ATGAGGAACCAGGAACAACTGAAGGTGAAGAAATCACTGAGTCAAGTAGC
ACTGAAGAAATGGAGGTCAGAAGTGTGGTGGCTGATACTGACCAAAAGGCT
TTAGGAAGTGAAGTTCAGGATGCTTCTAAAGTCACTACTCAGATAGATAAA
GAGAAAAAAGAAATTCCAGTGTCAATTAAAAAAGAGCCTGAAGTTACTGTA
GTTTCACAGCCCACTGAACCTCAGCCTGTTCTAATACCCAGTATTAATATCA
ACTCTGACAGTGGAGAAAATAAAGAAGAAATAGGTTCTTTATCAAAAACTG
AAACTATTCTGCCACCAGAATCTGAGAATCCAAAGGAAAATGATAATGATT
CAGGCACTGGTTCCACTGCTGATACTAGCAGTATTGACTTGAATTTATCCAT
CTCTAGCTTTCTAAGTAAAACTAAAGACAGTGGATCGATATCTTTACAAGAA
ACAAGAAGACAAAAGAAAACATTGAAGAAAACACGCAAATTTATTGTTGAT
GGTGTAGAAGTGAGTGTAACAACATCAAAGATAGTTACAGATAGTGATTCC
AAAACTGAAGAATTGCGGTTTCTTAGACGTCAGGAACTTCGGGAATTAAGA
TTTCTTCAGAAAGAAGAGCAAAGAGCCCAACAACAGCTCAATAGCAAACTA
CAGCAACAACGAGAACAAATTTTCCGGCGCTTTGAGCAGGAAATGATGAGT
AAAAAGCGACAATATGACCAGGAAATTGAGAATCTAGAAAAACAGCAGAA
ACAGACTATCGAACGCCTGGAACAAGAGCACACAAATCGCTTGCGAGATGA
AGCCAAACGCATCAAAGGAGAACAAGAGAAAGAGTTGTCCAAATTTCAGA
ATATGCTGAAGAACCGAAAGAAGGAGGAACAAGAGTTTGTTCAGAAACAA
CAGCAAGAATTAGATGGCTCTCTGAAAAAGATCATCCAGCAGCAGAAGGCA
GAGTTAGCTAATATTGAGAGAGAGTGCCTGAATAACAAGCAACAGCTCATG
AGAGCTCGAGAAGCTGCAATTTGGGAGCTCGAAGAACGACACTTACAAGAA
AAACACCAGCTGCTCAAACAGCAGCTTAAAGATCAGTATTTCATGCAAAGA
CATCAGCTACTTAAGCGCCACGAGAAGGAAACAGAGCAAATGCAGCGTTAC
AATCAAAGACTTATTGAGGAATTGAAAAACAGACAGACTCAAGAAAGAGC
AAGACTGCCCAAGATTCAGCGCAGTGAAGCCAAGACTCGAATGGCCATGTT
TAAGAAGAGTTTGAGAATTAACTCAACAGCCACACCAGATCAGGACCGTGA
TAAAATTAAACAGTTTGCTGCACAAGAAGAAAAGAGGCAGAAAAATGAGA
GAATGGCTCAGCATCAGAAACATGAGAATCAAATGCGAGATCTTCAGTTGC
AGTGTGAAGCCAATGTCCGCGAACTGCATCAGCTGCAGAATGAAAAATGCC
ACTTGTTGGTTGAGCATGAGACTCAGAAACTGAAGGAGTTAGATGAGGAAC
ATAGCCAAGAATTAAAGGAGTGGAGAGAGAAATTGAGACCTAGGAAAAAG
ACACTGGAAGAAGAGTTTGCCAGGAAACTACAGGAACAGGAAGTATTCTTT
AAAATGACTGGGGAGTCTGAATGCCTTAACCCATCAACACAGAGCCGGATT
TCCAAATTTTATCCTATTCCCAGCTTGCATTCCACCGGATCATAACAAAGGG
AAGCATTCTGTGCGTGGGTTTGGCTCTTTCAGTATGTCATTCTGTTCTCATCT
TCTGCCACAGTCTCTCAGATAGCTCATGAAGACAATCACCTGCCTCACCTTC
TAGGTGTTTTCCTTTTTTGTTTTTTTTGTTTTGTTTTGTTTTTAAGCAAAGATG
AAGGGAAAACGAACTAAGACAGACGCTAGGCCATGTTGGCAAAGTAGCAT
CTTGGTGACTAAGGTGACTTTGTATATTCATCTTAAAAATTATGTTCTTTAGA
CACTGCTACCTGAAAACTGTTGGAGAAATAATGTTTAAAGTTATTTAAGAA

AAACTGTTACATCACTAAGTATTAATAAATTCTTCTTACCTGACGTAACTTC
TCAATGCCTAAATTCTGTAGTTGAAGCTCTGCTGCAGAGAGTTGGGATAATT
TTCTTTTGGTGGATCAGCTCTCATAAAAAAGCTATGATTTGCTCAAATATGC
TGTTGACTCAGTAAATGAATATATTTTTTCTTTAAATAGGAACAACCTCTTT
TAAAAGAGAAAAATTATTTCAGTGATTTGTCAAAACGAATTACCTCTTTTGG
CATGAGCTAATAATTGAGGGTGCTAATTTTCTTAAGATAGTGCCTAAAACAC
TAAATTTCAGTCAAGTCGTAAGTAGGATTTTCTTTTTGATCAACAGGGACAA
AAACATCTTTAGAATTAAAAACATGGTTGTTTTGGAATTTTTGCTTCTCTTAC
CGTTTGATAGAAATTTTCATCCTAAAATACATGTACAAAGTTTGGAAAGATG
AAAAAAAGAGGTAGCTTTTAGATTGCAAACTGGAAATGTAAAACTCATGAA
ATTTAAGCAATATAGGTTTAGCTATCTGTGTTTATTTTCTAAAATAATACCTG
AGCTGGTTAAATGATTTCTCTCCATCTTAGCTAATTCTGTTTAAAACTCTGTC
AGAGGCCTGCAGGCTGTGAGTTATATTTATAAATATATCTTCAGAAATTAAT
CTTAAAAGAGGCATTAGTTCAGAATACTTTTTTAAAAGTTTAAATTAAATAT
TTAGGCACGTCAGGAATTACTTTTCCTTATTTTGAAATGAGGCTACTTATGT
CTTGGTTTTATTTTGTTCCATGTTTAAATCATTCACTTTGATTTGAGTGGGAA
AAGCCTGAAGCCTTTATCATGTGGTTGCTGGTGTGTGTAATTATTAATGAAA
TGTTCACTCCTAGTCCCTTATGAGGCTTAGAATTTCAACCACGTGTCAGGTC
AGACAGTATTATAAACTGTACTTTGCTGTCTGAGACAGCACATTTGTGAATG
ATGCTTGCTGCCTGCCATTTTCAACCTATTCTCTCTTAAGAGTGCTAGGTACC
AAATTGTGAAAGTTTGTTTTCAGTTATATTACTTTTGAGGCTGGTGAAAAAT
TTAAATGTAACTTTGTGGGAACACTGATTCATATTTAGAAAATGTAAATGTC
TGTAGCACTTTCTTGCAGTTAATTTGAAAACTTTGGATGCTGAACCTTGTTTG
TCAGTGATTTAGATGATTTAAAAATGCATGTGTGATTTGAATTTTATAATTG
TTTTGACAAGCATAATTTACTTGGACAACTTCGTAGGTAGCCTTAACTTCTG
GCCAAGTTTGTTTTTTATATAAATATATATACATATATACATATTATGTATGG
TTGTAAATTCATACACTTATCACATGAATGTGTTACTGTATACAAAACTCTT
AATGCTTTATTCTCAAATGCTGGGTTGAAAAATGTTTTGAAAGCCTTTTAAA
ATATATATCTTTATAAAGTAATATTCAGGATGATGATAAAAATTGTTTATAT
TGTTATGATAAAAATGACAGTATAATGTTGCCCAGTGTATTTAATGATTTAT
TTGAAGAGGGATTGGGAAGGAACGTCTTCATACCACTTTCTCCTTTGAAATT
TTCAGTTTATTGACTTTTAAAAAATGAATACCTCAGGCAGTAGACATTTTTT
TTCTAGTATCATTTAATTGATACCCTGTGCGCTAAATAGTGTGTGGTGCCTG
ATTAATTTGGTCTGAATATTTGATTCTTTCTGTTCCTTTCAACTTGACATTCA
GATTATTGACTCAAGGAGAGAGGCTCAGAGTGGAATGGTTGGCGCTGTGGG
TAAGGTTGGATCTCCCTTAAAACTGCCTTTTGGATTCAGTGTTTGTGCTTGA
GTTCGCTTTCAAATATGACCATAATCGTGTGGGTGCAAGACTGTACAGTGAT
ACATATGTAGAGGTAAAGCATTCATTTTAATACTTAAAGTTATATAAATCTT
TTCAAAAAGTGTTTTGTTATAAAATACGCTGTTTGTACCCATACCAGCCCAC
CTCTTCTGAGGCCCTGTATTCAAATAGATGATAGTGATCTATCTTTCCTGCAT
GAAGTGTAGGTGGCGAGTGGGCGAGGGGCGCAGACTTCTTTGAAATCGAAG
GGTACAGTCAAATCTACTGCTGATTTGGTTGTTTTGTTGCTGTGGCAGAATA
TGCCATGAAACACATACAGACTTCTCCGAACGTGCACCCTCATCAGCCACCT
CCTCCCCTCTTTCCCTGAGTGCTGTGAACACAGCAGACCTGCACACTTCTGC
AGATCCAGCTCCTACAGCTTGGGGCACTAGGCTGCCTTTCCTAGTCCTGTCA
ACAACCATACAGTGCGAATTGCTGAATTAGCTGCTATTCTATGTGGAGTCAC
ATTAAGCTTTTTCTTATCTTTTTCTATGGGGAAGCTATAGGGTGGGTAAGGA
AAAAATGTTGAATGCTTTTACTTTGCTGAAAATATTAGAACTCTCTTGTGAC
AGGATACAGCAAATTATAATTAAATATAAATTACCAGAACCAGAGCTACCT

CTAAGTCATACTTCCTCAAGCACAAAGCTCTCAGGCATATGAGACCCACCTT
AATGAAGGGTCTCTGATTTCTTGAGCATCAGCGAGTTTCAGAAGTGACTATT
TTTTTGTACTCTTCTAGTTTCCTTGTAACTATACACTTTTTCCCATTCCACACT
GTGCTTAAATGACAAAGACTCTTCTGAGAAGCCAAATTCTGTCCAAGTATTA
ACTAGAGATATTGTTGATTAAAGAAAATCTAGAACTGAAGTGAAAGAAGAG
AGTTCCAGTTCTAATAGTCTTTTGATTAACAATTCTTTTCTGAGAAATGATTT
TTATAAGAAATGGGGTGATTCTTTAAATGCTTTTCTTAAGTTGAAGGCACAA
CAGTTAATGGCTGTATTGTTGCTATTCCGTTGCTGACATGTTTTTGATAAAGC
TTTAACATTCCTGCTACTAATTTTGGCGGAGAGTGTTTGCCAGGTTTCAATG
TGGGCTGCAGCTTTTTGTGCTCCTTCTCTGGTTTGCAGTGTAATGAGTTCATA
AGCTAAATTTTCAGAAAGAATTTTGTTTAAGATTATGCCTCTTATCTACTTG
AGAGCAACATGTCTTTTCAATCATGGGATTGACACATGAAAAATAAAGTTA
TTTCTTAATCAA

Color code: coding sequences

Appendix B: Amino acid sequence of SLK isoform2.

>NP_001291672.1 STE20-like serine/threonine-protein kinase isoform 2 [Homo sapiens]

MSFFNFRKIFKLGSEKKKKQYEHVKRDLNPEDFWEIIGELGDGAFGKVYKAQN
KETSVLAAA**K**VIDTKSEEELEDYMVEIDILASCDHPNIVKLLDAFYYENNLWILI
EFCAGGAVDAVMLELERPLTESQIQVVCKQTLDALNYLHDNKIIHRDLKAGNIL
FTLDGDIKLADFGVSAKNTRTIQRRDSFIGTPYWMAPEVVMCETSKDRPYDYK
ADVWSLGITLIEMAEIEPPHHELNPMRVLLKIAKSEPPTLAQPSRWSSNFKDFLK
KCLEKNVDARWTTSQLLQHPFVTVDSNKPIRELIAEAKAEVTEEVEDGKEEDEE
EETENSLPIPASKRASSDLSIASSEEDKLSQNACILESVSEKTERSNSEDKLNSKIL
NEKPTTDEPEKAVEDINEHITDAQLEAMTELHDRTAVIKENEREKRPKLENLPD
TEDQETVDINSVSEGKENNIMITLETNIEHNLKSEEEKDQEKQQMFENKLIKSEEI
KDTILQTVDLVSQETGEKEANIQAVDSEVGLTKEDTQEKLGEDDKTQKDVISNT
SDVIGTCEAADVAQKVDEDSAEDTQSNDGKEVVEVGQKLINKPMVGPEAGGT
KEVPIKEIVEMNEIEEGKNKEQAINSSENIMDINEEPGTTEGEEITESSSTEEMEVR
SVVADTDQKALGSEVQDASKVTTQIDKEKKEIPVSIKKEPEVTVVSQPTEPQPV
LIPSININSDSGENKEEIGSLSKTETILPPESENPKENDNDSGTGSTADTSSIDLNLS
ISSFLSKTKDSGSISLQETRRQKKTLKKTRKFIVDGVEVSVTTSKIVTDSDSKTEE
LRFLRRQELRELRFLQKEEQRAQQQLNSKLQQQREQIFRRFEQEMMSKKRQYD
QEIENLEKQQKQTIERLEQEHTNRLRDEAKRIKGEQEKELSKFQNMLKNRKKEE
QEFVQKQQQELDGSLKKIIQQQKAELANIERECLNNKQQLMRAREAAIWELEE
RHLQEKHQLLKQQLKDQYFMQRHQLLKRHEKETEQMQRYNQRLIEELKNRQT
QERARLPKIQRSEAKTRMAMFKKSLRINSTATPDQDRDKIKQFAAQEEKRQKN
ERMAQHQKHENQMRDLQLQCEANVRELHQLQNEKCHLLVEHETQKLKELDE
EHSQELKEWREKLRPRKKTLEEEFARKLQEQEVFFKMTGESECLNPSTQSRISK
FYPIPSLHSTGS

K: Lysine residue at 63. Mutant residue in K63R.

Appendix C: Alignment of the catalytic domain of hSLK with that of other STE20 family members. Romain numbers are indicating the 11 conserved subdomains (Yamada et al., 2000).

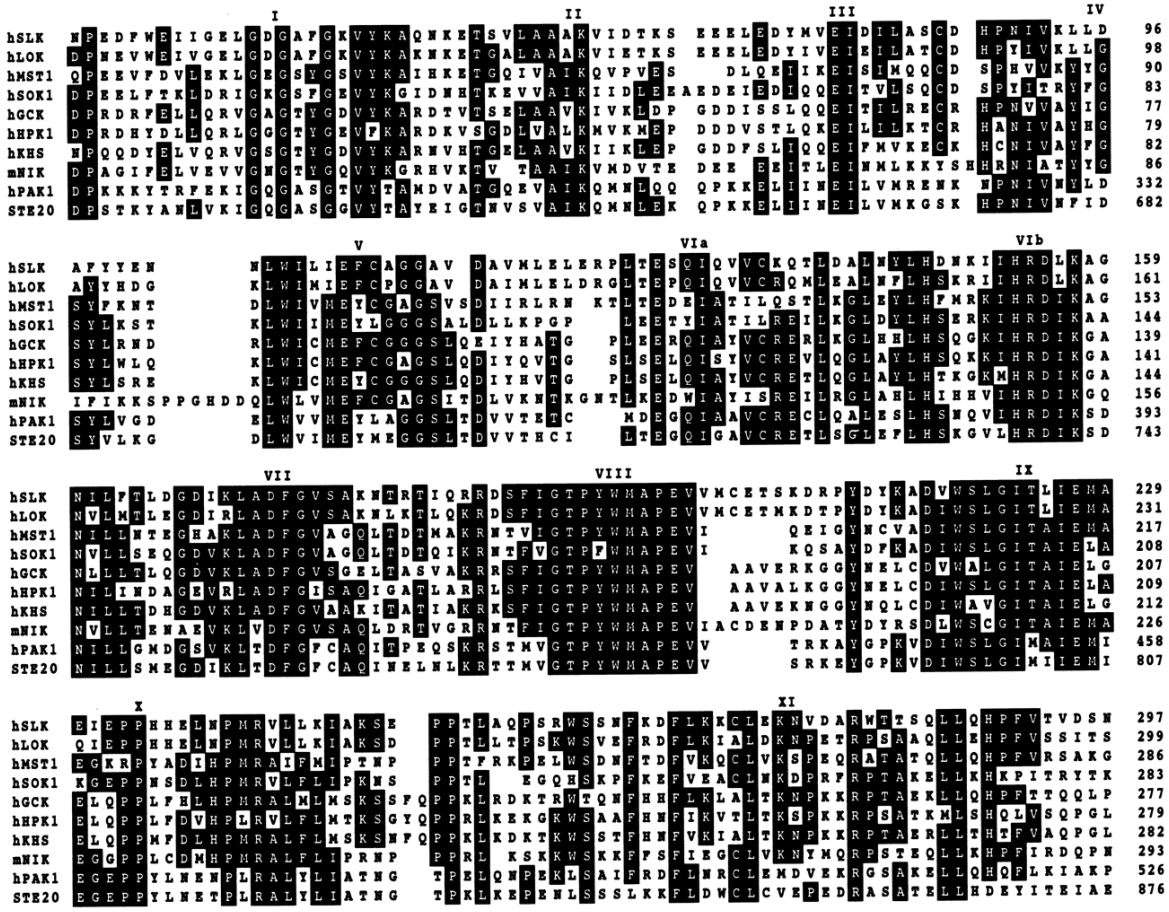

Appendix D: Alternative splicing of SLK. SLK-201 is the shorter isoform called as isoform 2 in Appendix A and B. **I.** Two different isoforms differ in presence of exon 13. **II.** Read counts of exons in primary and metastatic tumor. Exon 13 count is zero in metastatic sample. Gray region is UTR, blue parts are exons, and white regions are introns **III.** Scatter and box plots of two SLK isoforms. In the plots, it is shown that longer isoform (SLK-202) containing exon 13 is enriched in primary tumor while shorter isoform (SLK-201) lacking exon 13 is presented in primary tumors (Holland et al., 2022).

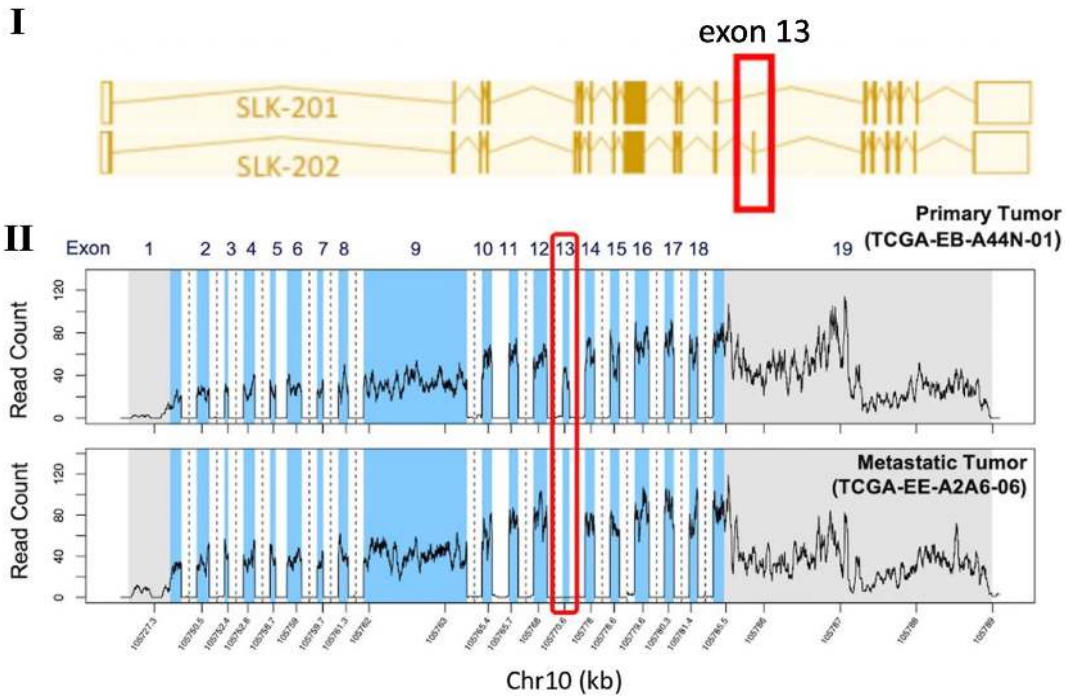

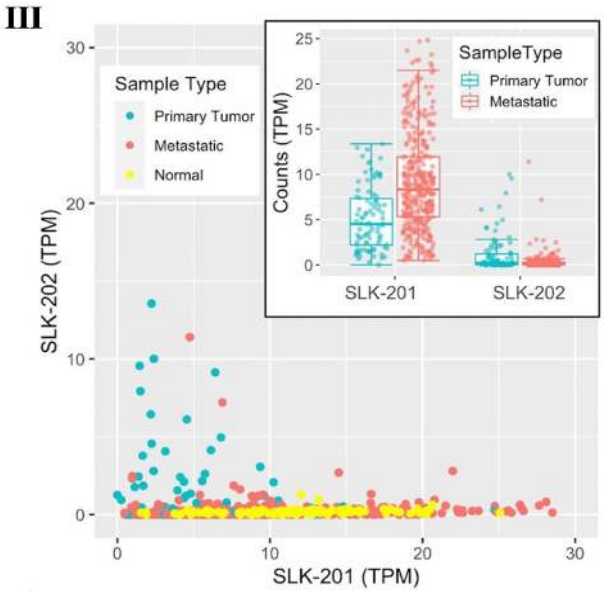

Appendix E Sequence of 50 amino acids of some target protein around phosphorylation site by SLK. It was shown that there is no conserved motif between these proteins and ATG5, Beclin1, ATG12, Bcl-2, and ATG16L1 proteins' aminoacid sequence.

Ezrin: Thr567
SSELSQARDENKRTHNDIIHNENMRQGRDKYK**T**LRQIRQGNTKQRIDEFE

Radixin: Thr564
SSELAQARDETKKTQNDVLHAENVKAGRDKYK**T**LRQIRQGNTKQRIDEFE

Moesin: Thr558
TSELANARDESKKTANDMIHAENMRLGRDKYK**T**LRQIRQGNTKQRIDEFE

Plk1: Thr210
KLGNLFLNEDLEVKIGDFGLATKVEYDGERKK**T**LCGTPNYIAPEVLSKKG

Paxillin: Ser250
ESLLDELESSVPSPVPAITVNQGEMSSPQRVT**S**TQQQTRISASSATRELD

RhoA: Ser188
GRDMANRIGAFGYMECSAKTKDGVREVFEMATRAALQARRGKKK**S**GCLVL

Appendix F Modifications of SLK protein. Data was obtained from Phosphosite.org (Https://Www.Phosphosite.Org/ProteinAction.Action?Id=2519&showAllSites=true)

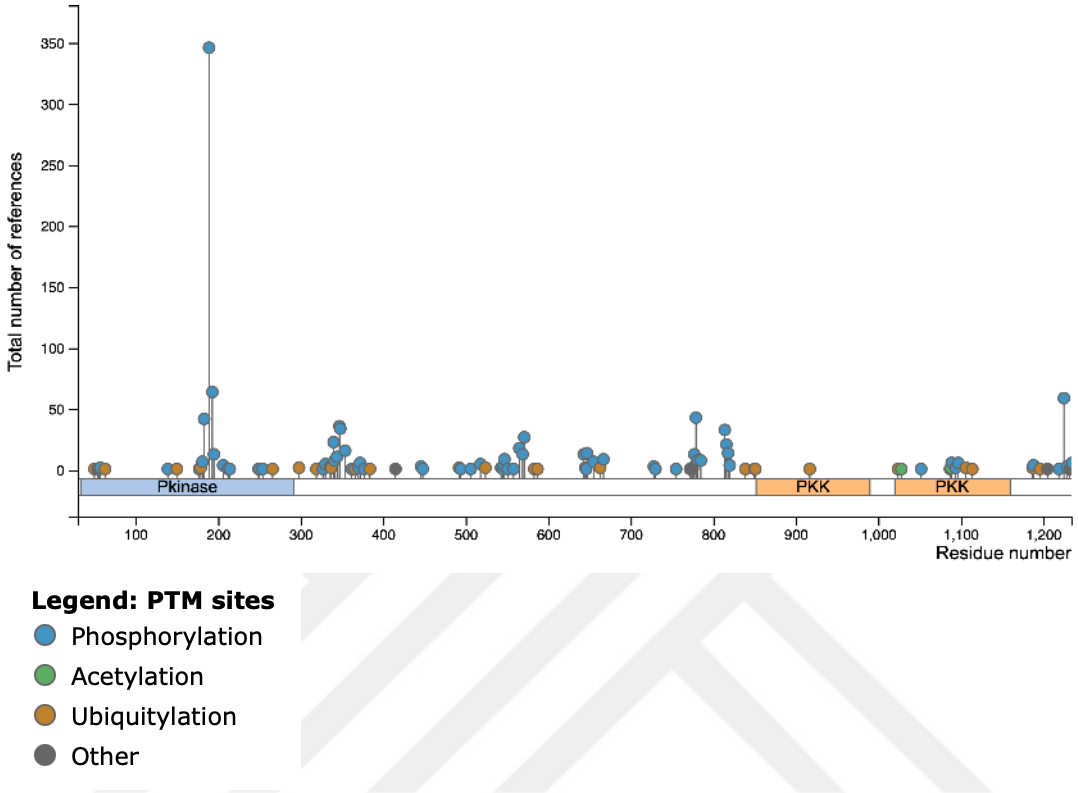

Appendix G Permissions from articles were presented respectively for figure 1.9 and 1.17.

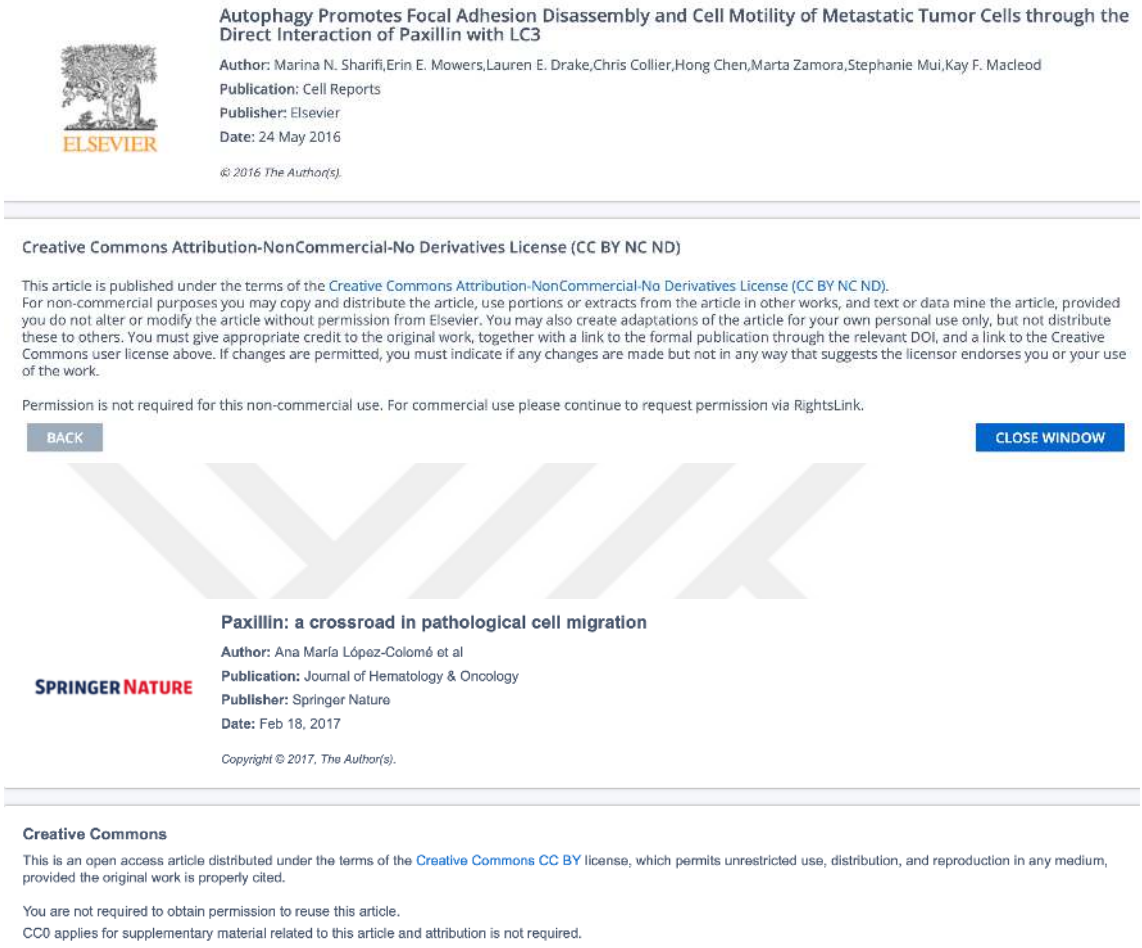

Autophagy Promotes Focal Adhesion Disassembly and Cell Motility of Metastatic Tumor Cells through the Direct Interaction of Paxillin with LC3

Author: Marina N. Sharifi,Erin E. Mowers,Lauren E. Drake,Chris Collier,Hong Chen,Marta Zamora,Stephanie Mui,Kay F. Macleod
Publication: Cell Reports
Publisher: Elsevier
Date: 24 May 2016

© 2016 The Author(s).

Creative Commons Attribution-NonCommercial-No Derivatives License (CC BY NC ND)

This article is published under the terms of the Creative Commons Attribution-NonCommercial-No Derivatives License (CC BY NC ND).
For non-commercial purposes you may copy and distribute the article, use portions or extracts from the article in other works, and text or data mine the article, provided you do not alter or modify the article without permission from Elsevier. You may also create adaptations of the article for your own personal use only, but not distribute these to others. You must give appropriate credit to the original work, together with a link to the formal publication through the relevant DOI, and a link to the Creative Commons user license above. If changes are permitted, you must indicate if any changes are made but not in any way that suggests the licensor endorses you or your use of the work.

Permission is not required for this non-commercial use. For commercial use please continue to request permission via RightsLink.

BACK CLOSE WINDOW

Paxillin: a crossroad in pathological cell migration

Author: Ana María López-Colomé et al
Publication: Journal of Hematology & Oncology
Publisher: Springer Nature
Date: Feb 18, 2017

Copyright © 2017, The Author(s).

Creative Commons

This is an open access article distributed under the terms of the Creative Commons CC BY license, which permits unrestricted use, distribution, and reproduction in any medium, provided the original work is properly cited.

You are not required to obtain permission to reuse this article.
CC0 applies for supplementary material related to this article and attribution is not required.